ABSTRACT

LI, JUN. **A Methodology to Evaluate Nuclear Waste Transmutation/Fuel Cycle Systems**. (Under the direction of Dr. Man-Sung Yim).

The nuclear waste issue is a major challenge to the nuclear energy industry. To reduce the nuclear waste impact, a number of advanced nuclear fuel cycles and transmutation schemes are being investigated. Reported herein is a methodology which was developed to evaluate and compare nuclear fuel cycles based on repository performance, proliferation resistance performance and fuel cycle cost.

To evaluate the repository performance efficiently, a simplified repository performance model was developed based on the Yucca Mountain Repository. By considering the temperature limits at different locations in the repository, maximum loading is estimated for given nuclear waste characteristics. The enrivonmental impact from the maximum loaded reprository is investigated in term of projected dose and health index based on accumulated risk.

A fuzzy logic based barrier method was developed to assess the proliferation resistance of three different nuclear fuel cycles. This model gives quantitative proliferation resistance information from the beginning to the end of a full fuel cycle.

A simple fuel cycle cost model was also used. Based on assumed nonproliferation charges, an adjusted fuel cycle cost was evaluated which included the impact from repository and proliferation resistance performance to the overall fuel cycle cost.

A case study investigates the three fuel cycles: PWR-OT (Pressurized Water Reactor-Once Through), MOX (Mixed Oxide) and DUPIC (Direct Use of spent PWR

fuel in CANDU). The PWR-OT cycle provides the highest level of proliferation resistance and lowest fuel cycle cost while the DUPIC cycle provides for maximum repository loading (based on the total electricity generated). The adjusted fuel cycle cost was found to be an inadequate means of combining repository impact, proliferation resistance, and cost to affect fuel cycle selection decisions. An alternative method of using an adjusted total electricity generation cost is presented.

A METHODOLOGY TO EVALUATE NUCLEAR WASTE TRANSMUTATION/FUEL CYCLE SYSTEMS

By
Jun Li

A dissertation submitted to the Graduate Faculty of
North Carolina State University
in partial fulfillment of the
requirements for the Degree of
Doctor of Philosophy

Nuclear Engineering

Raleigh, N.C.

2006

APPROVED BY:

_____	_____
Dr. David N. McNelis	Dr. Paul J. Turinsky
_____	_____
Dr. Robert E. Young	Dr. Man Sung Yim Chair of Advisory Committee

BIOGRAPHY

Jun Li was born in Wuhan, Hubei, China on Jan. 26th, 1975. He is the youngest of the three children of Mr. Liangkun Li and his wife Chuanzhi Zhang. He graduated from Tsinghua University in Beijing with a Bachelor of Science degree in Engineering Physics in 1997 and received a Master of Science degree in the same department in 2000.

He came to the United States to pursue his PhD in Nuclear Engineering at North Carolina State University in August 2000. Since the beginning of his PhD program in the Department of Nuclear Engineering at North Carolina State University, he has worked as a research assistant for Dr. Man-sung Yim. He received a Master of Industrial Engineering degree in Industrial Engineering in December 2003.

He married his wife Ramy N. Rabe from Madagascar in 2003 summer.

ACKNOWLEDGMENTS

I would like to thank God for the ultimate strength and courage He bestowed me in the fulfillment of this dissertation.

I would also like to express my gratitude and appreciation to my advisor Dr. Mansung Yim for his guidance, encouragement and valuable support throughout my dissertation research. Similar thanks go to Dr. David N. McNelis for his valuable and generous help during my graduate program and in the writing of my dissertation. I would also like to acknowledge my committee members, Dr. Paul J. Turinsky and Dr. Robert E. Young for their continued support, valuable suggestions and comments necessary for the completion of my research and dissertation.

I thank my parents and my wife, for their constant love and unending support that I most needed for the completion of my work.

Last but not least, I would like to acknowledge the Russell Family Foundation of Gig Harbor, Washington for their financial help without which I could not have finished my research.

TABLE OF CONTENTS

LIST OF FIGURES

LIST OF TABLES

LIST OF ABBREVIATIONS

AAA	Advanced Accelerator Applications
ADS	Accelerator Driven System
AFCI	Advanced Fuel Cycle Initiative
ALI	Annual Limit on Intake
AML	Areal Mass Loading
APD	Areal Power Density
ATR	Advanced Thermal Reactor
BEIR	Biological Effects of Ionizing Radiation
BF	Barriers Frame
CANDU	CANada Deuterium Uranium
CCDF	Complementary Cumulative Distribution Functions
CM	Critical Mass
DOE	Department Of Energy
DPUI	Dose Per Unit Intake
DUPIC	Direct Use of spent PWR fuel in CANDU)
EBS	Engineered Barrier System
EDA	Enhanced Design Alternatives
EPRI	Electric Power Research Institute
FCC	Fuel Cycle Cost
GIF	Generation IV International Forum
GTCC	Greater Than Class-C
GWD	Giga Watt Day

HI	Hazard Index
HLW	High-Level Waste
HTGR	High Temperature Gas cooled Reactor
ICRP	International Council on Radiation Protection
INFCE	International Nuclear Fuel Cycle Evaluation
IPA	Iterative Performance Assessment
IRIS-MOX	IRIS-MOX Fueled Concept
IRTP	Integrated Radiological Toxic Potential
ITP	Integrated Toxic Potential
LADS	License Application Design Selection
LANL	Los Alamos National Lab
LCOE	Levelized Cost Of Electricity
LET	Linear Energy Transfer
LEU	Low Enriched Uranium
LLNL	Lawrence Livermore National Laboratory
LLRW	Low-Level Radioactive Waste
LLW	Low-Level Waste
LWR	Light Water Reactor
LWR-MOX	LWR-MOX fuel cycle
LWROT	Light Water Reactor Once Through
LWR-OT-HB	LWR-OT with High Burnup
LWR-OT-Th	LWR-OT with a Heterogeneous Thorium Seed-Blanket Core

LWR-OT-ThU	LWR-OT with Homogeneously Mixed Thoria-Urania Fuel
MAU	Multi-Attribute Utility
MOX	Mixed Oxide
MTHM	Metric Tons of Heavy Metal
MTU	Metric Tons of Uranium
MWD	Mega Watt Day
NASAP	Nonproliferation Alternative System Assessment Program
NERAC	Nuclear Energy Research Advisory Committee
NRC	Nuclear Regulatory Commission
PA	Performance Assessment
PBR	Pebble-Bed Fuel High-Temperature Gas-Cooled Reactors
PDF	Probability Density Function
PNL	Pacific Northwest Laboratory
PP	Physical Protection
PR	Proliferation Resistance
PRA	Probabilistic Risk Assessment
PWR	Pressurized Water Reactor
PWR-OT	Pressurized Water Reactor-Once Through
RD	Relative Distance
RH	Relative Humidity
RIP	Repository Integration Program

SFN	Spontaneous Fission Neutron
SNF	Spent Nuclear Fuel
SNL	Sandia National Lab
SPA	Simplified Performance Assessment
STAR	Small, Transportable, Autonomous Reactor
TI	Toxicity Index
TOPS	Technical Opportunities To Increase the Proliferation Resistance of Global Civilian Nuclear Power Systems
TPA	Total System Performance Assessment
TRU	Transuranic Waste
TSPA-VA	Total System Performance Assessment - Viability Assessment
WIPP	Waste Isolation Pilot Plant
WP	Waste Package

1 Introduction

1.1 Background

Nuclear power is a technology that can reliably produce large quantities of energy safely and economically. It does not directly emit harmful pollutants including those associated with global climate change. About 20% of the electric power currently produced in the United States comes from nuclear power. However, the public's attitude toward nuclear power has been mixed with both interest and concern – particularly concern over the management of the nuclear waste. The spent nuclear fuel (SNF), once generated from nuclear power production, remains radioactive for very long periods of time and is highly radiotoxic for hundreds of thousands of years, a situation that creates a wide range of social, technical and public health concerns. If the SNF is to be placed behind a geological barrier in a repository, the entire SNF can be classified as waste. If the SNF is reprocessed and the fuel is recycled, there will still remain some waste materials which will require placement in a geological repository.

The United States recognizes three categories of nuclear waste, i.e., low-level waste, transuranic waste and high-level waste. High-level waste (HLW) is classified by the Nuclear Regulatory Commission as either: 1) spent fuel - irradiated commercial reactor fuel; or 2) reprocessing waste - liquid waste from solvent extraction cycles in reprocessing including the solids into which liquid wastes may have been converted. Transuranic waste (TRU) is man-made radioactive waste with particles whose atoms are heavier than uranium and a concentration greater than 10

nano-curies per gram of waste. It can be generated by nuclear weapons production and reprocessing of spent nuclear fuels. All other waste that is not considered high-level or TRU is classified as low-level waste (LLW), or low-level radioactive waste (LLRW). This classification would apply to the waste from pyroprocessing techniques as well.

When waste is classified as low-level, this does not directly depend on the level of radioactivity it contains, but rather on the materials it does not contain. The NRC has developed a classification system for low-level waste based on its potential hazards, and has specified disposal and waste form requirements for each of the general classes - A, B, C and greater than Class-C (GTCC). On average, Class A is the least hazardous while GTCC is the most hazardous. Class A waste typically contains "short-lived" radionuclides (average concentration: 0.1 curies/cubic foot). Class B is contaminated with a greater amount of "short-lived" radionuclides than Class A (average concentration: 2 curies/cubic foot). Class C is contaminated with greater amounts of long-lived and short-lived radionuclides than Class A or B (average concentration: 7 curies/cubic foot). GTCC is the most radioactive of the low-level classes (average concentration: 300 to 2,500 curies/cubic foot).

LLW, except for the GTCC wastes, is disposed of in one of the three commercial disposal facilities located in the U.S.: Barnwell, South Carolina (access authorized for all low-level waste generators except North Carolina), Hanford, Washington (restricted access to only the Northwest and Rocky Mountain compacts), and Clive, Utah (restricted to only Class A low-activity, high-volume waste, e.g., slightly contaminated soil). LLW generators in North Carolina manage the LLW through “a

combination of decay in storage, long term storage and disposal of low specific activity wastes" to Clive, Utah [Ref 1-1]. According to U.S. policy, GTCC wastes are to be disposed of in a deep geological repository along with HLW.

DOE is managing the TRU waste and the Waste Isolation Pilot Plant (WIPP) in New Mexico is potential final disposal site for most TRU waste.

HLW, for its disposal, will be placed in a geological repository designed for long-term isolation of the waste. Geological disposal of these materials, the U.S. option of choice, has been determined to be technically feasible and Yucca Mountain in Nevada is the designated SNF repository.

The Yucca Mountain repository has a statutory capacity of 70,000 metric tons of heavy metal (MTHM), 63,000 MTHM of commercial spent nuclear fuel, and 7,000 MTHM of DOE materials. In the United States, there are currently 104 commercial nuclear reactors with operating licenses at 64 sites in 31 states. As of 2010 [Ref 1-2], approximately 63,400 metric tons of SNF from commercial nuclear reactors will be accumulated and approximately 2,010 MTHM of additional spent fuel between 2001 to 2010 is accumulated each year. At this accumulation rate, the statutory capacity limit of Yucca Mountain for commercial spent fuel will be reached by 2010 (Figure 1-1) indicating a need for capacity expansion or a second repository.

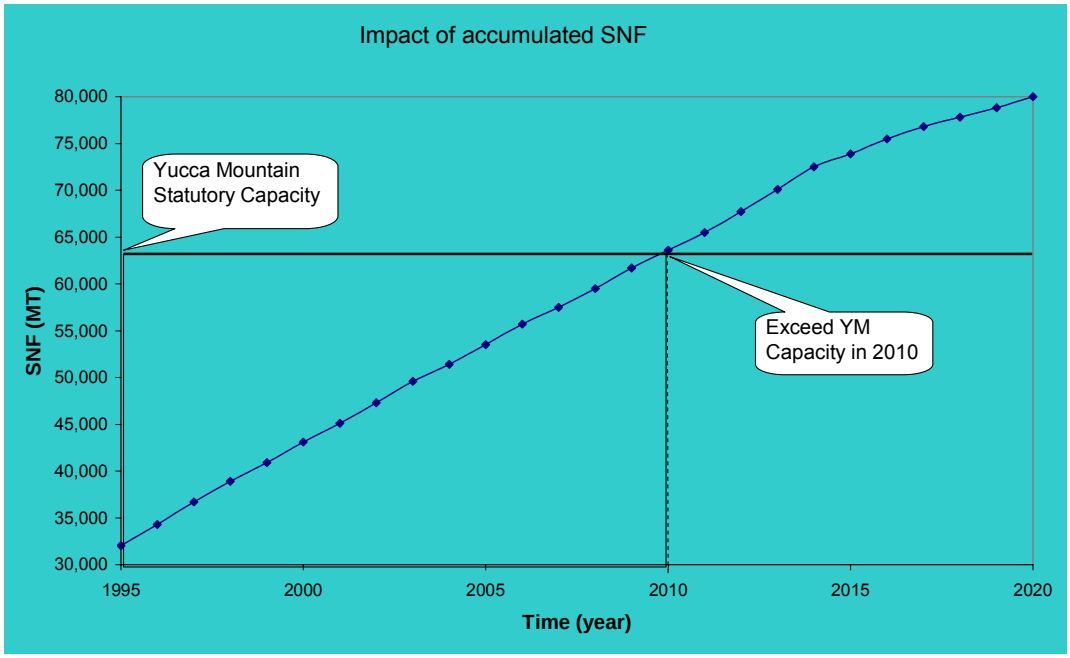

Figure 1-1: Civilian high-level waste generation in the US

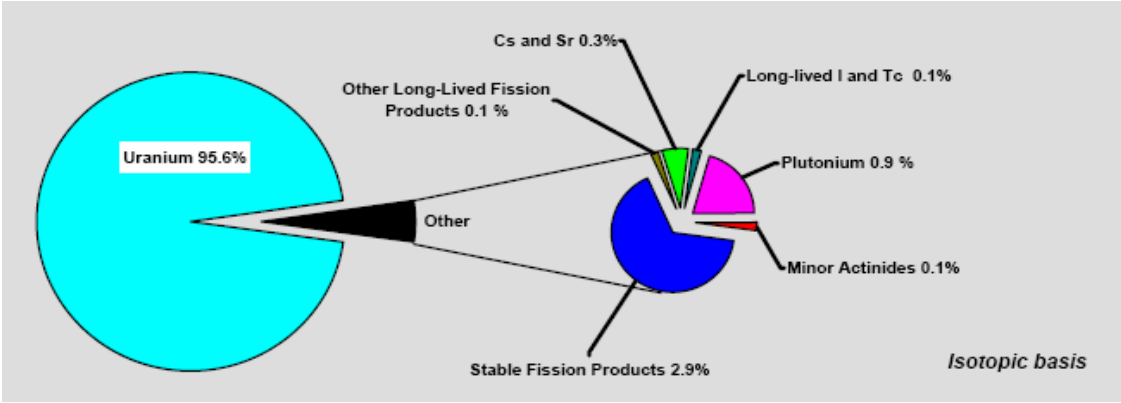

Figure 1-2: Isotopic basis of spent fuel

As shown in Figure 1-2, the composition of spent fuel (in weight percent, spent fuel of PWR, 3.2% initial enrichment, 33 GWD/MTU burnup) 10 years after removal from the reactor consists of approximately 95.6% Uranium, 0.9% Plutonium, 0.1% minor actinides, 0.1% long-lived fission products (e.g., ^{129}I and ^{99}Tc), 0.3% Cesium and Strontium and 2.9% other stable fission product nuclides. Through reprocessing, spent nuclear fuel can be partitioned into a number of components or

groupings including uranium, plutonium, minor actinides, fission products and stable isotopes. The uranium can be separated and disposed of as Class C, low-level waste, held in shallow land burial for potential reuse or recycled. This operation could significantly reduce the waste volume (as approximately 96% of spent fuel is uranium). Plutonium can be recycled and included in mixed oxide fuel or plutonium, minor actinides and possibly the long-lived iodine and technetium isotopes can be specially treated through transmutation to reduce the hazard of the HLW. Alternatively, these materials could, as a nonproliferation measure and to reduce the radiotoxic risk, be conditioned and fixed in a matrix for disposal in a geologic repository.

Transmutation is defined as the transformation of one isotope or element into another isotope or element by changing its nuclear structure. Through nuclear transmutation, hazardous long-lived nuclides can be transformed into shorter-lived, less radiotoxic or even stable nuclides. For example: ^{129}I has a half-life of 1.57×10^7 yrs and decays to stable ^{129}Xe. But if ^{129}I can absorb one neutron; it becomes ^{130}I, which has a half-life of only 12.36 hrs and decays to stable ^{130}Xe. Nuclear transmutation occurs naturally or can be induced by using photons or particles like electrons, protons or neutrons to interact with the nuclei. The neutron capture and the neutron-fission reactions are the most effective with respect to the treatment of the components of SNF. The neutrons can be produced in either a fission or fusion reaction or in a non-critical accelerator-driven system (ADS).

The Department of Energy (DOE), through various domestic and international collaborations, has been exploring the potential of advanced nuclear technologies

that can reduce the production of the hazardous components in spent nuclear fuel. In 2001, the United States and eight other countries established the Generation IV International Forum (GIF) to create a common, international nuclear research and development agenda for the future. The GIF has identified a number of candidate technologies and is developing partnerships within the participating countries for their development. These systems are described in the Generation IV (GenIV) technology Roadmap [Ref 1-4-Ref 1-5]. Beyond DOE's Advanced Accelerator Applications (AAA) and GenIV programs, the Advanced Fuel Cycle Initiative (AFCI) is designed to capitalize on the GenIV technology in reducing the volume and toxicity of the nuclear waste. The AFCI includes two major elements:

AFCI Series One addresses the intermediate-term issues associated with spent nuclear fuel, primarily by reducing the volume and heat generation of material requiring geologic disposition.

AFCI Series Two addresses the long-term issues associated with spent nuclear fuel. Specifically, this effort would explore fuel cycle technologies that could sharply reduce the long-term radiotoxicity and heat load of high-level waste sent to a geologic repository. Both Series One and Two assume the reprocessing of the SNF and recycling of the uranium and possibly other SNF components.

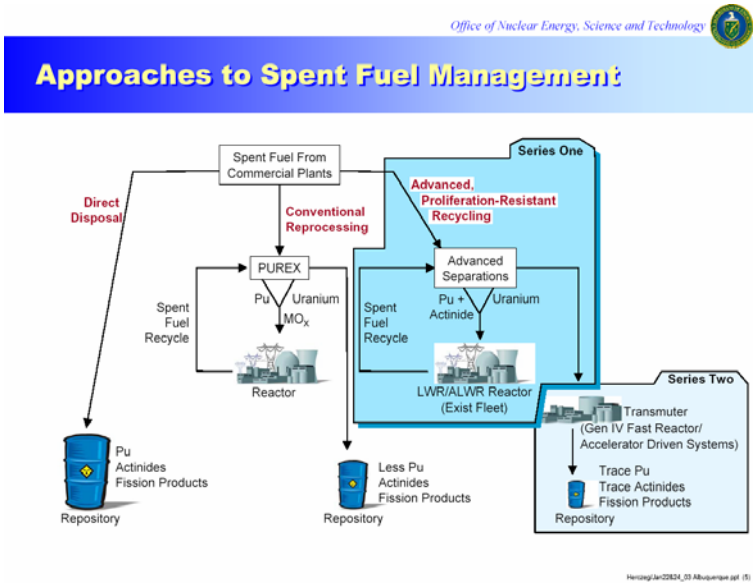

Figure 1-3: Approaches to spent fuel management

Figure 1-3 shows comparisons among direct disposal, conventional reprocessing and AFCI technologies, with respect to spent fuel management. Through separating and recycling the uranium and fissionable plutonium into new mixed oxide fuel, much less high-level waste remains for disposal in a geological repository. With the AFCI the waste volume would also be decreased though recycling some of the actinides and transmuting some of the other SNF components.

Within the research framework of the AFCI, some scenarios of waste transmutation have been proposed for further study [Ref 1-6-Ref 1-7]. Figure 1-4 [Ref 1-7] lists the examples as four different selected scenarios. All scenarios start with SNF from the Light Water Reactor Once Through (LWROT) cycle. In scenario one, SNF will be transmuted in a fast spectrum system (either accelerator-driven system or a Gen IV fast reactor system). In scenario two, SNF will be treated and burned in a low-recycle Mixed-Oxide (MOX) fueled light water reactor (LWR) before it is treated in the fast spectrum system. The difference between scenario three and

two is that a high-recycle MOX LWR fuel will be used in scenario three instead of the low-recycle MOX LWR fuel. In scenario four, a high temperature gas cooled reactor (HTGR) will be used to treat the SNF from the LWROT cycle.

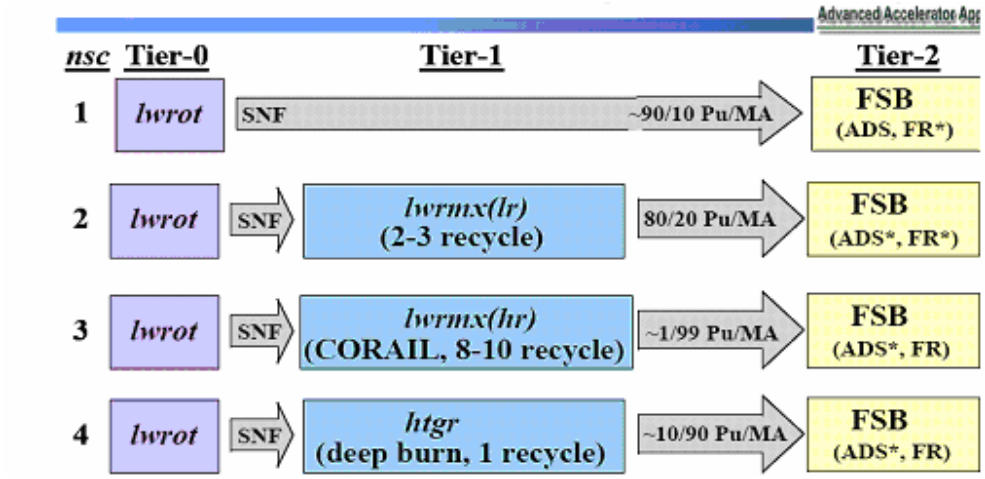

Figure 1-4: Collaborative distillation of possible advanced NFC scenarios adopted for temporal analyses

1.2 Fuel Cycle/Transmutation Strategy Modeling

To be resolved is how the above scenarios can be compared to find a better approach for advanced fuel cycle development and nuclear waste transmutation. Many researchers have contributed to modeling fuel cycle strategies [Ref 1-8 - Ref 1-13].

NFCSim [Ref 1-8] from Los Alamos National Lab (LANL) is an event-driven, fully time dependent simulation code modeling the flow of materials through the nuclear fuel cycle. The model generates life-cycle material balances for the demand required reactors and includes a process cost database. DYMOND/DANESS [Ref 1-9 - Ref 1-10] from Argonne National Lab (ANL) is developed to allow performing dynamic analysis of nuclear energy systems composed of multiple reactors and fuel

cycle options including cross-flow of fissile material between the different components of the system. The codes allow mass-flow analysis and economics analysis. Both DYMOND/DANESS and NFCSim have the ability to track the material flow in the fuel cycle and to do fuel cycle economics analyses. Both code development groups have included in their models, nonproliferation metrics and metrics showing the environmental impacts from the disposed waste. The Verifiable Fuel Cycle Simulation (VISION) model is currently under development at Idaho National Lab [Ref 1-13]. VISION is designed to serve as a system analysis and study tool for work conducted as part of the AFCI and GenIV reactor development studies. COSI [Ref 1-11, Ref 1-12] is a simulation software package developed by the Directorate of Nuclear Reactors at CEA, the French Atomic Energy Commission. It can also track the inventory of important nuclides during the whole fuel cycle for given scenarios with the capability to simulate various types of nuclear reactors.

These computer codes are typically provided with simplified system performance metrics such as fuel cycle cost, waste mass balance, and waste toxicity index. However, to effectively aid in fuel cycle development decision making, other fuel cycle performance measures such as repository capacity impact, radiation dose, and proliferation resistance need to be captured in fuel cycle systems modeling.

Details of model development to describe these fuel cycle system performance measures are described in this dissertation. Normally the metrics of disposed waste or non-proliferation are applied to the system separately from each other and from other analysis such as economics analysis. There is the desire to evaluate the fuel cycle comprehensively and integratedly. This research was carried out to develop a

methodology which has a set of indices to comprehensively characterize the fuel cycle and use those indices integratedly to compare different fuel cycles.

1.3 Purpose and Outline of Present Work

To compare different fuel cycle systems requires an understanding of various performance objectives of nuclear waste transmutation or fuel cycle systems and devising a series of metrics for their evaluation. As earlier mentioned, reduction of the amount of nuclear waste sent to a repository is one of the major objectives of an advanced fuel cycle. Other related goals could include cost reduction, minimizing human health impacts, enhanced system safety, and enhance the proliferation resistance of the fuel cycle against potential nuclear material diversion. Cost reduction could be the main driving force in the comparison as the economic consideration dominates the commercial market development in the U.S. with the inclusion of all risk factors.

The following performance objectives were included in this study:

- Repository performance
- Proliferation resistance
- Fuel cycle cost

Three models have been developed in this research. Repository performance model investigates the repository capacity by considering the temperature limits and the health risk from the disposed HLW. Fuzzy logic applied barrier method evaluates the relative proliferation resistance of nuclear fuel cycles quantitatively. And finally an integrated model compares the overall fuel cycle cost of nuclear fuel cycles by including the repository, proliferation and economic performances.

In Chapter 2, waste impact on the repository is addressed. Different methods have been investigated and compared. A new simplified performance assessment (PA) model to evaluate the repository benefits of different fuel cycle concepts was developed. In addition, for the purpose of expedient optimization studies, representing the system performance as a single performance index number is desirable. Accordingly, a single performance index number (a health-risk index) was developed which is based on the results of performance assessment that represent the residual human health risk for various fuel cycle strategies. By inputing nuclear waste information, this model calculates the maximum loading in Yucca Mountain according to the thermal design limits. Projected dose rate and health-risk index can also be obtained.

The proliferation resistance model is described in Chapter 3. A new method based on the application of fuzzy logic to Barriers Frame (BF), which was developed by the TOPS committee [Ref 1-14], was developed for quantitative assessment of proliferation resistance of nuclear reactor systems. This model considers a fully operational fuel cycle system, and yields a proliferation resistance evaluation for all facilities in the fuel cycle system based on measurable variables of the system. A fuzzy number can be generated which can be used to indicate the proliferation resistance of each fuel cycle system.

The fuel cycle model and integration model are discussed in Chapter 5. A simple fuel cycle cost model [Ref 1-15] was adopted for the study. A method to combine repository performance, proliferation resistance and fuel cycle cost, based on either

an adjusted fuel cycle cost or an adjusted total electricity generation cost was developed.

A case study is also included in Chapter 5. Three different fuel cycle systems are studied: pressurized water reactor once through (PWR-OT), pressurized water reactor with Mixed Oxide fuel (MOX) and Direct Use of spent PWR fuel in CANDU (DUPIC). The CANDU reactor is a pressurized-heavy water, natural-uranium power reactor designed in the 1960s by a partnership between Atomic Energy of Canada Limited and the Hydro-Electric Power Commission of Ontario as well as several private industry participants. These three systems were compared based on a number of different performance objectives included in the integration model. Uncertainty and sensitivity analyses were included in this investigation.

Chapter 6 includes discussions. Conclusions and recommendations are summarized in Chapter 7.

1.4 References

Ref 1-1 Greta Joy Dicus, “NATIONAL LOW LEVEL RADIOACTIVE WASTE DISPOSAL POLICY: A SUCCESS OR A FAILURE?”, U.S. Nuclear Regulatory Commision, April 14, 1998, <http://www.nrc.gov/reading-rm/doc-collections/commission/speeches/1998/s98-11.html>

Ref 1-2 Office of Environmental Management, U.S. Department of energy, November 6th 1997, <http://web.em.doe.gov/idb97/tab13.html>

Ref 1-3 Denis Beller, “RACE: The AFCI Reactor-Accelerator Coupling Experiments Program”, Seminar at NCSU, 2004

Ref 1-4 DOE, “Report to Congress on Advanced Fuel Cycle Initiative: the Future Path for Advanced Spent Fuel Treatment and Transmutation Research”, DOE, Jan. 2003

Ref 1-5 “A Technology Roadmap for Generation IV Nuclear Energy Systems: Technology Roadmap Report”, NERAC, Sept. 2003

Ref 1-6 C. G. Bathke, R. A. Kradowski, H. R. Trellue, A. M. Spearing, and C. M. Lovejoy, “Advanced Nuclear Fuel Cycle Systems Analyses for FY 2002”, LANL, LA-UR-02-6674, Oct. 2002

Ref 1-7 C. Bathke, W. Davidson, B. Krakowski, C. Lovejoy, S. Spearing, and H. Trellue, “Nuclear Fuel Cycle (NFC) Systems Studies Activities at Los Alamos”, LANL, AAA Third Quarterly Technical Review, July. 2002

Ref 1-8 Charles G. Bathke, Scott Demuth, Michael R. James and Erich A. Schneider, “NFCSim, A Dynamic Simulation Model of The Nuclear Economy”, Advances in Nuclear Fuel Management III, ANFM 2003

Ref 1-9 L. Van Den Durpel, A. Yacout, D. Wade, H. Khalil, “DANESS, Dynamic Analysis of Nuclear System Strategies”, Global 2003, p. 1613-1620, 2003

Ref 1-10 L. Van Den Durpel, A. Yacout, “DANESS v1.0.7 Users Manual”, Argonne National Laboratory, Feb. 2004

Ref 1-11 C. G. Bathke and E. A. Schneider, “Report of the COSI and NFCSim Benchmark”, LA-UR-03-8051, Sept. 2003

Ref 1-12 J.P.Grouiller et al, *COSI: a Code for Simulating a System of Nuclear Power Reactors and Fuel Cycle Plants*, in Proc. Fast Reactors ’91, Kyoto, Japan, 28 Oct.-1 Nov., 1991

Ref 1-13 “Software Requirements Specification Verifiable Fuel Cycle Simulation (VISION) Model”, AFCI Economic Benefits and Systems Analysis Team, Idaho National Engineering and Environmental Laboratory, Idaho Falls, Idaho, INEEL/EXT-05-02643, Rev. 0, 2005

Ref 1-14 NERAC TOPS Task Force, “Annex: Attributes of Proliferation Resistance for Civilian Nuclear Power Systems”, DOE, 2000

Ref 1-15 MIT, “The Future of Nuclear Power: an interdisciplinary MIT study”, MIT, July, 2003

2 Waste Disposal Impact

2.1 Introduction and Literature Reviews

Reduction/minimization of nuclear waste volume and its hazard is the major objective of waste transmutation. Following the work of DOE's Advanced Accelerator Applications (AAA) and GenIV, Advanced Fuel Cycle Initiative (AFCI) [Ref 2-1] program is designed to reduce the volume and toxicity of the nuclear waste.

Regardless of the specifics of a fuel cycle strategy, there is a need for permanent disposal of the residual nuclear waste. The risk from these residual materials needs to be properly assessed. Repository performance assessment [Ref 2-3] (hereafter called "PA" for simplification) is a tool for this assessment. Based on predictive modeling, PA projects the radiation dose from the radionuclides in the wastes when they are ultimately released and reach the environment accessible by future generations of humans. The PA models consider the behavior of the waste and the waste container in the repository environment; the fate and transport of radionuclides after their release to the environment; and the human exposure pathways and resultant dose. In this regard, the behavior of natural and engineered barriers to radionuclide migration is the key to the quantification of risk from waste disposal. Understanding which radionuclides contribute most to the health risk is also very important to effectively focus the effort of waste transmutation.

As PA represents a complex analysis covering various physical, chemical, biological, and human behavioral processes, it typically comes with a high

computational burden and significant uncertainty. Also the analysis is not transparent for permitting public understanding. For these reasons, PA has not been widely exercised in quantifying the safety benefits of nuclear waste transmutation.

There are several alternative methods which have been investigated to estimate the safety benefits of waste transmutation techniques. These include the study of the mass inventory change of key nuclides [Ref 2-2] and the assignment of a waste toxicity measure (or toxicity index) [Ref 2-2, Ref 2-4, Ref 2-5]. In fact, the waste toxicity index (TI) has commonly been used to demonstrate the benefit of advanced fuel cycles and waste transmutation [Ref 2-6, Ref 2-7]. The waste TI, typically refers to the volume of water (in m^3) in which wastes would have to be diluted to meet standards for radionuclide concentrations in drinking water. Waste TI methods offer advantages over PA due to computational simplicity, low input data requirements, and transparency for presentation [Ref 2-8]. However, the methods do not take into account the influence of engineered and natural barriers employed in nuclear waste disposal. Appropriateness of these methods is investigated in Section 2.2.

Agencies such as DOE, NRC, and Electric Power Research Institute (EPRI) have made various efforts to evaluate the environmental impact from the repository disposal of nuclear waste. Various computer models have been developed out of these efforts. The work of DOE is mainly based on the model developed by Godler Associates Inc. named Repository Integration Program (RIP) [Ref 2-15 - Ref 2-20]. RIP has been one of the major tools of PA for DOE. RIP is a fully integrated probability-based PA tool that investigates the possible release of radionuclides to

the accessible environment. RIP utilizes a “top down” approach to PA that concentrates on the integration of all system components. Less detailed process models are utilized, with both model and parameter uncertainties included. RIP uses a simulation approach utilizing the Monte Carlo method to sample the probability distributions of uncertain parameters for each realization. A large number of system realizations are performed in order to determine probability distributions of repository performance such as rate and magnitude of radionuclide release. For DOE’s 1999 Total System Performance Assessment – Viability Assessment (TSPA-VA), RIP was used to link all the various component computer models. Iterative Performance Assessment (IPA) is NRC’s computer model for PA and is a major component of the NRC’s program in high-level waste [Ref 2-12, Ref 2-21, Ref 2-22]. A primary objective of IPA is to provide the NRC staff with a working knowledge of modeling approaches and techniques used to estimate repository performance, so that the staff will be able to comment on the adequacy of DOE’s License Application and pre-licensing performance assessment analyses. The Total System Performance Assessment (TPA) computer code is a major part of IPA and is used to estimate overall system performance as a function of the specific characteristics of the proposed repository site and design. The TPA code includes the repository system description, conceptual models, and parameter values with enough details to provide meaningful insights on respository performance. The model includes infiltration and deep percolation, near-field environment, radionuclide releases from engineered barrier systems, aqueous-phase radionuclide transport through the

unsaturated and saturated zone, airborne transport from direct radionuclide releases, and exposure scenarios and reference biosphere.

For independent technical reviews for Yucca Mountain from DOE and NRC, EPRI has developed their own total system performance assessment model labeled “IMARC” (Integrated Multiple Assumptions and Release Code) [Ref 2-23 - Ref 2-27]. IMARC has evolved with the developments of Yucca Mountain repository design and the supporting scientific knowledge since 1990. IMARC calculates dose vs. time using a logic tree format in which specific critical conceptual models or input parameters are identified and treated as uncertain. The program organizes the uncertainties into a “logic tree” and calculates all possible combinations of these models or parameters (and their weights), and for each combination estimates radionuclide concentration and dose vs. time. The SUMO (System Unsaturated Model) code [Ref 2-28] is an integrated system model and computer code to address the cumulative radionuclide release criteria (i.e., CCDF (complementary cumulative distribution functions)) established by the U.S. Environmental Protection Agency (EPA) and to estimate population risks in terms of dose to humans. SUMO is an outgrowth of the preliminary Yucca Mountain risk assessment analysis that was completed by the Performance Assessment Scientific Support Program at Pacific Northwest Laboratory (PNL) in 1988. Sandia National Lab (SNL) did its performance assessment based on DOE’s request in1991 [Ref 2-29 - Ref 2-38]. SNL’s performance-assessment work was primarily based on prior HYDROCOIN [Ref 2-30], COVE-2A [Ref 2-31], and PACE-90 [Ref 2-32] work and expressed the measure of total system performance as CCDFs of radionuclide cumulative

releases. In terms of analytical solution approaches to PA, the research performed by Professor T.H. Pigford and his associates needs to be noticed. Although limited by the assumptions made to allow analytical solutions, the method provided very useful insights into PA [Ref 2-39 - Ref 2-46].

Other countries, such as the United Kingdom, Switzerland and Japan, also have developed performance assessment methodologies for the repository in their countries [Ref 2-54 - Ref 2-56]. For example, Kristallin-I [Ref 2-54, Ref 2-55] is an integrated analysis model from Nagra (the National Co-operative for the Storage of Nuclear Waste) in Switzerland to investigate the option of disposal of vitrified high-level waste in the subsurface crystalline structure of Northern Switzerland. H3 [Ref 2-56] is post-closure performance assessment model for the conceptual or proposed granite repository in Japan.

Wide implementation of PA in fuel cycle studies requires the computational burden of PA to be reduced. Another important consideration in assessing repository waste impact for a fuel cycle is the corresponding required repository capacity. The capacity of a HLW repository, i.e., Yucca Mountain, is mainly dictated by thermal design limits which establish the maximize temperature that can exist at the surface of the disposal container, at the drift wall and at the centerline between drifts. This requires the use of a thermal analysis model. The thermal analysis model describes temperature changes in the rock around the waste packages as a function of the HLW/spent fuel composition. Modeling repository thermal impact has been pursued by various researchers. Both analytical and numerical solutions have been developed. Examples of analytical solution approaches in modeling repository

thermal behavior include the works of Estrada-Gasca [Ref 2-48], Malbrain [Ref 2-53], and The Swedish SKB (Svensk Kärnbränslehantering AB) [Ref 2-47]. The Swedish SKB has developed a general purpose analytical model for a geologic repository based on the heat conduction model described by Carlslaw and Jaeger [Ref 2-47]. In C.A. Estrada-Gasca's dissertation [Ref 2-48], analytical methods were described to predict the far-field thermal impact of a nuclear waste repository. One-dimensional linear and non-linear models were studied and analytical solutions or finite element solutions are presented. The finite method solution is also given for two-dimensional, linear and non linear models. Temperature distributions and temperature histories are given as results. Carl Malbrain and Richard K. Lester [Ref 2-53] developed a semi-analytical model to investigate the optimal design for a repository based on thermal constraints. In their work, semi-analytical models for predicting the time-dependent temperature distribution in the region of a high-level waste repository was developed. Three models were developed for thermal behavior in the far-field region, the near-field region and within the waste package itself respectively. The repository itself is modeled as an infinite plane source at a depth corresponding to the mid-plane of the waste canisters, with a thermal strength equal to the average areal loading of the repository. For the near-field region, the host rock is assumed to be infinite, homogeneous, and an isotropic conducting medium with temperature-independent physical properties. The canisters are represented by finite-length line sources. A simple one-dimensional, quasi steady-state model is used to predict the temperature distribution within the waste package. The model has been applied to a determination of the maximum permissible

repository mass loading and canister loading for spent PWR fuel and reprocessed PWR high-level waste in salt and granite media, subject to several independent thermal constraints. It is found that the repository loading and the canister loading are controlled by the bentonite backfill temperature constraint (<100 °C) [Ref 2-49].

In W.M. Kays, F. Hossaini-Hashemi and J.S. Busch's work [Ref 2-50], an approximate semi-analytical model has been developed. Each individual canister is treated as finite-length line source in a continuous medium. The combined effect of multiple canisters is established in the medium at selected point of interest by superposition of the temperature rises calculated for each canister. Lawrence Livermore National Lab also developed a model for the thermal performance of a repository [Ref 2-51, Ref 2-52]. The V-TOUGH code [Ref 2-52] is used to investigate impacts of different repository areal power densities (APDs) to the flow along preferential fracture pathways in the unsaturated zone at Yucca Mountain. This study indicates that thermal and hydrological performance of the unsaturated zone will be dominated by conduction of heat generated by the repository. The performance of a system dominated by heat conduction is most sensitive to the thermal properties of the system and the thermal loading conditions.

2.2 Case Study to Examine TI Methods

In this section, toxicity index methods (including Hazard Index [Ref 2-6], Number of ALI (Annual Limit on Intake) [Ref 2-59], Integrated Radiological Toxic Potential [Ref 2-8], and Integrated Toxic Potential [Ref 2-60]) were evaluated along with mass inventory method by assuming performance assessment result from TPA as base. For a comprehensive PA, the TPA code [Ref 2-12] was used.

2.2.1 Scenario Assumption

Under a transmutation scenario, spent fuel would be processed for the removal of uranium and the separation of long-lived actinides, such as plutonium, neptunium, americium, and curium. Uranium would be recycled or disposed of as low-level radioactive waste. The separated long-lived actinides would be manufactured into transmutation assemblies which become the fuel in a transmutation device. It was assumed for this study that the spent nuclear fuel was first processed using an aqueous uranium extraction that is assumed to recover 99.995% of the irradiated uranium [Ref 2-9]; then all residual materials were further processed at a pyrochemical facility. The pyrochemical process was assumed to recover 99.9% of the actinides (including remained uranium), remove 95% of the rare earth fission products, and remove 100% of all other fission products. The composition of the transmutation fuel assembly used in this study is shown in Table 2-1. In-reactor neutron irradiation with a thermal or fast neutron spectrum was chosen as the methods of transmutation. Finally, it was assumed that the byproducts/waste would be disposed of at a HLW repository (i.e., Yucca Mountain), after these fuel assemblies had been subjected to neutron bombardment.

Performance of waste transmutation was compared for four different options: (a) burning in a thermal reactor for 100 days (this is referred to as “T100” hereafter), (b) burning in a thermal reactor for 200 days (referred to as “T200”), (c) burning in a fast reactor for 100 days (referred to as “F100”), and (d) burning in a fast reactor for 200 days (referred to as “F200”). Waste composition is assumed and summarized in Table 2-1. The performance benefit of waste transmutation was calculated by

comparing the potential health risk from the disposal of byproducts of each transmutation method with respect to that from the “no transmutation – natural decay only” case.

Table 2-1 Composition of the representative fuel for transmutation

Nuclide	Composition by mass	Nuclide	Composition by mass	Nuclide	Composition by mass
U235	0.004%	Pu240	21.231%	Cm243	0.002%
U236	0.002%	Pu241	3.870%	Cm244	0.116%
U238	0.423%	Pu242	4.677%	Cm245	0.013%
Np237	4.313%	Am241	9.184%	Cm246	0.001%
Pu238	1.236%	Am241M	0.007%		
Pu239	53.901%	Am243	1.021%		

ORIGEN2 [Ref 2-10] was used to simulate the changes in the isotopic inventory of the fuel (due to depletion, decay and generation of radionuclides) from neutron irradiation. ORIGEN2 is a point-depletion and radioactivity-decay computer code that simulates the changes in nuclide composition and characteristics of materials. The methods employed in the study to assess the safety benefits of transmutation are described in the following sections.

2.2.2 Environmental Impacts Metrics Comparison

2.2.2.1 Mass Inventory Changes of Key Nuclides

Examining mass inventory changes of key nuclides provides a simple picture of waste transmutation performance. Results of fuel composition change due to transmutation by the assumed methods are shown in Figure 2-1. The nuclides listed represent the top six dose contributors in the Department of Energy’s Total System Performance Assessment [Ref 2-11]. These six nuclides, however, may not represent the most important ones in PA in general.

As shown, the amount of ^{237}Np, ^{234}U and ^{239}Pu decreased after irradiation in both a thermal and in the fast reactor system. ^{242}Pu decreased following irradiation in a fast reactor but increased as a result of the irradiation in the thermal reactor. At the same time, the amount of fission products began to build-up during the transmutation process. The inventory change was mainly affected by the fission cross sections of the respective nuclides and the neutron flux levels in each system.

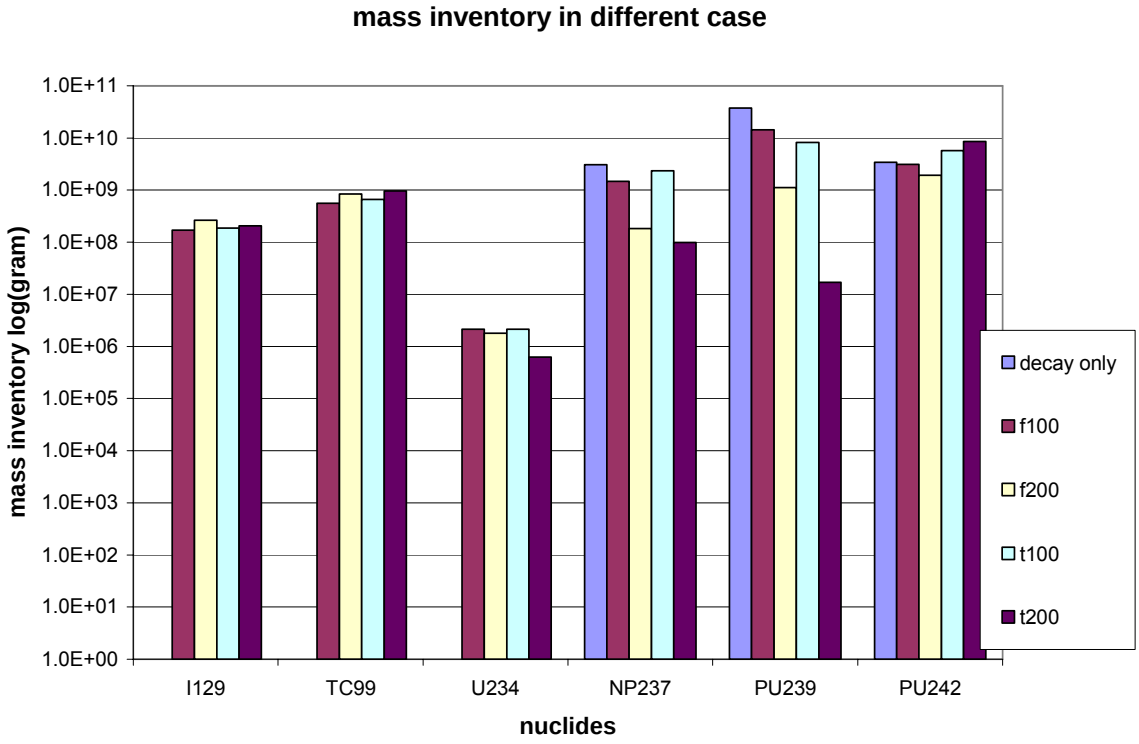

Figure 2-1 Predicted changes in the inventory of key radionuclides after transmutation

It is commonly argued that the harder, high-energy neutrons improve actinide burning because the fission cross section of the actinides is typically larger in a fast system. But this is not always the case. Reduction of ^{239}Pu activity was larger with the thermal system as the fission cross section of ^{239}Pu is about a factor of four higher in a thermal spectrum than in a fast spectrum. The largest reduction of ^{237}Np

activity was observed with the T200 method. These observations indicated that it is difficult to see which method performed better overall based on the inventory changes. As the mass inventory does not directly translate into health risk, the comparison is useful only for qualitative screening and points to the need for the development of a better comparison metric.

2.2.2.2 Performance Assessment to Represent the Health Risk

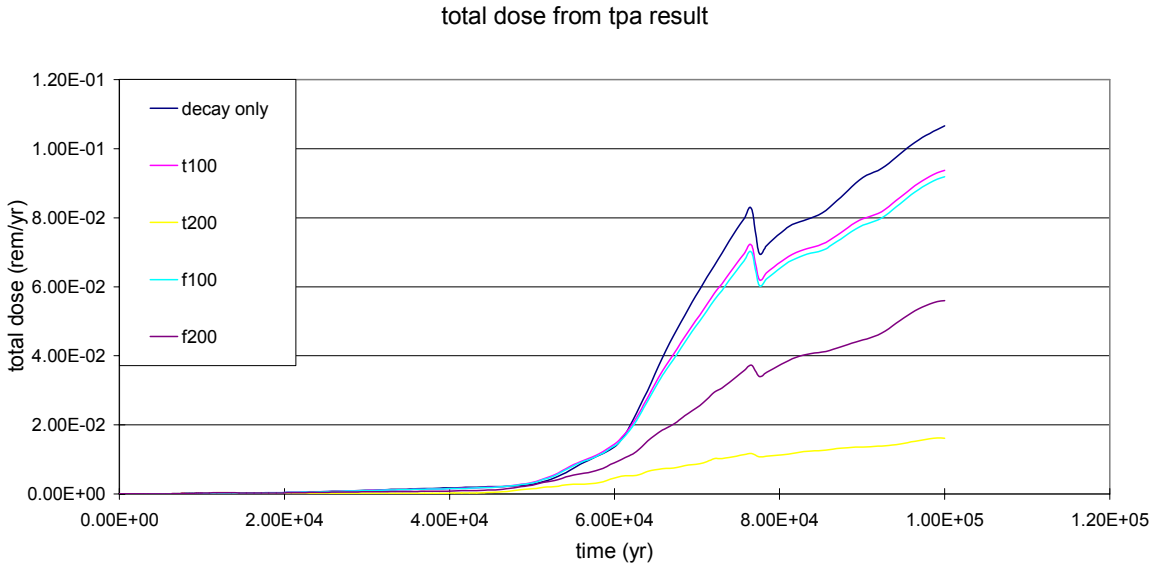

Figure 2-2 Comparisons of transmutation methods and benefits using performance assessment

Calculations using the TPA code were made using the built-in default parameter values that represent the conditions at the Yucca Mountain repository. Results are shown in Figure 2-2. The curves represent the mean values of projected human dose rate (based on 300 histories) at each simulation time step up to 100,000 years from the closure of the repository. The results show that all four methods of transmutation provide some performance benefits in comparison to the case without transmutation. The largest reduction in dose was calculated for the T200 method

(86% dose reduction), followed by F200 (58% dose reduction), F100 (21% dose reduction), and T100 (19% dose reduction). Radionuclides that contributed most to the peak dose at the end of the simulation period (100,000 years) were ^{237}Np, ^{129}I, ^{99}Tc, ^{234}U, and ^{230}Th as shown in Table 2-2.

Table 2-2 Results of TPA analysis as comparison of different transmutation methods

	Initial		F100		F200		T100		T200	
average dose	1.00E-01 (rem/yr) at 100,000 yrs		7.91E-02 (rem/yr) at 100,000 yrs		4.21E-02 (rem/yr) at 100,000 yrs		8.12E-02 (rem/yr) at 100,000 yrs		1.37E-02 (rem/yr) at 100,000 yrs	
ratio (to initial)	100%		78.78%		41.98%		80.87%		13.69%	
peak dose for the top nuclides	nuclide	value	nuclide	value	nuclide	value	nuclide	value	nuclide	value
	Np237	1.34E-01	NP237	1.03E-01	NP237	5.75E-02	NP237	1.06E-01	NP237	1.52E-02
	U234	1.84E-03	I-129	8.72E-03	I-129	1.34E-02	I-129	9.52E-03	I-129	1.05E-02
	Th230	1.53E-04	U-234	5.34E-03	Tc-99	7.77E-03	Tc-99	6.22E-03	Tc-99	8.94E-03
	Pb210	6.52E-05	Tc-99	5.05E-03	U-234	2.58E-03	U-234	4.79E-03	U-234	1.77E-04
	Ra226	2.65E-05	Th-230	3.24E-04	Th-230	1.38E-04	Th-230	2.82E-04	Se-79	2.50E-05
	U238	3.50E-07	Pb210	1.77E-04	Pb210	8.27E-05	Pb210	1.58E-04	Th-230	8.59E-06
	Pu239	9.57E-08	Ra226	7.09E-05	Ra226	3.32E-05	Ra226	6.35E-05	Pb210	5.46E-06
	Pu240	5.51E-10	SE 79	1.52E-05	SE 79	3.03E-05	SE 79	1.67E-05	Ra226	2.17E-06
	Cm245	1.10E-16	Pu239	9.18E-08	Pu239	8.72E-08	Pu239	8.30E-08	Pu239	9.89E-08
	Cm246	2.64E-18	Pu240	1.14E-09	U-238	2.65E-08	Pu240	2.39E-09	U-238	6.56E-08

2.2.2.3 Hazard Index (HI)

The HI for water ingestion is the volume of water (m^3) in which wastes would have to be diluted to meet standards for radionuclide concentrations in drinking water. The HI is defined as,

$$HI_w = \sum(\lambda_i N_i / C_{iw}) = \sum(A_i / C_{iw})$$

where, λ_i is the decay constant for i^{th} element (s^{-1}); N_i is the number of atoms for i^{th} element; A_i is the activity of i^{th} element (Bq); C_{iw} is the maximum permissible concentration of i^{th} element in water (Bq/m^3). In the past, a large reduction in HI with waste transmutation based on the HI calculation, provided justifications for the development of research in waste transmutation [Ref 2-6].

Based on the use of HI, the performance of the four methods was compared (Figure 2-3). As shown, the HI result without transmutation was the lowest between 3,000 and 10,000 years among all the options indicating no benefit of transmutation. This does not agree with the results observed from PA (Figure 2-2). Among the four burning options, the T200 method was the best although the performance difference between T200 and F200 was very small. Ranking of the methods based on the HI (T200>F200>T100~F100) was similar to what was observed with PA (Figure 2-2 and Table 2-2). The top nuclides dose contributors from the HI results are the actinides ^{239}Pu, ^{231}Pa, ^{227}Th, ^{227}Ac, ^{242}Pu, and ^{237}Np. The list is markedly different from the one identified from PA in Table 2-2. This is not surprising as toxicity index does not consider the performance of waste package and repository.

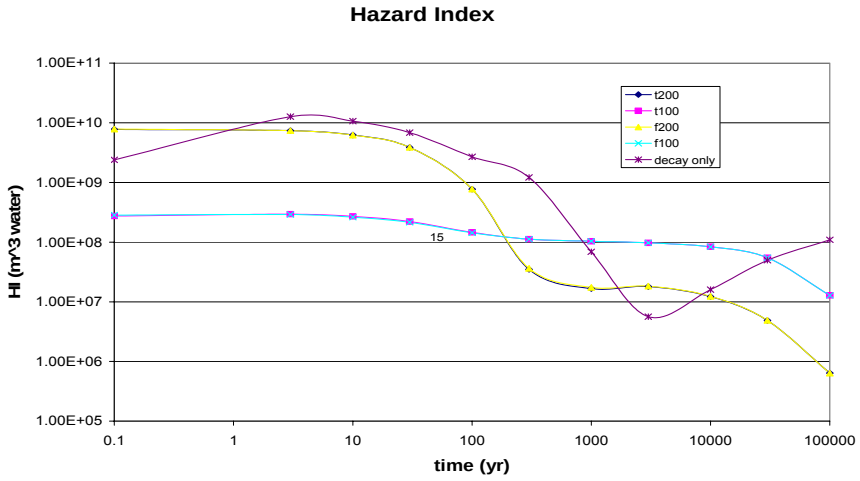

Figure 2-3 Comparisons of transmutation methods and benefits using the HI method

2.2.2.4 Number of ALI (Annual Limit on Intake) in the waste

The number of ALI contained in the waste material can be calculated as,

$$\#\ \text{of ALI} = \sum(A_i / ALI_i) \quad (\text{yr})$$

where, A_i is the activity of i^{th} element at time t (Bq) and; ALI_i is the annual limit on intake for nuclide i (Bq per year) [Ref 2-59]. Results (Figure 2-4) based on this method were similar to what was observed with the HI method, including the top nuclide list.

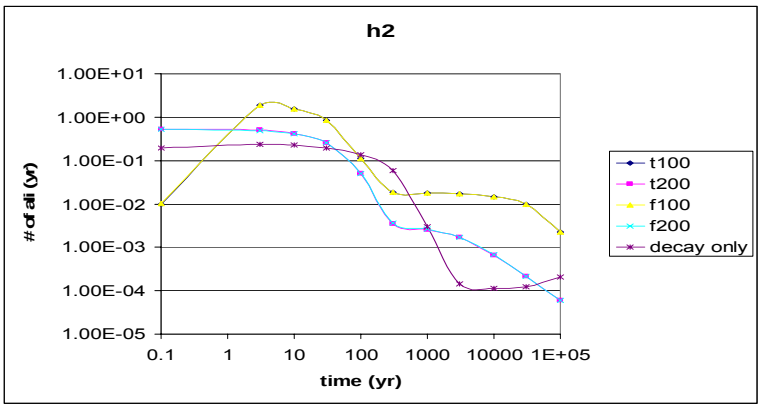

Figure 2-4 Comparisons of transmutation methods and benefits using the number of ALI method

2.2.2.5 Integrated Radiological Toxic Potential

The so-called "integrated radiological toxic potential" (IRTP) is the time integral of the volume of water required to dilute a unit volume (1 m^3) of waste to a level at which it could be drunk by an individual member of the public without exceeding a current dose limit. The IRTP is an approach proposed in a report by the European Commission [Ref 2-8] and expresses toxic potential of nuclear wastes based on the HI concept but can take account of the time delays in groundwater transport. The IRTP is calculated as,

$$IRTP = \sum_i C.\, A_i.\, DPUI_i\, .\, \exp(-\lambda_i t_{gw})/\ \lambda_i \ \ (m^3.y)$$

where, C is a numerical factor (identical for all radionuclides) derived from the annual individual intake of drinking water and the dose limit (m^3Sv^{-1}); A_i is the activity of the radionuclide i at time t (Bq); $DPUI_i$ is the dose per unit intake of the radionuclide i by ingestion (Sv/Bq); λ_i is the decay constant (1/y), and; t_{gw} is the groundwater travel time (y).

The comparison of the transmutation methods based on IRTP is shown in Figure 2-5. Ranking of the transmutation methods (T200>F200>T100~F100) was similar to that from the HI method. The top nuclide list (^{237}Np, ^{242}Pu, ^{231}Pa, ^{239}Pu, ^{234}U, ^{230}Th) was again similar to that from the HI approach, thus was very different from the list from PA. The benefit of transmutation was not shown by the method.

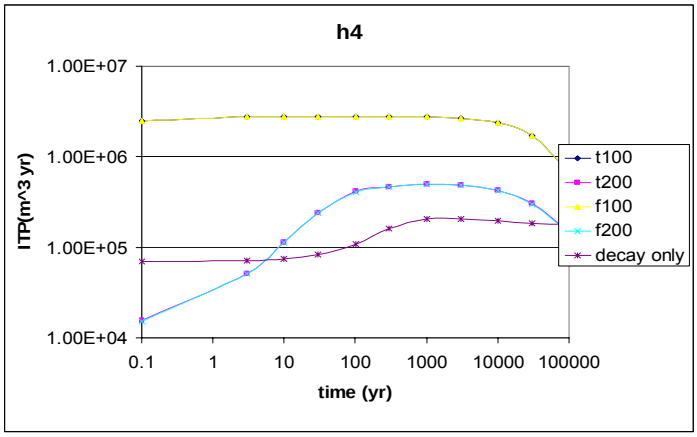

Figure 2-5 Comparison of transmutation methods and benefits using IRTP

2.2.2.6 Integrated Toxic Potential

A slightly different measure of integrated toxic potential (ITP) has recently been proposed [Ref 2-60]. It is based on International Council on Radiation Protection (ICRP) recommendations for radionuclide-specific ALI values for ingestion exposure,

the average annual water intake of ICRP reference man, the effective dose coefficient of each radionuclide, and the specific activity of each radionuclide considered. ITP is calculated by using:

$$\mathrm{ITP} = \sum_i ITP_i m_i = \sum_i \frac{AWI \times \alpha_i}{ALI_i} m_i = \sum_i \frac{AWI \times A_i}{ALI_i},$$

$$\text{Revised HI} = \int_0^T ITP\,dt \quad (\mathrm{m^3 yr})$$

where, AWI is the average annual water intake of ICRP reference man (0.712 m^3); α_i is the activity for a unit mass of each radionuclide i.; m_i is mass of i^{th} element at time t; A_i = Activity of i^{th} element at time t (Bq); ALI_i = Annual limit on intake for nuclide i (Bq per year), and; T is the time period of interest (year).

Comparison of the transmutation methods based on the ITP approach is shown in Figure 2-6. Ranking of the transmutation methods (T200>F200>T100~F100) was the same with other methods. The top nuclide list (^{237}Np, ^{231}Pa, 239Pu, ^{242}Pu, ^{230}Th, ^{234}U) was similar to that from the HI or IRTP approach, thus was very different from the TPA results. The benefit of transmutation was not shown by the method.

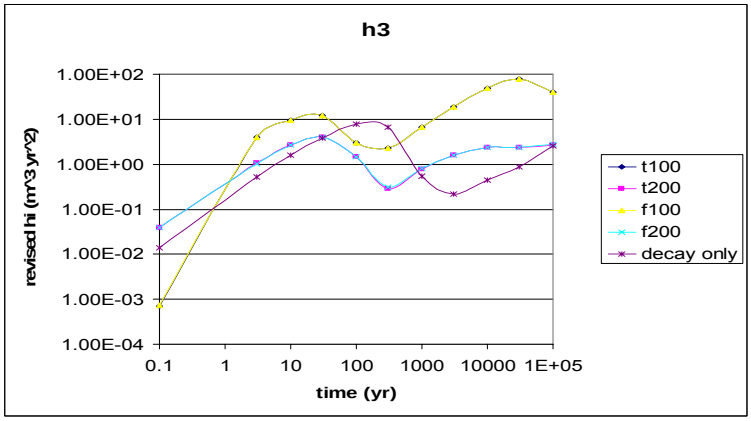

Figure 2-6 Comparisons of transmutation methods and benefits using the ITP

2.2.3 Summary Observation from the Evaluation of Existing Methods

As shown, these Toxicity Index methods did not show consistent results with PA result for the performance benefits of waste transmutation. And mass inventory or toxicity index does not take into account the performance of waste package and repository. If the waste packages were constructed to maintain their integrity over the life of the repository, then the radiotoxicity of the waste would not be an issue.

2.3 A New Simplified PA Model

In this study, a new simplified PA model was developed which consisted of four main parts: source term model, unsaturated zone transport model, saturated zone transport model, and dose analysis model. Monte Carlo uncertainty analysis capability was also provided to the computer model. Water infiltration into the waste region was assumed to be at steady state.

2.3.1 Source term model

Source term model is adopted from sub-model in TPA code [Ref 2-57, Ref 2-58]. It includes models to represent processes (i.e. thermal, chemical environment, humid-air and aqueous corrosion) that govern the failure of waste packages and the release of radionuclides from the engineered barrier system. The conduction-only thermal model predicts the temperature distribution and relative humidity (RH) as a function of time and position within the EBS. The near-field environment model provides chemical environment as a function of time in the immediate neighborhood of the waste package. Chemical parameters of the groundwater including solution pH, oxygen fugacity, chloride and bicarbonate concentration, and dissolved silica are

taken into account. To simulate the corrosion of waste package, dry-air oxidation model, humid-air and aqueous model are used at different RH. The Conceptualization of engineered barrier system (EBS) is shown in Figure 2-7 [Ref 2-57]. Water enters EBS and contacts with waste package and causes waste package to fail. Radionuclide releases from the waste package and dissolves in the water and enters the near field with water. Two processes are modeled: waste package degradation and radionuclide release from the EBS and represented as two modules: EBSFAIL (originally as part of EBSPAC code) [Ref 2-57] and EBSREL (derived from EBSPAC code) [Ref 2-58].

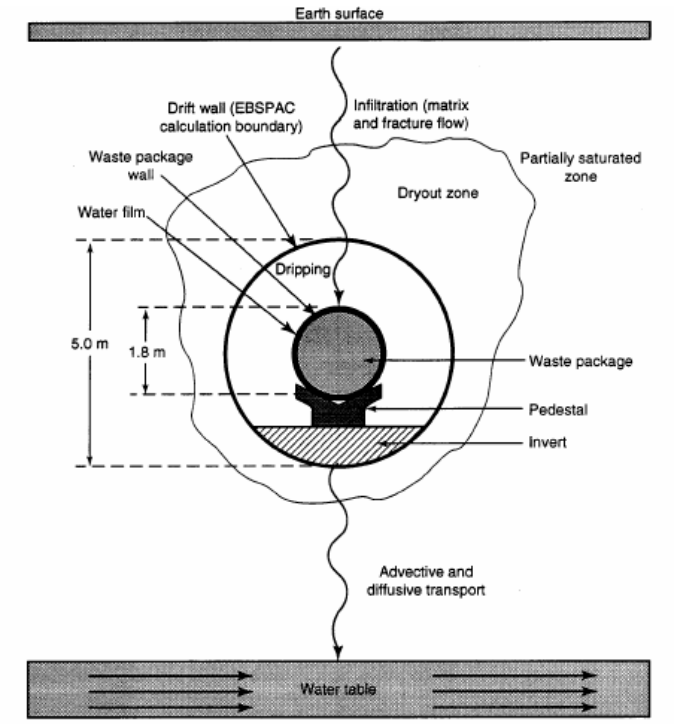

Figure 2-7 Conceptualization of the radionuclide release from waste packages emplaced in a horizontal drift

EBSFAIL simulates the corrosion and mechanical failures of waste packages. Figure 2-12 [Ref 2-57] shows the flow of EBSFAIL to evaluate the WP failure. Its

thermal model provides the temperature distribution and relative humidity (RH) as a function of time and position within the EBS. Its environment model provides chemical environment as a function of time in the immediate neighborhood of the waste package. Chemical parameters of the groundwater including solution pH, oxygen fugacity, chloride and bicarbonate concentration, and dissolved silica are taken into account. Dry-air oxidation model, humid-air and aqueous model are used at different RH to simulate the corrosion of waste package. Results from EBSFAIL become part of inputs for EBSREL module.

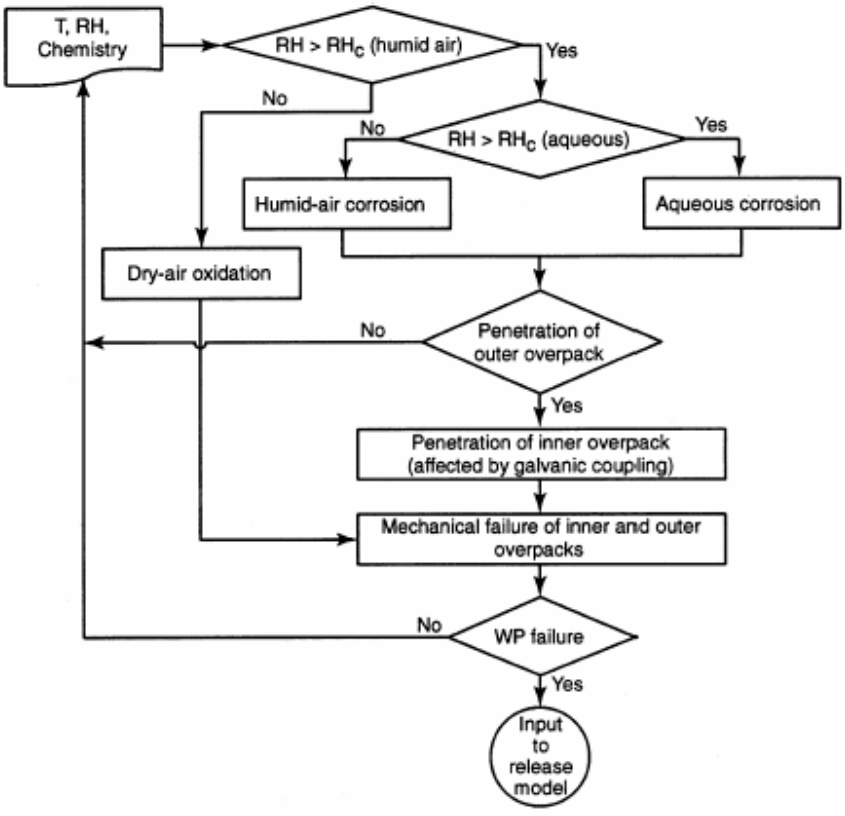

Figure 2-8 Flow diagram models in EBSFAIL to evaluate the WP failures

WP failure information from EBSFAIL and near-field chemistry, temperature, and liquid flow rate information from NFENV are inputs for EBSREL. NFENV [Ref 2-12]

module calculates temperature, groundwater reflux and groundwater chemistry. EBSREL computes the release of radionuclides from a WP. Only advective release from the WP is considered because its dominance. There are two models for aqueous release of nuclides: the bathtub model and the flow-through model. The difference is two holes are assumed as inlet and outlet for water in the bathtub model and water will not flow out until its level reaches the outflow position (defined by inputs), but in the flow-through model, the flow-out is assumed to be immediately equal to the flow in.

When the water enters the WP after its failure, the overall mass balance model for the nuclide inventory in the water in a failed WP is [Ref 2-12]:

$$\frac{dm_i}{dt} = w_{li}(t) - w_{ci}(t) - m_i\lambda_i + m_{i-1}\lambda_{i-1}$$

where: m_i amount of ith radionuclide in the WP water at time t [mol]

$w_{li}(t)$ rate of transfer from the SF into the WP water through leaching of SF [mol/yr] (function of flow rate of water, composition of the water and the element solubility in the water)

λ_i decay constant of ith radionuclide [1/yr]

m_{i-1} amount of i-1th radionuclide in the WP water at time t [mol]

λ_{i-1} decay constant of i-1th radionuclide [1/yr]

$w_{ci}(t)$ rate of advective transfer out of the WP [mol/yr]

$w_{ci}(t) = C_i(t)\ q_{out}(t)$

where: $C_i(t)$ concentration of i[th] radionuclide in the WP water [mol/m^3]

(mass m_i divided by volume of water in the WP)

$q_{out}(t)$ water leaving the WP at time t [m^3/yr] (in flow-through model, the flow out of a WP is equal to the flow in all times.)

The failure time of the waste package and the release rate from the engineered barrier system to the unsaturated zone of each nuclide $q_c(t)$ [Ci/yr] are outputted from this model and used as input for unsaturated zone model.

2.3.2 Unsaturated Zone Model

The unsaturated zone is assumed to be a homogeneous, isotropic, porous media with constant, unidirectional flow in the vertical (downward) direction. The contaminant transit time in the unsaturated zone is:

$$T_a = \frac{X_u}{U_u} R_{du} \qquad \text{[yr]}$$

X_u = the distance from the base of the source volume to the top of the aquifer [m]

U_u = the unsaturated pore velocity [m/yr]

$$U_u = \frac{P}{\theta_u}$$

P = the net water percolation rate [m/yr]

θ_u = effective porosity in the unsaturated zone

R_{du} = the retardation factor in the unsaturated zone

Release rate from unsaturated zone to saturated zone:

$$q_a(t) = e^{-\lambda_d T_a} \; q_c(t) \qquad \text{[Ci/yr]}$$

2.3.3 Saturated Zone Transport Model

The transport in the saturated zone was modeled based on a 2D analytic solution [Ref 2-61] to the advection dispersion equation. The advection-dispersion mass balance equation that describes contaminant transport is:

$$\frac{\partial C}{\partial t} + U\frac{\partial C}{\partial x} = D_x\frac{\partial^2 C}{\partial x^2} + D_y\frac{\partial^2 C}{\partial y^2} + D_z\frac{\partial^2 C}{\partial z^2} - \lambda C$$

In the case of instantaneous release of mass, q [Ci], at t=0 at the surface of the source area and initial concentration of zero everywhere in the domain, the solution to this equation becomes:

$$C(x,y,t) = \frac{q}{\eta R_d}\frac{1}{dilutionvolume}\left(erf\left(\frac{x+\frac{L}{2}-\frac{Ut}{Rd}}{\sqrt{\frac{4D_x t}{R_d}}}\right)+erf\left(\frac{x-\frac{L}{2}-\frac{Ut}{Rd}}{\sqrt{\frac{4D_x t}{R_d}}}\right)\right)\times$$

$$\left(erf\left(\frac{\frac{W}{2}+y}{\sqrt{\frac{4D_y t}{R_d}}}\right)+erf\left(\frac{\frac{W}{2}-y}{\sqrt{\frac{4D_y t}{R_d}}}\right)\right)\times e^{-\lambda_d t}\ \text{[Ci/m^3]}$$

where: $dilutionvolume$ = the water pumping out from the well every year [m^3]

erf = the error function

Dx = α_L U dispersion coefficient at x direction [m^2/yr]

Dy = α_T U dispersion coefficient at y direction [m^2/yr]

α_L = the longitudinal dispersivity [m]

α_T = the transverse dispersivity [m]

U = groundwater velocity [m/yr]

For an arbitrary release:

$$C_{longterm}(x,y,t) = \int_0^t C(x,y,t-\tau)q(\tau)d\tau$$

2.3.4 Human Exposure/Dose Model

Human exposure to radionuclides was modeled by considering the consumption of the drinking of contaminated groundwater from a well at 20 km down gradient from the repository. In EPRI's 1996 report [Ref 2-27] table 8-2, top three exposure pathways contributing to peak total dose for different nuclides are listed. For ^{237}Np, drinking water pathway contributes 21.1%, for ^{129}I, this number is 15.3%, ^{99}Tc 5.4%, and ^{238}U 11.6%. Considering the importance of ^{237}Np to total dose, it is assumed that the dose from drinking water is 20% of total dose from all pathways in this study. The drinking water dose can be calculated as follows:

$$\text{Dose}_{DW} = \text{Usage} \times \sum_i Ci \times Dcfi \times \exp(-\lambda i \times Tp) / 1000 \text{ [rem/yr]}$$

Usage = a usage factor that specifies the exposure time or intake rate for an individual of age group associated with pathway [m^3/yr]

Ci = the concentration of nuclide i in groundwater [pCi/m^3]

Dcfi = the dose factor of radionuclide i [mrem/pCi]

λi = the decay constant [1/yr]

Tp = the average transit time required for nuclides to reach the point of exposure [yr]

2.3.5 Health Risk Index Model

Development of a performance index to represent human health risk from waste disposal from a given fuel cycle strategy was performed in two steps. First, the human dose from the disposal of residual nuclear materials was projected by using a simplified PA model which was developed in the study. Secondly, the results obtained from the PA as a time-dependent dose history were converted to a cumulative health risk by integrating the projected dose curve and performing a dose-to-risk conversion.

The BEIR V relative risk models were used to estimate the cancer risk from the radiation exposure due to the repository waste [Ref 2-35]. The Relative (Multiplicative) Risk Model [Ref 2-34] is:

$$\varepsilon(D, a_0, a, s) = \varepsilon_0(a, s) \times R(D, a_0, a, s)$$

where: $\varepsilon_0(a, s)$ is the natural incidence or mortality in year a, which is given in table.

$R(D, a_0, a, s)$ is the relative risk

a_0 is the starting year of exposure

a is the ending year of exposure

s is sex

D is total dose received from year a0 to a in Gy

The relative risk may be expressed in this form:

$$R(D, a_0, a, s) = \alpha(a_0, a, s)D + \beta(a_0, a, s)D^2$$

The BEIR-V committee has developed relative mortality risks in terms of the year t after exposure for different cancer types including leukemia, respiratory cancer,

breast cancer (female only), digestive cancer and all other cancers [Ref 2-34, Ref 2-35].

For leukemia:

$$R(D, a_0, t) = (0.243D+0.271D^2)\, e^{\gamma(a_0, t)}$$

γ =4.885, $t \le 15,\ a_0 \le 20$

γ =2.380, $15 < t \le 25,\ a_0 \le 20$

γ =2.367, $t \le 25,\ a_0 > 20$

γ =1.638, $25 < t \le 30,\ a_0 > 20$

For respiratory cancer, risk is zero during a 10 years latent period, after that:

$$R(D, a_0, t, s) = 0.636De^{(-1.437 \ln(t/20)+\gamma)}$$

γ =0 for the male and 0.711 for the female

For breast cancer (female only), risk is zero during a 10 years latent period, after that:

$$R(D, a_0, t) = 1.220De^{(\gamma_1 - 0.104 \ln(t/20) - 2.212 \ln(t/20) - \gamma_2 (t-20))}$$

γ_1 =1.385, a_0 <15, or γ_1 =0, $a_0 \ge 15$

γ_2 =0, a_0 <15, or γ_2 =0.0628, $a_0 \ge 15$

For digestive cancer, risk is zero during a 10 years latent period, after that:

$$R(D, a_0, t, s) = 0.809De^{(\gamma_1 - \gamma_2)}$$

γ_1 =0 for males or 0.553 for females

γ_2 =0, $a_0 \le 25$, or γ_2 =0.198(a_0 -25), $25 < a_0 \le 35$, or γ_2 =1.98, a_0 >35

For all other cancers, risk is zero during a 10 years latent period, after that:

$$R(D, a_0, t) = 1.220De^{(-\gamma)}$$

γ =0, $a_0 \leq 10$ or γ =0.0464(a_0-10), a_0>10

The lifetime cancer risk for a person who receives dose D at age a_0 [Ref 2-34]:

$$U(a_0, D) = \sum_a \frac{N(a)}{N(a_0)} \varepsilon_0(a) R(D, a_0, a)$$

where $U(a_0, D)$ is the probability that this person will have cancer fatality at some future time in his natural life expectancy. The summation is over the years beyond the age time receives the dose. N(a) is natural cancer fatalities at age a per 100,000 per year and is function of age at death, sex and cancer type [table 3.7 at p. 149 in Ref 2-34].

Using these relative cancer risk models, tables of natural cancer mortality [table 3.7 at p. 149 in Ref 2-34], and life table with population characteristic of the United States [table 3.10 at p. 152 in Ref 2-34], the average cancer risk from exposed population was calculated. Assuming the whole population receives the same amount of dose (1 Gy), the expected fatality over 100,000 years during lifetime is 4636. It means a fatality risk of 0.046 per Gy. This number was used as an overall cancer risk factor. Quality factor of low Linear Energy Transfer (LET) was used in this study.

It was assumed that for an exposed individual, the exposure to radiation occurs throughout the lifetime of the person at a constant level. In this study, the resulting cumulative health risk index is normalized against a reference fuel cycle (e.g., LWR-once through fuel cycle) for comparative analysis.

$$\sum_{totalrisk}(t_1, t_2)$$

$$= \int_{t_1}^{t_2} OverallCancerRiskFactor \bullet DoseRate(t) \bullet ValueofLifeAdjustmentFactor(t)dt$$

Where:

Overall Cancer Risk Factor = 5.0×10^{-4} per rem

t_1, t_2 are the start and end time of interest period. t_1=0 and t_2=100,000 years in this study

DoseRate(t) is total dose rate due to the release of nuclear waste [rem/yr]

Value of Life Adjustment Factor (t) = Adjustment for the relative changes in value of human life as a function of time, if the adjustment is needed for future generations (This factor is assumed to be one in this study).

A health risk performance number for a fuel cycle is defined as the ratio of total cumulative health risk from the fuel cycle to the base case fuel cycle risk (spent fuel direct disposal).

2.4 Repository Capacity Impact Model

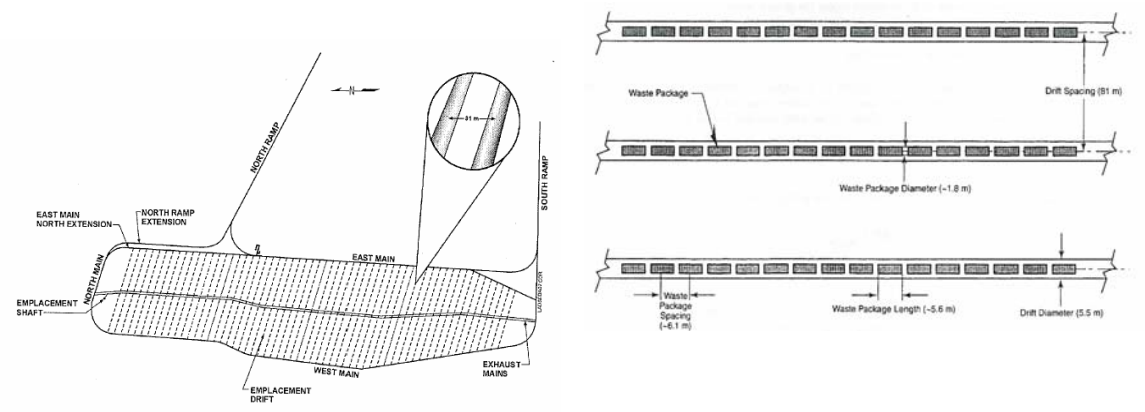

Figure 2-9 Repository layout

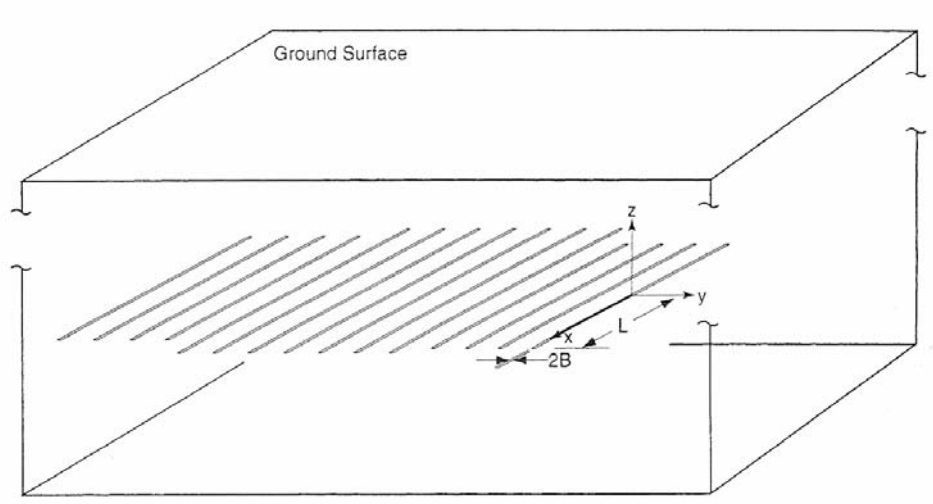

Figure 2-10 Mountain-scale heat-transfer model with line sources

In this study, the repository-horizon average rock temperature was computed using an analytic conduction model for mountain-scale heat transfer [Ref 2-12]. The modeled repository region has line sources laid out parallel to each other to cover the proposed repository (Figure 2-9). Each line source is at a depth of H below the ground surface and is represented as a high aspect-ratio rectangular element with a length of 2L and width of 2B (the drift diameter) (Figure 2-10). The temperature increase in the semi-infinite medium is the sum of contributions from each line source. The general solution for the temperature increase at any point in space and time is given as:

$$\Delta T(x,y,z,t) = \int_0^t \frac{\alpha q''_{rep}(t')}{4k\sqrt{\pi}} \frac{1}{\sqrt{4\alpha(t-t')}} \left[erf\left(\frac{L-x}{\sqrt{4\alpha(t-t')}}\right) + erf\left(\frac{L+x}{\sqrt{4\alpha(t-t')}}\right)\right]$$

$$\left[erf\left(\frac{B-y}{\sqrt{4\alpha(t-t')}}\right) + erf\left(\frac{B+y}{\sqrt{4\alpha(t-t')}}\right)\right] \left[\exp\left(\frac{-z^2}{4\alpha(t-t')}\right) - \exp\left(\frac{-(z-2H)^2}{4\alpha(t-t')}\right)\right] dt'$$

where: $\Delta T(x, y, z, t)$ is the increase in temperature at time t at point(x,y,z) in the semi-infinite medium due to one line source [°C]; $q''_{rep}(t)$ is the time-dependent repository heat flux [W/m^2]; α is the thermal diffusivity of the semi-infinite medium [m^2/s]; k is the thermal conductivity of the semi-infinite medium [W/(m-°C)]; L is the half-length of a line source [m]; B is the half-width of a line source [m]; H is the depth of a line source below the ground surface [m]; t is the actual time after the activation of the heat flux [s]; and x,y,z are the locations of interest [m].

In this model, the ground surface is assumed to be at a constant temperature. The repository-scale heat flux is related to the areal mass loading (AML) and the heat output per MTU of waste as following:

$$q''_{rep}(t) = \text{AML } Q_{mtu}(t)$$

Likewise, the thermal output for a single WP is related to the WP payload:

$$Q_{wp}(t) = MTU_{wp}\, Q_{mtu}(t)$$

where, AML is areal mass loading for the area occupied by the drifts [MTU/m^2]; MTUwp is the metric tons of uranium in a representative WP; $Q_{mtu}(t)$ is the time-dependent heat output per MTU of waste [W/MTU]

2.5 An Integrate Repository Impact Model

In this study, an integrated repository impact model was developed by coupling the thermal analysis model and the simplified PA model.

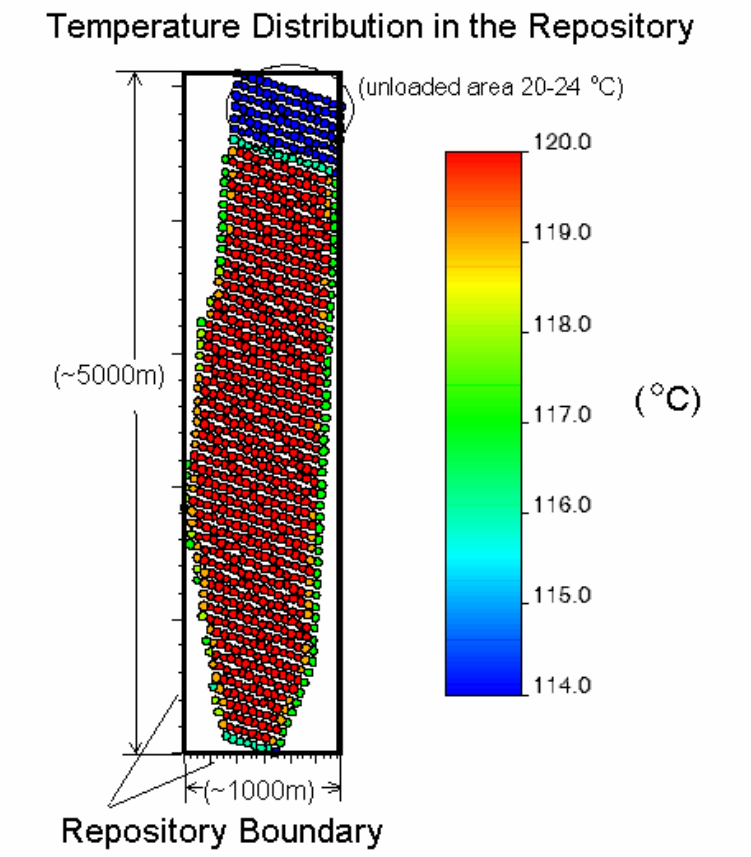

Figure 2-11 Spatial temperature distribution

Calculation for the integrative repository impact assessment proceeds as following: For a given fuel loading density per waste package (WP), the external gamma dose to the wall is calculated. From this, the rock-wall temperature and the rock temperature at the midway between drifts are estimated. If the estimated drift wall temperature and midway temperature are lower than the limit, the fuel loading density per WP is increased and rock temperatures are recalculated. This continues until the maximum temperature limit is reached. Based on the maximum fuel loading density per WP, the corresponding spent fuel loading capacity is estimated for the repository. The maximum spent fuel loading capacity for the repository was estimated based on the maximum drift wall temperature limit and maximum midway

temperature [Ref 2-62]. Then by using the total waste inventory for the repository, waste package failure, release of radionuclides and post-closure human dose history are projected. Time-dependent projected dose rate is converted into a risk-based health index. All of these calculations were integrated and coordinated in a computer code by using a master and slave module interactions. For a full loaded repository, two representative points are chosen for warmest drift wall point and midway point by investigating spatial temperature distribution over the whole repository. The Figure 2-11 shows a typical spatial temperature distribution at certain loading condition. It can be observed that the temperature in the central part of the repository does not change much. The temperature at two representative points (one is on drift wall, the other one is at the midway between two drifts) are used to supervise the temperature changing with loading change. Figure 2-12 shows the flow chart of the calculations.

A computer model was developed in this study to efficiently evaluate repository impact for a given fuel cycle strategy with respect to maximum repository loading capacity in accordance with temperature limits and projected health risk to humans.

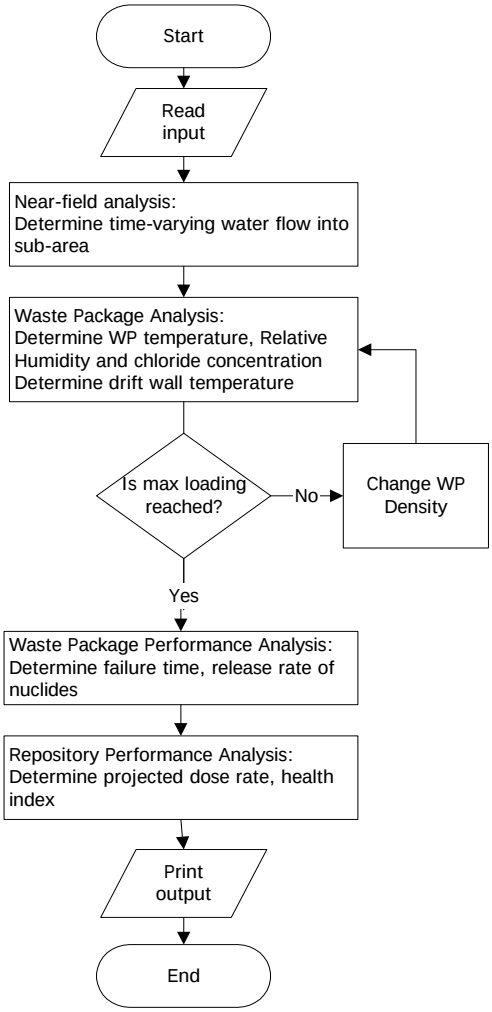

Figure 2-12 Flowchart of calculations for the integrated repository impact analysis

2.6 Test Case Analysis for Repository Impact

By applying the integrated repository impact model, two different fuel cycle scenarios were analyzed and compared as a test case. These two fuel cycles were the PWR once-through fuel cycle and the DUPIC (Direct Use of Spent PWR Fuel in CANDU reactors) fuel cycle.

The ORIGEN2.2 code [Ref 2-10] was used to simulate the mass and isotope inventory and their decay heat rates of the spent fuels from the two fuel cycle

scenarios. PWR once-through scenario was based on the use of 3.2% enriched UO_2 fuel burned up to 33,000 MWD/MTHM. The spent fuel is disposed of after 26 years of cooling period. In the DUPIC scenario, the spent fuel from the PWR once-through scenario was refabricated into a CANDU fuel after 10 years of cooling. The fuel is subsequently burned in a CANDU reactor up to 7500 MWD/MTHM and then disposed of after another 26 years of cooling.

The thermal analysis performed in this study was based on the revised repository design as specified in the License Application Design Selection (LADS) [Ref 2-63]. The LADS is characterized as a low thermal impact design which includes thermal blending of spent nuclear fuel assemblies, closer spacing of the waste packages, wider spacing of the waste emplacement tunnels (drifts), and preclosure ventilation. The maximum repository loading capacity was sought after within the given thermal design limit after assuming that the spacing between drifts and WP was fixed to be constant as specified in the EDA II (enhanced design alternatives II) of LADS [Ref 2-63].

The results of time-dependent temperature history at the two representative points for the two cases are shown in Figure 2-13 and Figure 2-14. From the figures, we can see the repository capacity is limited by the temperature limit (96°C) at midway between drifts in both scenarios. The peak temperature appears at around 80 years for temperature at driftwall and around 500-800 years for temperature at midway between drifts after disposal.

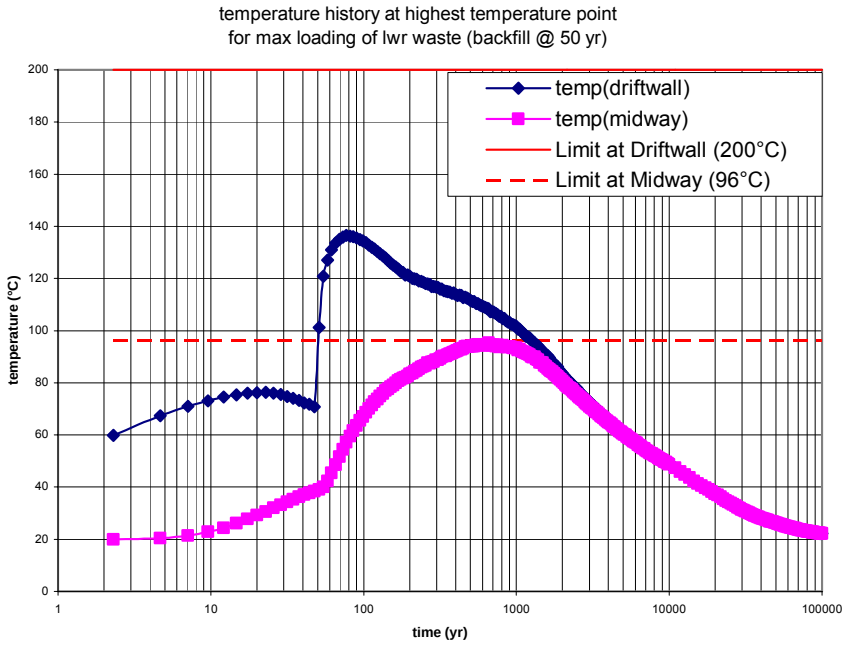

Figure 2-13 Temperature history at highest temperature point for LWR

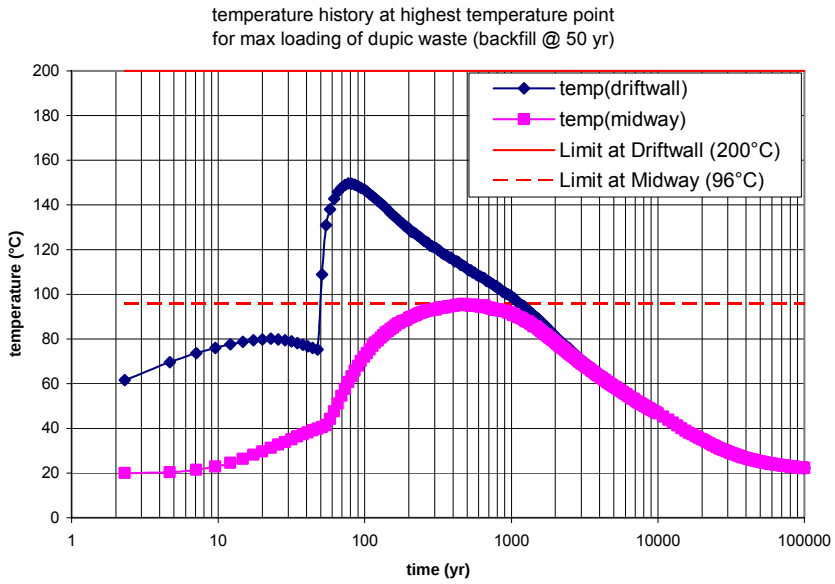

Figure 2-14 Temperature history at highest temperature point for DUPIC

These results are in good agreement with the results obtained from Argonne National Laboratory (Figure 2-15) [Ref 2-64]. Their results show that the maximum

loading is limited by the temperature limit at the midway between drifts for PWR SNF which contains Pu and Am actinides. The peak temperature at midway shows up at around 1000-2000 years after disposal. The peak temperature at drift wall appears at around 25 years after the airflow turned off.

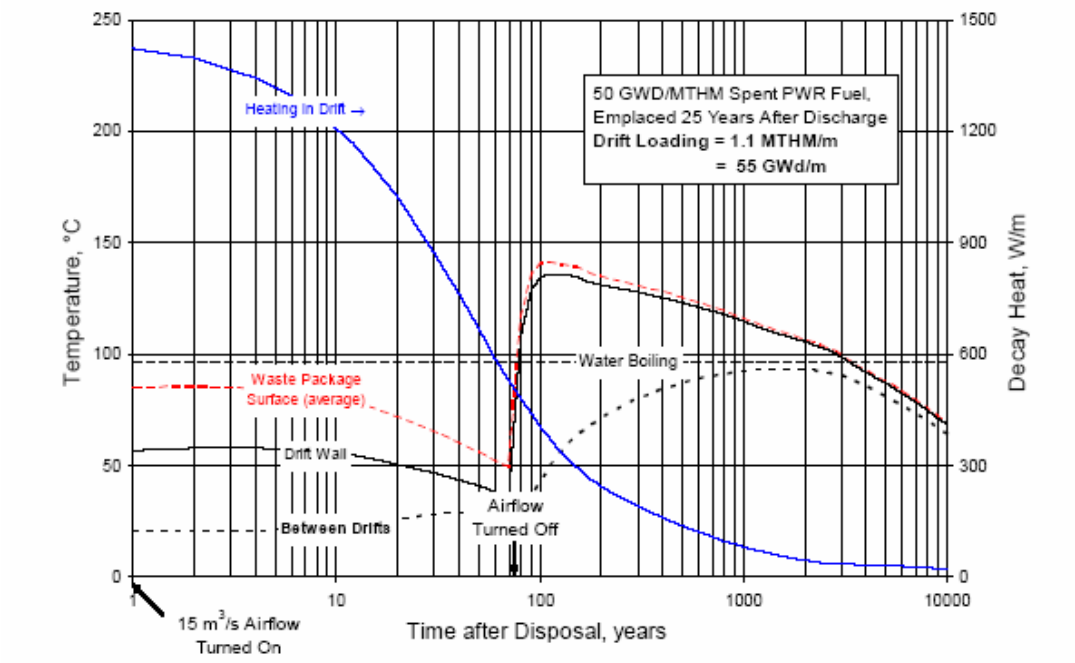

Figure 2-15 Temperature history result for PWR SNF

Table 2-3 Comparison of TPA and SPA results

	PWR	DUPIC	Ratio (DUPIC/PWR)
Peak Dose Rate (rem/yr) [TPA]	7.24E-02	9.54E-02	1.32
Peak Dose Rate (rem/yr) [SPA]	2.48E-02	3.03E-02	1.23
Accumulated Dose (rem) [TPA]	1.85E+02	2.29E+02	1.23
Accumulated Dose (rem) [SPA]	4.36E+01	5.35E+01	1.23

Environmental impacts from the repository of fixed loading (assumed 70,000 MTHM) for PWR SNF and DUPIC SNF were analyzed by using TPA4.1 code [Ref 2-12] and the new Simplified Performance Assessment (SPA) model. The results

are shown in Table 2-3. Both peak dose and accumulated dose in 100,000 years were calculated and listed. The estimated ratios of peak dose rate and accumulated dose between the DUPIC SNF case and the PWR SNF case indicate that that the predictions from new SPA model are in good agreement with those from TPA.

2.7 References

Ref 2-1 “Report to Congress on Advanced Fuel Cycle Initiative: The Future Path for Advanced Spent Fuel Treatment and Transmutation Research,” Department of Energy Office of Nuclear Energy, Science and Technology, January 2003.

Ref 2-2 Hoffman, E. A., “Neutron Transmutation of Nuclear Waste”, Ph.D. Dissertation, Georgia Institute of Technology, July 2002.

Ref 2-3 Savage, D., The Scientific and Regulatory Basis for the Geological Disposal of Radioactive Waste, John Wiley and Sons, Chichester, UK, 1995.

Ref 2-4 Benedict, M., T. H. Pigford, and H. W. Levi, Nuclear Chemical Engineering, McGraw-Hill Inc., New York, NY, 1981.

Ref 2-5 Kang, C. H., “Transmutation Effects on Transuranic Waste Inventory and Its Repository Risk”, M.S. Thesis, MIT, June, 1993

Ref 2-6 Pigford, T. H., “Actinide Burning and Waste Disposal,” UCB-NE-4176, MIT International Conference on the Next Generation of Nuclear Power Technology, October 1990.

Ref 2-7 Griffith, J. D., “Actinide Recycle: Presentation to National Research Council Committee on Future Nuclear Power Development,” Department of Energy, Office of Nuclear Energy, January 1990.

Ref 2-8 European Commission, “Comparison of Waste Toxicity Index and Repository Performance Assessment Approaches to Providing Guidance for R&D on Partitioning and Transmutation,” EUR 16167, Luxembourg, 1995.

Ref 2-9 “A roadmap for developing accelerator transmutation of waste (ATW) technology”, U.S. Department of Energy, October, 1999

Ref 2-10 A. G. Croff, “A User’s manual for the ORIGEN2 Computer Code”, ORNL/TM-7175, 1980.

Ref 2-11 “Viability Assessment of a Repository at Yucca Mountain”, U.S. Department of Energy, Office of Civilian Radioactive Waste Management, 1998

Ref 2-12 Mohanty, S., T. J. McCartin, and D. W. Esh, “Total-System Performance Assessment (TPA) Version 4.0 Code: Module Descriptions and User’s Guide”, Center for Nuclear Waste Regulatory Analyses, San Antonio, Texas, Jan. 2002

Ref 2-13 G.J. Saulnier, K.P. Lee, D.A. Kalinich, S.D. Sevougian, J.A. McNeish, “Total System Performance Assessment Model for the Final Environmental Impact Statement for the Potential High-level Nuclear Waste Repository at Yucca Mountain”, Proceedings of ICONE10, P. 311-319, 2002

Ref 2-14 CRWMS M&O, “Total System Performance Assessment for the Site Recommendation”, TDR-WIS-PA-000001 REV 00 ICN 01, 2000

Ref 2-15 W.M. Nutt, R.N. Hill and D. B. Bullen, “Performance Assessment Modelling of Pyrometallurgical Process Wasteforms”, Waste Management, vol. 15, No. 8, pp. 629-639, 1995

Ref 2-16 Golder Associates Inc., “RIP Repository Performance Assessment and Strategy Evaluation Model: Theory and Capabilities, Version 3.20”, Report No. 933-1469, 1994

Ref 2-17 Golder Associates Inc., “RIP Repository Performance Assessment and Strategy Evaluation Model: User’s Guide, Version 5.19.01”, Report No. 933-1469, 1998

Ref 2-18 DOE, Office of Civilian Radioactive Waste Management, “Total System Performance Assessment – 1995: An Evaluation of the Potential Yucca Mountain Repository”, B00000000-01717-2200-00136, Rev. 01, 1995

Ref 2-19 DOE, Office of Civilian Radioactive Waste Management, “Viability Assessment of a Repository at Yucca Mountain, Volume 3: Total System Performance Assessment”, DOE/RW-0508/V3, 1998

Ref 2-20 DOE, Office of Civilian Radioactive Waste Management, “Environmental Impact Statement for a Geologic Repository for the Disposal of Spent Nuclear Fuel and High-Level Radioactive Waste at Yucca Mountain, Nye County, Nevada”, DOE/EIS-0250, 2002

Ref 2-21 N.A. Eisenberg, R.G. Wescott, M.V. Federline, M. Silbergerg and B. Sagar, “IPA PHASE 2 and NRC’s HLWM Regulatory Program”, 5th HLW, pp. 1451-1460, 1994

Ref 2-22 J.R. Park, R.G. Baca, N.A. Eisenberg, R.W. Janetzke and B. Sagar, “IPA PHASE 2 Total System Code and Scenario Analysis”, 5th HLW, pp. 1461-1468, 1994

Ref 2-23 “Demonstration of a risk-based approach to high-level waste repository evaluation”, EPRI, Palo Alto, CA, Report NP-7057, 1990

Ref 2-24 “Demonstration of a risk-based approach to high-level waste repository evaluation: phase 2”, EPRI, Palo Alto, CA, Report TR-100384, 1992

Ref 2-25 “Yucca Mountain Total System Performance Assessment, Phase 3”, EPRI, Palo Alto, CA, Report TR-107191, 1996

Ref 2-26 “Alternative Approaches to Assessing the Performance and Suitability of Yucca Mountain for Spent Fuel Disposal”, EPRI, Palo Alto, CA, Report TR-108732, 1998

Ref 2-27 “Evaluation of the Candidate High-Level Radioactive Waste Repository at Yucca Mountain Using Total System Performance Assessment: Phase 5”, EPRI, Palo Alto, CA, Report TR-1000802, 2000

Ref 2-28 Eslinger, P. W., D. W. Engel, T. B. Miley, and P. J. Chamberlain, “SUMO-System Performance Assesment for High-Level Nuclear Waste Repository: Mathematical Models,” PNL-7581, Pacific Northwest Laboratory, September 1992

Ref 2-29 R.W. Barnard, M.L. Wilson, H.A. Dockery, J.H. Gauthier, P.G. Kaplan, R.R. Eaton, F.W. Bingham, T.H. Robey, ”TSPA 1991: In Initial Total-System Performance Assessment for Yucca Mountain”, SAND91-2795 UC-814, Sandia National Laboratories, Albuquerque, NM., September 1992

Ref 2-30 R.W. Prindle and P.L. Hopkins, “On Conditions and Parameters Important to Model Sensitivity for Unsaturated Flow Through Layered, Fractured Tuff: Results of Analyses for HYDROCOIN Level 3 Case 2”, SAND89-

0652, Sandia National Laboratories, Albuquerque, NM. (NNA.900523.0211), 1990

Ref 2-31 R.C. Dykhuizen and R.W. Barnard, “Groundwater Flow Code Verification ‘Benchmarking’ Activity (COVE-2A): Analysis of Participants’ Work”, SAND89-2558, Sandia National Laboratories, Albuquerque, NM. (NNA.920130.0016), 1992

Ref 2-32 R.W. Barnard and H.A. Dcckery, editors, “Technical Summary of the Performance Assessment Calculational Exercises for 1990 (PACE-90), Vol. 1: ‘Nominal Configuration’ Hydrogeologic Parameters and Calculational Results,” SAND90-2726, Sandia National Laboratories, Albuquerque, NM. (NNA.910523.0001), 1991

Ref 2-33 M.L. Wilson, J.H. Gauthier, R.W. Barnard, G.E. Barr, H.A. Dockery, E. Dunn, R.R. Eaton, D.C. Guerin, N. Lu, M.J. Martinez, R. Nilson, C.A. Rautman, T.H. Robey, B. Ross, E.E. Ryder, A.R. Schenker, S.A. Shannon, L.H. Skinner, W.G. Halsey, J.D. Gansemer, L.C. Lewis, A.D. Lamont, I.R. Triay, A. Meijer, and D.E. Morris, “Total-System Performance Assessment for Yucca Mountain —SNL Second Iteration (TSPA-1993),” SAND93-2675, Sandia National Laboratories, Albuquerque, N. Mex., 1994

Ref 2-34 R.E. Faw and J.K. Shultis, “Radiological Assessment: sources and doses”, La Grange Park, Ill, American Nuclear Society, ISBN: 0-89448-455-9, 1999

Ref 2-35 “Health Effects of Exposure to Low Levels of Ionizing Radiation: BEIR V”, Committee on the Biological Effects of Ionizing Radiation (BEIR V), National Research Council, 1990

Ref 2-36 R.W. Barnard and H. A. Dockery, editors, “Technical Summary of the Performance Assessment Calculational Exercises for 1990 (PACE-90), Vol. 1: ‘Nominal Configuration’ Hydrogeologic Parameters and Calculational Results”, SAND90-2726, andia National Laboratories, Albuquerque, N. Mex., NNA.910523.0001, 1991

Ref 2-37 R.C. Dykhuize and R.W. Barnard, “Groundwater Flow Code Verification ‘Benchmarking’ Activity (COVE-2A): Analysis of Participants Work”, SAND89-2558, Sandia National Laboratories, Albuquerque, N. Mex., NNA.920130.0016, 1992

Ref 2-38 R.W. Prindle and P.L. Hopkins, “On Conditions and Parameters Important to Model Sensitivity for Unsaturated Flow Through Layered, Fractured Tuff: Results of Analyses for HYDROCOIN Level 3 Case 2”, SAND89-0652, National Laboratories, Albuquerque, N. Mex., NNA.900523.0211, 1990

Ref 2-39 M. Harada, P.L. Chambre, M. Foglia, K. Higashi, F. Iwamoto, D. Leung, T.H. Pigford, D. Ting, “Migration of Radionuclides Through Sorbing Media Analytical Solutions-I”, ONWI-359, LBL-10500, UC-70, Lawrence Berkeley Laboratory, University of California, Feb. 1980

Ref 2-40 T.H. Pigford, P.L. Chambre, M. Albert, M. Foglia, M. Harada, F. Iwamoto, T. Kanki, D. Leung, S. Masuda, S. Muraoka and D. Ting, “Migration of

Radionuclides Through Sorbing Media Analytical Solutions-II", LBL-11616, UCB-NE-4003, UC-70, Lawrence Berkeley Laboratory, University of California, Oct. 1980

Ref 2-41 P.L. Chambre, T.H. Pigford, A. Fujita, T. Kanki, A. Kobayashi, H. Lung, D. Ting, Y. Sato, S.J. Zavashy, "Analytical Performance Models for Geologic Repositories", Vol. 1&2, LBL-14842, UCB-NE-4017, UC-70, Lawrence Berkeley Laboratory, University of California, Oct. 1982

Ref 2-42 P.L. Chambre, T.H. Pigford, W.W.L. Lee, J. Ahn, S. Kajiwara, C.L. Kim, H. Kimura, H. Lung, W.J. Williams, S.J. Zavoshy, "Mass Transfer and Transport in a Geologic Environment", LBL-19430, DE87 000888, Lawrence Berkeley Laboratory, University of California, April 1985

Ref 2-43 J. Ahn, D. Kavasaki, P. L. Chambre, "Relationship among performance of geologic repositories, canister-array configuration, and radionuclide mass in waste", Nuclear Technology, 126, p. 94-112, 2002

Ref 2-44 D. Kawasaki, J. Ahn, P.L. Chambre, W. G. Halsey, "Canister-array configuration and congruent release of long-lived radionuclides", 10th int. High-Level Rad. Waste Mange. Conf. (IHLRWM), Las Vegas, Nevada, March 30-April 3, 2003

Ref 2-45 J. Ahn, "Possibility of safety improvement for vitrified HLW geologic disposal by partitioning and transmutation", Proc. Global '99, Int. Conf. on Future Nuclear Systems, Jackson Hole, Wyoming, 1999

Ref 2-46 J. Ahn, “An environmental impact measure for nuclear fuel cycle evaluation”, Journal of Nuclear Science and Technology, vol. 41, No. 3, p. 296-306, March 2004

Ref 2-47 J. Claesson and T. Proberts, “Temperature Field Due to Time-Dependent Heat Sources in a Large Rectangular Grid – Derivation of Analytical Solution”, SKB 96-12, Stockholm, Sweden: Swedish Nuclear Fuel and Waste Management Co. 1996

Ref 2-48 C.A. Estrada-Gasca, “Analytical Methods of Heat Transfer Compared With Numerical Methods as Related to Nuclear Waste Repositories”, Dissertation, Mechanical Engineering, New Mexico State University, Las Cruces, NM, 1986

Ref 2-49 International Atomic Energy Agency, “International Nuclear Fuel Cycle Evaluation, Volume 7: Waste Management and Disposal”, IAEA, 1980

Ref 2-50 W.M. Kays, F. Hossaini-Hashemi and J.S. Busch, “Calculation of Media Temperatures for Nuclear Sources in Geologic Depositories by a Finite-Length Line Source Superposition Model (FLLSSM)”, Nuclear Engineering and Design 67 p.339-347, 1981.

Ref 2-51 Thomas A. Buscheck and John J. Nitao, “The Impact of Thermal Loading on Repository Performance at Yucca Mountain”, 3rd hlw, 1992

Ref 2-52 Nitao, J.J., “V-TOUGH – An Enhanced Version of the TOUGH Code for the Thermal and Hydrological Simulation of Large-Scale Problems in Nuclear Waste Isolation”, UCID-21954, Lawrence Livermore National Laboratory, Livermore, CA, 1989

Ref 2-53 Carl Malbrain and Richard K. Lester, “Impact of Thermal Constraints on the Optimal Design of High-Level Waste Repositories in Geologic Media”, Nuclear Engineering and Design 73, p. 331-341, 1982

Ref 2-54 M. Thury et al., “Geologie und Hydrogeologie des Kristallins der Nordschweiz”, Nagra Technical Report, NTB 93-01, Wettingen, Switzerland, 1994

Ref 2-55 NAGRA, “Kristallin-I: Safety Analysis Overview”, Nagra Technical Report, NTB 93-22, Wettingen, Switzerland, 1994

Ref 2-56 PNC, “Research and development on geological disposal of high level radioactive waste. First progress report.”, PNC, TN 1410 93-018, Japan, 1992

Ref 2-57 G.A. Cragnolino, S. Mohanty, D.S. Dunn, N. Sridhar, T.M. Ahn, “An Approach to the Assessment of High-level radioactive Waste Containment. I: Waste Package Degradation”, Nuclear Engineering and Design 201 289-306, 2000

Ref 2-58 G.A. Cragnolino, S. Mohanty, D.S. Dunn, N. Sridhar, T.M. Ahn, “An Approach to the Assessment of High-level Radioactive Waste Containment. II: Radionuclide Releases from an Engineered Barrier System”, Nuclear Engineering and Design 201 307-325, 2000

Ref 2-59 International Council on Radiation Protection, “Annual Limits on Intakes of Radionuclides by Workers, Based on the 1990 Recommendations of the ICRP,” ICRP Publication 61, Ann. ICRP 21, No. 4, 1991

Ref 2-60 Hogget-Jones, C., C. Robbins, G. Gettinby, and S. Blythe, “Modeling the Inventory and Impact Assessment of Partitioning and Transmutation Approaches to Spent Nuclear Fuel Management,” Annals of Nuclear Energy, 29, 491-508, 2002

Ref 2-61 Codell, R. B. and J. D. Duguid, “Transport of Radionuclides in Groundwater,” in Radiological Assessment, Till, J. E. and H. R. Meyer (editors), NUREG/CR-3332, Nuclear Regulatory Commission, 1983

Ref 2-62 M. M. Goldberg, T.H. Bauer, R.A. Wigeland, and J.C. Cunnane, “Corrosion Prevention Effect of Spent Nuclear Fuel Decay Heat”, Global 2003, New Orleans, LA, Nov. 2003

Ref 2-63 C.R. Hastings, “License Application Design Selection Report, REV 01. August 1999”, B00000000-01717-4600-00123 REV 01 ICN 01, Aug 30 1999

Ref 2-64 R.A. Wigeland and T.H. Bauer, “Repository Benefits of Partitioning and Transmutation”, Eighth Information Exchange Meeting on Actinide and Fission Product Partitioning and Transmutation, Las Vegas, NV, November 9-11 2004

3 Proliferation Resistance

Any nuclear reactor system that produces/handles fissile nuclear materials is potentially vulnerable to diversion or misuse of the fissile materials. At the same time, depending upon the technological effort or the degree of complexity required for any diversion/misuse attempts, proliferation resistance of a particular nuclear system can differ. Since proliferation resistance is as an important aspect of civilian nuclear power systems as cost, safety and environment impacts, a quantitative assessment is necessary to compare different nuclear fuel cycle options for AFC development. In this chapter, development of a new method of quantifying proliferation resistance based on a fuzzy logic and TOPS barrier concept is described.

3.1 Introduction and Literature Reviews

The concern over the connection between the worldwide spread of nuclear power and nuclear weapons proliferation rose up in 1970's, especially after the so called "peaceful nuclear explosion" in India on May 18, 1974. This concern was expressed by former US President Carter in his April 1977 decision to defer commercial reprocessing and the breeder reactor [Ref 3-2]. And he initiated the International Nuclear Fuel Cycle Evaluation (INFCE) program [Ref 3-3] and the U.S. Nonproliferation Alternative System Assessment Program (NASAP) [Ref 3-4] to evaluate alternative nuclear fuel cycles. Over 50 countries were involved in the INFCE project and after two years of deliberation, the study concluded that the connection between civilian nuclear power and weapons proliferation is a problem

that technology can not handle alone. However, the NASAP, the study parallel to INFCE, concluded that the once-through fuel cycle is the most resistant fuel cycle. At 1978, Harold A. Feiveson reviewed studies on the proliferation resistance of nuclear fuel cycle and concluded that it was generally agreed that no fuel cycle can be completely proof against diversion of fissile materials for use in weapons [Ref 3-5]. These studies also identified the need for the development of quantitative methods to assess proliferation resistance of a nuclear fuel cycle.

Based on the principles of multi-attribute decision analysis, MIT Energy Lab developed a quantitative methodology for proliferation resistance assessment [Ref 3-6, Ref 3-7]. Five attributes were defined to express the proliferation resistance of a given system for a given country with a given nuclear-weapons aspiration. The least resistance of a pathways among many choices is considered to constitute the resistance of the system for the given country-aspiration combination. Multi-attribute decision analysis was also used by Heising, et al., to address proliferation risk of nuclear energy systems [Ref 3-8, Ref 3-9]. Value functions were defined to derive a quantitative indicator of the relative diversion resistance of a fuel cycle. The dimensionless numerical indicators can be calculated from the value functions and are multiplied by importance weighting factors and summed over all attributes to obtain one single indicator for each fuel cycle. The weighting factors reflect expert opinions. In Silvennoinen and Vira's work [Ref 3-10, Ref 3-12], the proliferation risk is defined as a combined utility of the different fuel cycle processes or materials for the proscribed acquisition of a nuclear weapon. Based on a set of selected weighted criteria, the process utilities are calculated employing two schemes: utility

functions or fuzzy expectation values. The techniques of pair-wise comparisons as proposed by Saaty have been used to assigning weighting factors. The order of the utility values for different processes is not sensitive to the scaling of the weights. Ahmed and Husseiny developed a quantitative decision model based on MAU theory to arrive at the relative ranking of 14 important proliferation routes [Ref 3-13]. The proliferation resistance index was also modeled in the imitation of an electrical circuit and linked with multi-attribute utility theory to quantify the proliferation resistance of nuclear fuel cycles [Ref 3-15]. A fuel cycle is modeled as an electrical circuit and for each facility in the fuel cycle; an equivalent resistance is generated to represent the proliferation resistance. Both political issues and technical issues relevant to the proliferation resistance can be included. All facilities and activities in a nuclear fuel cycle from mining to disposal can be considered. The motivations of the potential proliferators are represented as the electromotive force V.

Krakowski [Ref 3-16, Ref 3-17] used pair-wise comparison method combined together with the multi-attribute utility approach to generate proliferation resistance metrics. This method combines two earlier applications of multi-attribute utility analysis to quantify, on a subjective scale, the risks of nuclear weapons proliferation from the nuclear fuel cycle into a parametric algorithm.

Application of fuzzy theory was explored to evaluate the efficiency of safeguards in 2002 [Ref 3-19]. Matsuoka, Nishiwaki, Ryjov and Belenki developed a simple logic tree to evaluate the safeguards effectiveness. Fuzzy linguistic variables are used as inputs and fuzzy operation “and” and “or” are defined in their study. It

demonstrates a useful application of fuzzy theory in the evaluation of integrated safeguards.

A more refined MAU-based methodology was developed at the University of Texas in collaboration with Oak Ridge National Lab [Ref 3-20 - Ref 3-21]. The methodology is focused on the material moving through a fuel cycle instead of the facilities or processes. The method tracks the proliferation resistance of a unit mass of material input into a fuel cycle all the way from its initial input through its eventual disposal.

A comprehensive evaluation methodology has also been developed by the U.S. DOE through the PR&PP (proliferation resistance and physical protection) Working Group to assess PR&PP of Generation IV nuclear energy systems as recommended in the Generation IV Roadmap [Ref 3-22 - Ref 3-25]. The evaluation methodology [Ref 3-26, Ref 3-27] identifies the threats, relevant elements of the nuclear power system and targets. PR&PP measures are defined as high-level parameters to represent the proliferation resistance and physical protection. Pathways are identified for proliferation, theft or sabotage and are analyzed. The resistance of the system to those pathways is determined and expressed in terms of PR&PP measures. This methodology is under development and provides an intuitive, structured and comprehensive tool. It is in need of data to support the application of this tool [Ref 3-28].

These assessment methods can be categorized into two approaches: attribute analysis and scenario analysis. Attribute analysis examines proliferation resistance of a reactor system, a commercial fuel cycle, or transportation of nuclear material by

identifying and examining various attributes related to potential fissile material diversion attempts. The MAU approach belongs to this category. MAU is an approach associated with the field of decision analysis. Decision analysis enables complex problems to be systematically analyzed to obtain a solution; thus decision-makers can make an educated decision between alternatives. MAU analysis allows proliferation objectives and metrics to be weighted according to their degree of influence. MAU enables diverse metrics to be integrated into a model to obtain a value for comparison. The current MAU models only treat the technical aspect of the proliferation problem, but proliferation resistance of nuclear fuel cycle includes both intrinsic and extrinsic attributes and also heavy reliance on subjective judgments/expert opinions.

In the scenario analysis approach, specific scenarios leading to proliferation are identified and modeled and typically proliferation risk is quantified. Probabilistic risk analysis is a prime example of a scenario analysis. A probabilistic approach is analogous to probabilistic risk assessments (PRAs), which have mainly been used for safety analyses. In a probabilistic approach, causal relationships resulting in an undesirable outcome are identified in the form of event trees, which are then used to determine the risk of a postulated event. This allows identification of key risk contributors in the event tree; yet it does not readily allow comparison between alternatives. Also it suffers the lack of data regarding probabilities of events leading to proliferation makes assigning probabilities to each node of the event tree difficult. The approach can apply to actions or activities not necessarily part of a physical nuclear complex. Attribute analysis is quite useful when details of design

information are not available (i.e., at a conceptual design stage), whereas scenario analysis is most useful when detailed design information is available. If the purpose of the assessment is for comparison of relative merits of conceptual design alternatives (for fuel cycle or a reactor system), using attribute analysis to examine proliferation resistance would be a preferred method of analysis.

The barrier framework (BF) [Ref 3-29, Ref 3-30] developed by the TOPS (Technical Opportunities To Increase the Proliferation Resistance of Global Civilian Nuclear Power Systems) task force of the Nuclear Energy Research Advisory Committee (NERAC) of the Department of Energy is a key example of attribute analysis. The TOPS approach provides a very comprehensive framework, supported by an extensive list of the basic metrics (both intrinsic and extrinsic) related to proliferation assessments. But due to the qualitative nature of the assessment, the method is not amenable to quantitative analysis. Also, due to the subjective nature of assessment, the method is subject to large uncertainty.

Application of the theory of fuzzy sets and possibility to the BF appears meritorious in this regard. The fuzzy logic approach is particularly well suited for representing information that is vague, imprecise, and uncertain. Fuzzy logic was first introduced in the early 1960's [Ref 3-36] and was not accepted initially by the U.S. scientific community. In 1970's, fuzzy logic was first applied in control engineering in Europe, and later in 1980's; Japanese researchers adopted fuzzy logic and further developed it. With the broad applications of fuzzy logic in Europe and Japan, the U.S. community recently started to take a serious look at the method.

The specific objective of the research described in this chapter is to develop a comprehensive proliferation resistance assessment method by applying fuzzy number and rendering Barrier Framework (BF) from TOPS to a quantitative tool. The method, as is based on the TOPS BF, is comprehensive in covering proliferation barriers associated with a reactor system. The method is capable of describing the effect of time-varying inventories of materials to be processed. The method allows direct interpretation of the numbers in terms of the qualitative effectiveness of the proliferation barrier of the system, as characterized in the TOPS report [Ref 3-29, Ref 3-30].

3.2 Fuzzy Logic and Fuzzy Number

Fuzzy number is a set of number and their membership function that shows how much the number is close to this set. Normally a fuzzy number A can be expressed as:

A = $\{(x, \mu_A(x)) \mid x$ is element of A, and $\mu_A(x)$ shows how true the element x belongs to A, and $0 \le \mu_A(x) \le 1\}$

Fuzzy number can be used to represent regular human concept like “hot”, “cold”, “high” and “low”. For example, we can define “hot” as a fuzzy number A = $\{(x, \mu_A(x)) \mid \mu_A(x)$=1 when x >80F, $\mu_A(x)$=0 when x <70F, $\mu_A(x)$=(x-70)/10 when $70F \le x \le 80F\}$ where x is the F degree of temperature. So if x=90, $\mu_A(x)$=1, and it means it is definitely “hot”. And if x=60, $\mu_A(x)$=0, and it means it is definitely not “hot”. And if x=75, $\mu_A(x)$=0.5, and it means it is half true to say it is “hot”.

3.3 Barrier Method

In 1999, the U.S. Department of Energy (DOE) office of Nuclear Energy, Science, and Technology and DOE's Nuclear Energy Research Advisory Committee (NERAC) established a special Task Force to identify near and long-term technical opportunities to increase the proliferation resistance of civilian nuclear power system (TOPS) and to recommend specific areas of research that should be pursued to further these goals. As one of two methods considered by TOPS Task Force, the Barrier Framework (BF) is an attributes methodology that addresses both intrinsic (technical features) and extrinsic (institutional measures) aspects of fuel cycle system. By applying the BF method and considering only technical features, Hassberger [Ref 3-37] studied ten systems (LWR-ONCE THROUGH (LWR-OT), LWR-OT with high burnup (LWR-OT-HB), LWR-OT with Homogeneously Mixed Thoria-Urania Fuel (LWR-OT-ThU), LWR-OT with a Heterogeneous Thorium Seed-Blanket Core (LWR-OT-Th), LWR-MOX fuel cycle (LWR-MOX), Prismatic Fuel High-Temperature Gas-Cooled Reactor (HTGR), Pebble-Bed Fuel High-Temperature Gas-Cooled Reactors (PBR), Small, Transportable, Autonomous Reactor (STAR), IRIS-MOX Fueled Concept (IRIS-MOX), IFR/PRISM/BREST Fuel Cycle) and he gave the results similar to Table 3-1 which is the result for LWR, one of the ten systems he studied. "VH" means "Very High", "I" means "Ineffective", "M" means "Moderate", "H" means "High", and "L" means "Low".

Table 3-1 Barriers of once-through LWR cycle [Ref 3-37]

Stage of the fuel cycle	Material Barriers					Technical Barriers					
	Isotopic	Radiological	Chemical	Mass & Bulk	Detectability	Facility Unattractiveness	Facility Access	Available Mass	Facility Detectability	Skills, Expertise, & Knowledge	Time
Front-end of the cycle											
Transport of fresh fuel	VH	I	M	H	M	VH	I	L-M	M	VH	VH
Reactor operations											
Fresh fuel storage	VH	I	M	VH	M	VH	I	I	VH	VH	VH
…	…	…	…	…	…	…	…	…	…	…	…
On-site SNF dry storage	L	H-VH	VH	VH	VH	VH	M	I	VH	VH	L-M
Back-end of the cycle											
Transport of SNF	L	H-VH	VH	VH	VH	VH	M	I	VH	VH	VH

3.4 Fuzzy Logic Based Barrier Method

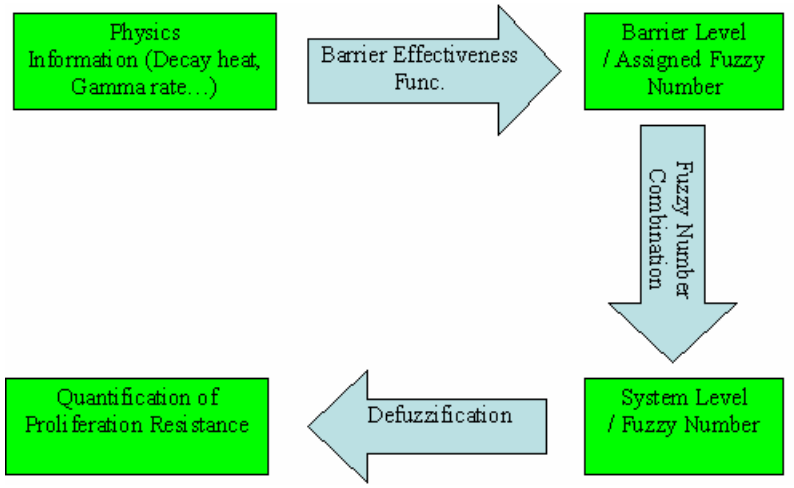

Figure 3-1 Information process of fuzzy logic based barrier method

The fuzzy logic applied barrier method is based on BF method. Fuzzy logic is used to mimic the information process of experts when they use the BF method to assess the proliferation resistance of a system. The information process can be shown in Figure 3-1. For each stage of a system, the basic related physics information is collected and barrier level which is represented by a fuzzy number is generated by using defined barrier effectiveness function. Barrier effectiveness function expresses the relationship between the basic physics information and barrier level (strength of proliferation resistance). A system associates with several stages and each stage is evaluated based on 11 intrinsic barriers out of 14 total barriers in the TOPS report (which includes 3 extrinsic barriers). For each barrier level of a barrier in one stage, there is one fuzzy number to express the strength of the barrier level. By appropriately combining the fuzzy numbers for each barrier and fuel cycle stage, a fuzzy number for the fuel cycle system is calculated to represent the proliferation resistance of the system. This fuzzy number can be used to extract

meaningful and quantifiable proliferation resistance of the system. Important quantities to reflect proliferation resistance of a system were first selected. Secondly, barrier effectiveness functions were defined to mathematically link the important quantities to barrier level. Then, for 15 different barrier levels, 15 fuzzy numbers are defined to represent the barrier levels quantitatively. The fuzzy numbers for all barriers at all stages in a nuclear fuel cycle are further combined to generate one fuzzy number for the nuclear fuel cycle which can represent the proliferation resistance level for the fuel cycle. Through defuzzification, the centroid value of a fuzzy number is defined to represent the proliferation resistance of a system.

3.4.1 Determination of Quantities to Represent PR

The barriers considered in the TOPS BF include material barrier characteristics (i.e., isotopic, chemical, radiological, mass and bulk, and detectability considerations) and technical barriers (i.e., facility unattractiveness, facility accessibility, available mass, diversion detectability, skills/expertise/knowledge required and time requirement). Relative differences in the effectiveness of each barrier between different reactor systems or fuel cycle systems depend upon the system characteristics and the nature of the design (i.e., the time- and fuel cycle strategy-dependent isotopic mass balance). The barrier effectiveness functions were developed to represent the characteristics of different reactor systems as a function of a system-dependent variable that is measurable or quantifiable. This is described in the following.

The isotopic barrier relates to the quality of the fissile material once available and indicates how difficult it would be to construct a weapon from this fissile material. The quality of the fissile material depends on the fissile material isotopes, enrichment, impurities and the concentrations (especially even Pu isotopes for ^{239}Pu), and radiation level that would affect the assembly process of a nuclear device. Presently the enrichment of fissile material, critical mass, spontaneous fission neutron (SFN) rate, gamma radiation rate and heat rate are used as indicators for the barrier. Enrichment and critical mass directly affect how much materials are needed to make one successful nuclear device. SFN, gamma rate and heat rate can affect the quality of the fissile material for weapon use. High SFN and high gamma rate may cause the device difficult to control. High heat rate may cause the explosive difficult to be assembled. For a system that contains both ^{239}Pu and ^{235}U, an equivalent fissile value was used.

The chemical barrier represents the extent and difficulty of chemically partitioning or separating the weapons-usable material(s) from the given materials. The difficulty depends on how many processes are involved, how long the processes take, and what kinds of facilities are required. The extent of these efforts can be summarized in terms of cost, which is used as a key attribute of the chemical barrier effect.

The radiological barrier affects the ease of theft or diversion and complication of chemical processing. The unshielded dose rate at one meter from the surface of the material is chosen to represent the effect of this barrier.

For mass and bulk barrier, the concentration of fissile material and the size of the material involved are important attributes. The higher the concentration, the lower

the barrier is. The size also matters in terms of handling and/or ease of concealment. The concentration of fissile materials is chosen as the key indicator, adjusted by the size effect when necessary (e.g., a very large size should be noted).

For the detectability barrier, the extent of how difficult to track sensitive material is used as the indicator. Currently, five different levels are assigned.

The extent to which facilities, equipment, and processes are resistant to the production of weapon-usable materials is an important intrinsic barrier. As the modification involves time and labor, the cost of modification is used as indicator for the facility unattractiveness barrier.

The extent to which facilities and equipment inherently restrict access to fissile materials represents the facility accessibility barrier. Facilities with a high degree of remote, autonomous processes and operations present a higher barrier than those with more hands-on operations. Reactors with on-line refueling (especially those involving manual fuel-handling) have a lower barrier as the fissile materials can easily be accessed by the operator than those requiring special procedures designed for un-refueled operations throughout their lifetime. Time available for possible assess during one year of operation is used to indicate the effect of facility accessibility barrier.

The “available mass” barrier shows how much fissile material is in the facility. The amount of fissile material in the facility in terms of total number of critical mass is used as an indicator for this barrier.

Diversion detectability is a measure of the extent to which diversion or theft of materials from processes and facilities can be detected. The ability and efficiency of

accounting system will be important for this barrier. The uncertainty of the accounting system in terms of the lower limit of accounting capability can show the strength of this barrier.

Skills, Expertise, and Knowledge barrier is similar to the facility unattractiveness barrier and the time needed to modify the skills and apply them to a weapon programs is used as an indicator for the barrier.

The amount of time available for a potential proliferator to access the fissile materials is an important element in determining the overall effectiveness of the barriers to proliferation. The residence time of the fissile material in a given system is used as an indicator for the barrier.

Table 3-2: Indicators used for each intrinsic/technical barrier

Barrier	Proposed Quantities
Isotopic barrier	Bare sphere Critical Mass(CM) (kg)
	Equivalent Enrichment (%) (^{233}U, ^{235}U, ^{239}Pu)
	Spontaneous neutron generation rate (n/sec/kg)
	Heat generation rate (W/kg)
	Gamma Radiation (MeV/sec/kg)
Chemical Barrier	Cost to extract the fissile materials ($/Kg)
Radiological Barrier	Dose rate at 1-meter distance (mrem/hr/kg)
Mass and Bulk Barrier	Concentration of fissile material (# of CM/kg)
Detectability Barrier	Detectability levels
Facility Unattractiveness	Modification time needed to produce 1 CM in a year (weeks)
Facility Accessibility	Frequency of possible access to facility (days/yr)
Available Mass	Available fissile materials (# of CM)
Diversion Detectability	Uncertainty of measurement(# of CM/yr)
Skills, Expertise, and Knowledge	Time needed to modify the skills and apply it to weapons programs (yr)
Time	Time of residence of the materials of interest (yr)

The important quantities for all barriers are summarized in Table 3-2. To calculate bare sphere critical mass, two group of fissile material have to be treated in

different ways: U based and Pu isotopes and other actinides based. It can be seen in the Table 3-3 that Pu isotopes and other actinides have much higher spontaneous fission neutron rate and heat generation rate than ^{235}U. Table 3-4 shows the assumed isotopic composition of three types of materials.

Table 3-3 Nuclear properties of fissile and fertile nuclear materials [Ref 3-30]

Isotope	Half-life (y)	Neutrons/ sec-kg	Watts/kg	Bare Sphere Critical Mass (kg)
^{231}Pa	3.28E+04	nil	1.3	162
^{232}Th	1.41E+10	nil	nil	infinite
^{233}U	1.59E+05	1.23	0.281	16.4
^{235}U	7.00E+08	0.364	6.00E-05	47.9
^{238}U	4.50E+09	0.11	8.00E-06	infinite
^{237}Np	2.10E+06	0.139	0.021	59
^{238}Pu	88	2.67E+06	560	10
^{239}Pu	2.40E+04	21.8	2	10.2
^{240}Pu	6.54E+03	1.03E+06	7	36.8
^{241}Pu	14.7	49.3	6.4	12.9
^{242}Pu	3.76E+05	1.73E+06	0.12	89
^{241}Am	433	1540	115	57
^{243}Am	7.38E+03	900	6.4	155
^{244}Cm	18.1	1.10E+10	2.80E+03	28
^{245}Cm	8.50E+03	1.47E+05	5.7	13
^{246}Cm	4.70E+03	9.00E+09	10	84
^{247}Bk	1.40E+03	nil	36	10
^{251}Cf	898	nil	56	9

Table 3-4 Composition of ^{239}Pu based fissile materials

In Percentage	^{239}Pu	^{240}Pu	^{241}Pu	^{242}Pu	^{238}Pu
Super grade	96	3	1	0	0
Weapons grade	91	6	2	1	0
Reactor grade	51	28	14	5	2

Origen2.2 [Ref 3-34] is used to calculate spontaneous neutron rate, decay heat rate and gamma radiation from the selected materials: weapon grade U, super grade Pu, weapon grade Pu, and reactor grade Pu. MCNP4C2 [Ref 3-35] is used to calculate critical mass of all materials. As shown in Table 3-5, CM of ^{239}Pu based material is very smaller compared with ^{235}U based material, but the spontaneous

fission neutron generation rate, heat generation rate and gamma rate is much higher. It is complex to use Origen2.2 and MCNP to obtain SFN rate, heat rate, gamma rate and CM. To simplify the calculation, SFN, Heat and Radiation are calculated by using simple equation instead of ORIGEN2.2 in this study:

$$\text{SFN} = \sum_i w_i SFN_i$$

$$\text{Heat} = \sum_i w_i Heat_i$$

$$\text{Radiation} = \sum_i w_i Radiation_i$$

Where, w_i is mass fraction of isotope i in the material, SFN_i, $Heat_i$, $Radiation_i$ are SFN, Heat and Radiation from unit mass material i. Isotopes in Table 3-3 are considered. The rationality of this simplification is based on the fact that self-shielding effect is ignored in the ORIGEN2.2 calculation. The results are compared in the following figures. The results based on simplified equations for the materials in Table 3-5 are compared with results from ORIGEN2.2 (Figure 3-2-Figure 3-4). Mat. #s in Figure 3-2-Figure 3-4 mean the mat. # of material in Table 3-5. The figures show very good match.

Table 3-5 Quality of different fissile materials

Mat.#	Material	SFN (neutron/sec/kg)	Heat (W/kg)	Gamma rate (MeV/s/kg)	Critical Mass (Kg)
1	weapon grade U (80% ^{235}U)	1.55E+00	4.62E-05	9.93E+00	69.27
2	Super grade Pu	2.73E+04	2.09E+00	1.91E+03	10.36
3	Weapons grade Pu	7.15E+04	2.24E+00	2.38E+03	10.76
4	Reactor grade Pu	3.92E+05	1.48E+01	2.66E+04	14.22
5	U with ^{235}U enrichment 50%	6.52E+00	3.26E-05	6.21E+00	153.59
6	U with ^{235}U enrichment 35%	8.37E+00	2.54E-05	4.35E+00	283.74
7	U with ^{235}U enrichment 20%	1.02E+01	1.82E-05	2.49E+00	766.37
8	U with ^{235}U enrichment 1%	1.26E+01	9.01E-06	1.39E-01	9999.00
9	U with ^{235}U enrichment 0.72%	1.26E+01	8.88E-06	1.04E-01	9999.00

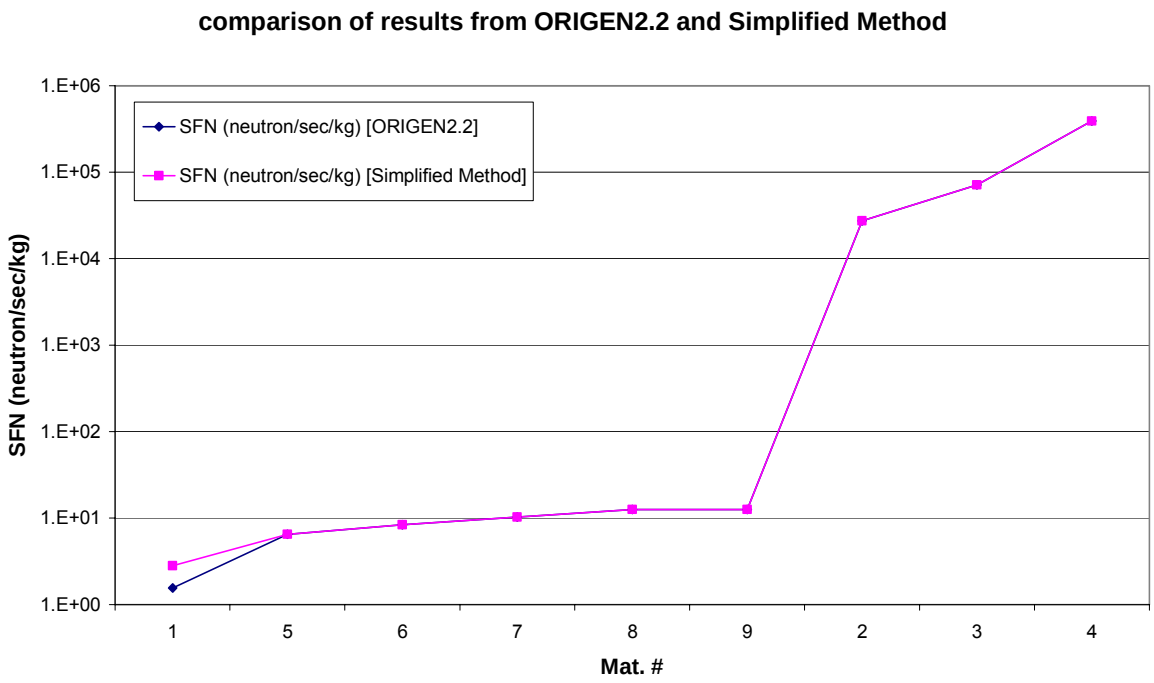

Figure 3-2 SFN rate comparison

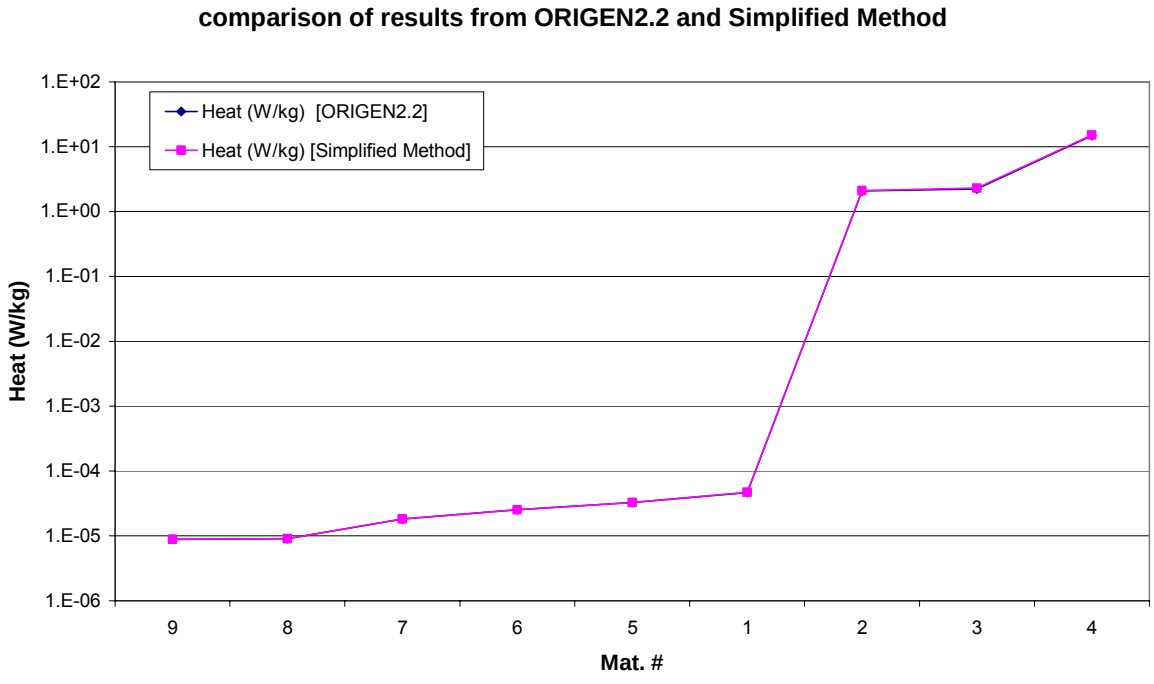

Figure 3-3 Heat rate comparison

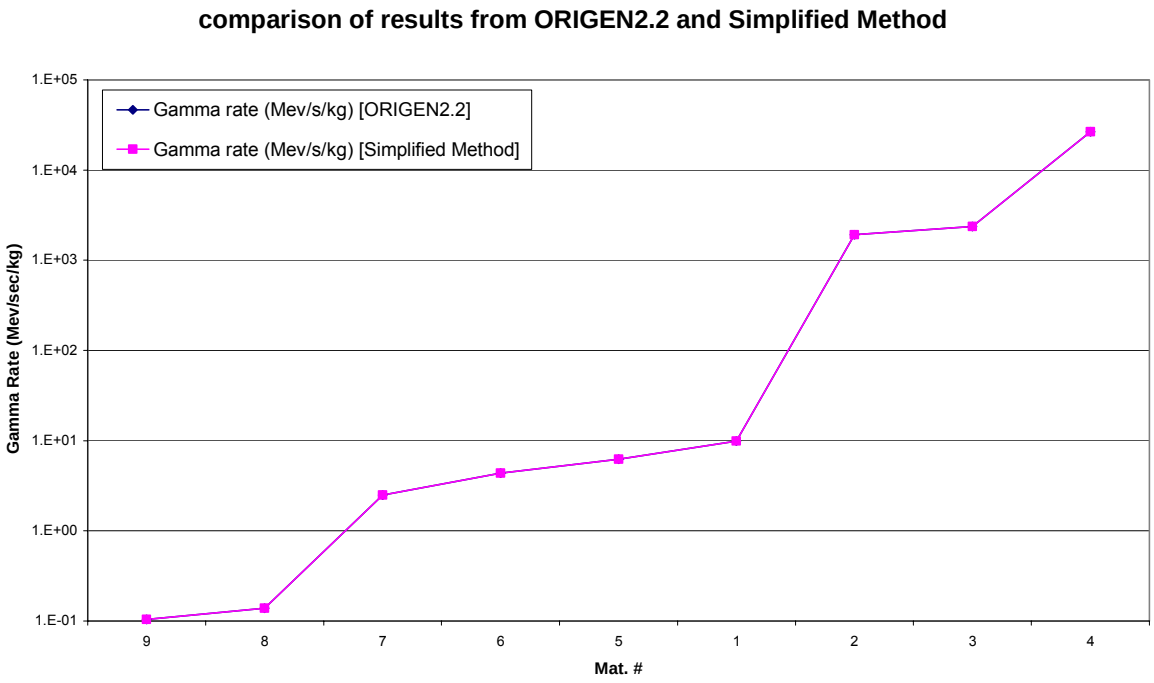

Figure 3-4 Gamma rate comparison

For critical mass, notice that two group of fissile material, U and actinides, the CM of mixture of actinides is always very small (most likely around 10 to 15). This is easily understandable, because most of the actinides have very small CM. But the story is very different for U. U, with varying fractions of ^{235}U, has very different CM from 70 to more than 700. When the CM is considered for the proliferation problem, the different effect for CM in the range of 10-20 kgs is small. But there is big difference for U material.

Based on previous analysis, a simplified method is proposed to calculate the CM of fissile material. If the fissile material is actinides based, the CM is always very small, the barrier level is always I- (ineffective minus), and there is no need to calculate the CM value. If the fissile material is U based, the CM can be calculated

by a simple proposed formula, the formula is obtained by fitting the CM calculation results from MCNP for different fraction ^{235}U:

$$CM = 41.69 * (EnrichmentofU235) ** (-1.824)$$

Table 3-6 CM calculation comparison

enrich. Of U235	Critical Mass (Kg) [MCNP]	calculated CM (kg) [Simple formula]
1	46.78	41.69
0.9	49.89	50.52
0.8	69.27	62.63
0.7	77.45	79.90
0.6	99.93	105.85
0.5	153.59	147.61
0.4	199.19	221.76
0.35	283.74	282.91
0.3	326.98	374.77
0.2	766.37	785.15
0.15	1217.27	1326.91
0.1	3385.97	2779.92

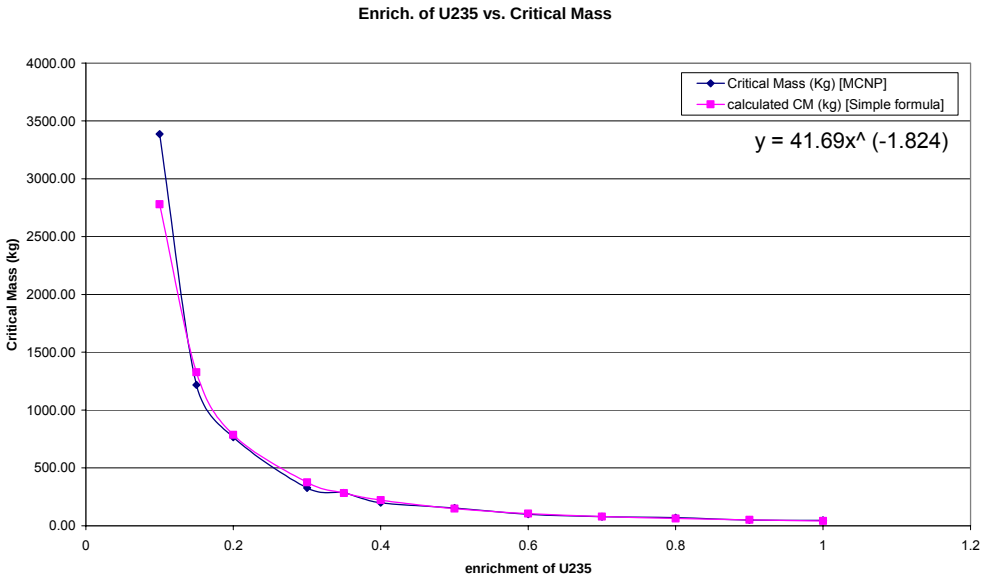

Figure 3-5 CM comparison

The differences of these two methods are shown in Figure 3-5 and Table 3-6. The variance can be observed but it is minor considering the vagueness of the effectiveness function.

Equivalent Enrichment is calculated based on fraction of ^{233}U, ^{235}U and ^{239}Pu. For U based material, it is assumed 12% enriched ^{233}U is "critically equivalent" to 20% ^{235}U (in mixture with ^{238}U) [Ref 3-30], then:

Equivalent Enrich. = 1.67 Enrichment of ^{233}U + Enrichment of ^{235}U

For Pu based material, as 35-50% enriched ^{235}U is treated as the same level as reactor grade Pu (~40% ^{239}Pu) in TOPS, and assume 70% enriched ^{235}U is the same effective for weapon use as Pu with 93% ^{239}Pu, an assumed formula is setup to calculate the equivalent enrichment:

Equivalent Enrich. = (percentage of ^{239}Pu in Pu- 40) $\times$0.44 + 40)

Concentration of fissile material is defined as concentration by mass (stage weight) divided by CM. Calculation of stage weight is shown in Table 3-20.

Dose rate at 1-meter to the surface can be obtained by using the MicroShield code [Ref 3-38].

Cost to extract the fissile materials is assigned by referred information from references. In this study, Ref 5-2 is used as main source for separation cost.

Concentration of fissile materials and available fissile materials can be calculated based on mass inventory from reactor simulation and critical mass.

Five levels can be assigned to detectability levels according the definition of the levels (Table 3-11) and system characteristics.

Uncertainty of measurement, time needed to modify the skills and stay time of materials are assumed in this study. The values of these quantities can be assigned by experts.

3.4.2 Barrier Effectiveness Function

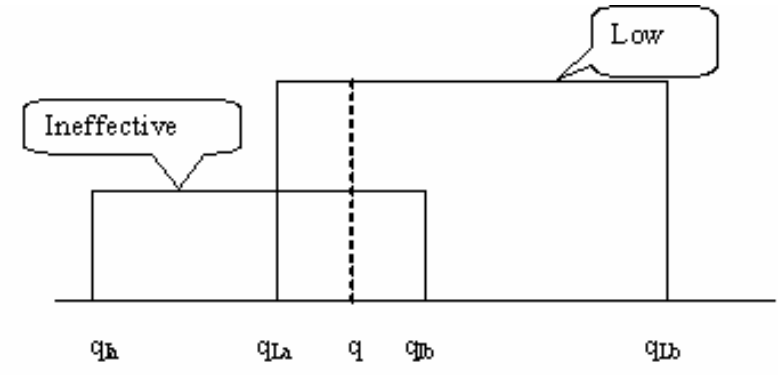

Figure 3-6 Barrier effectiveness function sample

For each variable and related barrier, a barrier effectiveness function was defined. The nature of the problem of quantifying proliferation resistance is still perceived to be uncertain and subjective. Instead of trying to define a clear relationship, a fuzzy relationship was setup to capture understanding of the relationship of a variable and its barrier. For certain values of each variable, a barrier level was defined to represent the barrier effectiveness. Step functions are used to show these relationships quantitatively. The concept is described in the following example (see Figure 3-6).

For an indicator or a quantity q, the range is from 0 to q_{max}, $0<q<q_{max}$, where q_{max} can be infinite. The range is divided into several sub-ranges for different barrier levels from Ineffective minus (I-) to very high plus (VH+). The adjacent sub-ranges can be overlapped, and no sub-range can be totally included by the other sub-

ranges. If a value of the quantity is located in the overlap area, the barrier level will be sum of fractional barrier levels represented by the overlapped sub-ranges. The fraction is determined by the location of the value in the overlap area. For example, in Figure 3-6, $q_{Ia}<q<q_{Ib}$ represents I (Ineffective) barrier level, and $q_{La} < q < q_{Lb}$ represents L (Low) barrier level, where $q_{Ia}< q_{La} <q_{Ib} < q_{Lb}$, it means these two sub-ranges overlaps. If $q_{La} < q <q_{Ib}$, q means mixed level of I and L level,

$$\text{barrier level} = \frac{q-q_{La}}{q_{Ib}-q_{La}}\ \text{L} + \left(1-\frac{q-q_{La}}{q_{Ib}-q_{La}}\right)\text{I};$$

Use of a fuzzy number for the variable captures its uncertainty. For each quantity Qi, there is a barrier effectiveness function g(Qi), a fuzzy number Bi which is the barrier level indicated by the quantity is obtained: Bi = g(Qi)

For quantity Qi with uncertainty, assuming the distribution of Qi is f(q): Qi = f(q)

Then the fuzzy number of level Bi can be obtained as:

$$\text{Bi} = \int g(q)\,f(q)dq \,/ \int f(q)dq$$

Based on available data for the fuel cycle under consideration, the barrier effectiveness functions calculated the barrier level for each respective barrier in a given fuel cycle step.

Barrier Effectiveness Functions are defined by the author based on a previous study [Ref 3-30, Ref 3-37] and shown in following tables.

Table 3-7 Barrier effectiveness functions of quantities for isotopic barrier

Critical Mass [kg]		
LevelID	Qmin	Qmax
I-	0	100
I	100	150
I+	150	200
L	200	300
M	300	700
H	500	800
VH	800	Max

Equivalent Enrichment [%]		
LevelID	Qmin	Qmax
I-	80	Max
I+	50	80
L-	45	50
L	40	45
L+	30	40
M-	20	30
M	10	20
H-	5	10
H	1	5
VH	0	1

SFN Rate [n/sec/Kg]		
LevelID	Qmin	Qmax
I-	0.E+00	1.E+02
I	1.E+02	1.E+03
I+	1.E+03	1.E+04
L-	1.E+04	1.E+05
L	1.E+05	5.E+05
M	5.E+05	1.E+06
H	1.E+06	Max

Heat Rate [W/Kg]		
LevelID	Qmin	Qmax
I-	0	1
L-	1	10
L	10	100
M	100	500
H	500	Max

Gamma Rate [MeV/sec/Kg]		
LevelID	Qmin	Qmax
I-	0.E+00	1.E+03
I	1.E+03	1.E+04
L	1.E+04	1.E+05
M	1.E+05	1.E+06
H	1.E+06	Max

Table 3-8 Barrier effectiveness functions of quantity for chemical barrier

Separation Cost [$]		
LevelID	Qmin	Qmax
I	0	10
I+	10	50
L-	50	150
L	150	250
L+	250	400
M-	400	600
M	600	800
M+	800	1000
H-	1000	1500
H	1500	2000
H+	2000	2500
VH-	2500	3000
VH	3000	5000
VH+	5000	Max

Table 3-9 Barrier effectiveness functions of quantity for radiological barrier

Dose Rate [mrem/hr/Kg]		
LevelID	Qmin	Qmax
I	0.E+00	1.E-05
L	1.E-05	5.E-05
M	5.E-05	1.E+00
H	1.E+00	1.E+01
VH	1.E+01	Max

Table 3-10 Barrier effectiveness functions of quantity for mass and bulk barrier

Concentration of fissile material [1/kg]		
LevelID	Qmin	Qmax
I	0.1	Max
L	0.02	0.1
M	0.01	0.02
H	0.005	0.01
VH	0	0.005

Table 3-11 Barrier effectiveness functions of quantity for detectability barrier

Detectability	
LevelID	Levels
I	No signature
L	No reliably signature
M	Moderately detected by active mean
H	Reliably detected by active means
VH	Easily detected by passive means

Table 3-12 Barrier effectiveness functions of quantity for facility unattractiveness barrier

Facility Modification Time [week]		
LevelID	Qmin	Qmax
I	0	0.1
L	0.1	1
M	1	5
H	5	30
VH	30	100
VH+	100	Max

Table 3-13 Barrier effectiveness functions of quantity for facility accessibility barrier

Frequency of Access [days/yr]		
LevelID	Qmin	Qmax
I	365	Max
L	243	365
M	180	243
H	100	180
VH	10	100
VH+	0	10

Table 3-14 Barrier effectiveness functions of quantity for available mass barrier

Available Mass [#ofCM]		
LevelID	Qmin	Qmax
I	10	Max
L	1	10
M	0.1	1
H	0.01	0.1
VH	0	0.01

Table 3-15 Barrier effectiveness functions of quantity for diversion detectability barrier

Uncertainty of Measurement [#ofCM/yr]		
LevelID	Qmin	Qmax
I	0.96	Max
M	0.82	0.96
H	0.65	0.82
VH	0.29	0.65
VH+	0	0.29

Table 3-16 Barrier effectiveness functions of quantity for skills/expertise/knowledge barrier

Knowledge Modification Time [yr]		
LevelID	Qmin	Qmax
I	0	0.1
L	0.1	0.5
M	0.5	2
H	2	10
VH	10	Max

Table 3-17 Barrier effectiveness functions of quantity for time barrier

Stay Time [yr]		
LevelID	Qmin	Qmax
I	10	Max
L	5	10
M	2	5
H	0.5	2
VH	0	0.5

3.4.3 Fuzzy Number Definition and Operation

To quantify the proliferation resistance represented by each barrier, the barrier effectiveness was defined as fuzzy numbers to represent the information that is imprecise and uncertain. Following the TOPS BF, the effectiveness was classified into 5 classifications (Insignificant, Low, Medium, High, Very High) to differentiate the effectiveness of each barrier, representing the strength against proliferation. For example, $\tilde{H}$ represents "H", or "high", where $\tilde{H}$ = { x_H | $\mu_{\tilde{H}}(x_H)$ }, x_H is relative proliferation resistance, and $\mu_{\tilde{H}}(x_H)$ is the membership function of x_H. Then $\tilde{A}_i$ = {($x_{\tilde{A}_i}$, $\mu_{\tilde{A}_i}(x_{\tilde{A}_i})$)} (i=1,2…N) represents barrier level or barrier strength of each barrier i. (N is the total number of barriers including material and technical barriers and is 11 for in the study).

A fuzzy number can be defuzzified to a crisp value. And Yager has proposed one function to mapping each fuzzy set into the real line, where a natural order exists [Ref 3-43, Ref 3-44]. The function is:

$$F_1(\tilde{u}) = \frac{\int x\mu_{\tilde{u}}(x)dx}{\int \mu_{\tilde{u}}(x)dx}$$

This number is also called the centroid value of a fuzzy number. It will be called as mean value of a fuzzy number in the rest of the report.

To define fuzzy number for 15 levels used in TOPS report, a Gaussian distribution shape is assumed for each fuzzy number $\mu(x) = e^{\frac{-(x-c)^2}{2\sigma^2}}$ [Ref 3-33]. The shape is controlled by c and σ, where c is the centroid value/mean value. The mean value of each level follows one based consideration: for five main group

Ineffective, Low, Moderate, High, Very High, the mean value increases from Ineffective to Very High. And mean value of one main group is two times of the mean value of next lower level. One set of definition is listed in Table 3-18. σ is assumed as 5% of the mean value.

Table 3-18 Fuzzy number definition for all 15 levels

Level ID	Level Name	Mean
1	I-	0.038
2	I	0.044
3	I+	0.05
4	L-	0.07
5	L	0.088
6	L+	0.111
7	M-	0.14
8	M	0.176
9	M+	0.222
10	H-	0.279
11	H	0.352
12	H+	0.443
13	VH-	0.559
14	VH	0.704
15	VH+	0.887

Fuzzy numbers (Bi) of each barrier are combined to get a fuzzy barrier value, $\tilde{S}_j$ ={($x_{\tilde{S}_j}$, $\mu_{\tilde{S}_j}(x_{\tilde{S}_j})$)} for a stage *j* in a fuel cycle (for a given fuel cycle, there could be up to 35 fuel cycle stages starting from mining). Calculation of $\tilde{S}$ ={($x_{\tilde{S}}$, $\mu_{\tilde{S}}(x_{\tilde{S}})$)} is based on the following:

$x_{\tilde{S}} = \frac{\sum_{i=1}^{11} x_{\tilde{A}_i} w_i}{\sum_{i=1}^{11} w_i}$, $\mu_{\tilde{S}}(x_{\tilde{S}}) = \max_{x_{\tilde{A}_i}} (\min(\mu_{\tilde{A}_i}(x_{\tilde{A}_i}), \text{ i=1,2,…,11}))$, which means take maximum membership function among all groups $x_{\tilde{A}_i}$ that satisfy $x_{\tilde{S}} = \frac{\sum_{i=1}^{11} x_{\tilde{A}_i} w_i}{\sum_{i=1}^{11} w_i}$, and membership function of each group is minimum membership function of $x_{\tilde{A}_i}$, i=1,2,…,11. The different weights in w_i represent the relative importance of each barrier against a potential diversion attempt by a "developing" nation.

Table 3-19 Barrier weights as relative importance of each barrier with respect to a covert proliferation attempt by a "developing" nation

Barrier	COST (M$)	Source	Weight
Isotopic barrier	1300	1.3 billion includes from research to commercial scale [Ref 3-31]. One tenth is used for covert weapon program.	130
Chemical Barrier	55	1977 OTA report for a U.S.-built simplified reprocessing plant [Ref 3-32]	55
Radiological Barrier	5	Personal conversation with expert giving hot cell service	5
Mass and Bulk Barrier	0.15	Assuming 3 trip needed, 5 persons per trip, one hour per trip, and $10000/hour/person	0.15
Detectability Barrier	0.14	$500/kg shielding fee, and 280 kg/assembly of BWR	0.14
Facility Unattractiveness	13.3	Capital cost for a reactor comparable to Brookhaven graphite research reactor	13.3
Facility Accessibility	1	To access the facility without notice is a tough job. Assuming 1 million job	1
Available Mass		Assumed as the same as chemical barrier	55
Diversion Detectability		Assumed as the same as time barrier	1
Skills, Expertise, and Knowledge	3.2	8 specialists, 4 year of work, 100 k/year (nuclear proliferation with particle accelerators)	3.2
Time	1	Assume 1 million	1

Different weights, w_i, represent relative importance of each barrier against the threat under consideration. In this study, the threat under consideration was a

"developing" nation who may be interested in nuclear weapon development out of the civilian nuclear power program. Considering this, the effort needed to overcome each barrier was approximately estimated as cost and used as weights to distinguish the relative strengths of the barriers (Table 3-19). The barrier effectiveness values for each fuel cycle steps were combined to represent the proliferation resistance of the entire fuel cycle. In this combination process, a different set of weighting factors are also needed to represent the relative importance of different fuel cycle stages with respect to proliferation. Concentration of sensitive nuclear materials in the mass flow was used as weights in this process as Table 3-20. Where,

Table 3-20 Concentration of sensitive nuclear materials (sample)

	Material form	Mass fraction of U	Mass fraction of Pu	Enrich (^{235}U)	Enrich (^{239}Pu)	Con (^{235}U+^{239}Pu)
Beginning of the cycle						
Storage of fresh fuel	UO2	88	0	4	0	3.5200
Fuel handling	UO2	88	0	4	0	3.5200
Reactor irradiation	UO2	88	0	4	0	3.5200
Spent-fuel handling	spent fuel	88	1	0.8	40	2.5260
Storage of spent fuel	spent fuel	88	1	0.8	40	2.5260

$con(^{235}U+^{239}Pu) = con(^{235}U) + con(^{239}Pu) \times CM(^{235}U / CM(^{239}Pu)$.

$con(^{235}U)$ = Enrichment of $^{235}U \times$ mass fraction of U

$con(^{239}Pu)$ = Enrichment of $^{239}Pu \times$ mass fraction of Pu

The fuzzy barrier value for each fuel cycle stage can then be combined to generate a fuzzy number to represent the proliferation resistance of the entire fuel cycle system.

To qualitatively explain the quantitatively result, one way is to define relative distance (RD) of a system mean PR to mean PR of each level:

RD = non-negative value of (system mean PR – mean PR of the level)/ mean PR of the level

The smallest relative distance indicates the level the system belongs. Sample shown in Table 3-21, if the mean value is 0.2938, the smallest RD is 0.05 for level "H-". It means a system with mean PR value equals 0.2938 can be grouped into level "H-".

Table 3-21 Qualitative explanation of quantitative result

Level ID	Level Name	Level Mean	RD (if the mean = 0.2938)
1	I-	0.038	6.73
2	I	0.044	5.68
3	I+	0.05	4.88
4	L-	0.07	3.20
5	L	0.088	2.34
6	L+	0.111	1.65
7	M-	0.14	1.10
8	M	0.176	0.67
9	M+	0.222	0.32
10	H-	0.279	0.05
11	H	0.352	0.17
12	H+	0.443	0.34
13	VH-	0.559	0.47
14	VH	0.704	0.58
15	VH+	0.887	0.67

3.5 Fuzzy Number Defuzzification and Ranking

Fuzzy number is different from a crisp number as it contains more information than a crisp number. There are many different fuzzy number ranking methods [Ref 3-40-Ref 3-42] to explain the fuzzy number and help decision-making. Dubois and Prade proposed a set of four indices able to completely describe the relative location of two fuzzy numbers $\tilde{u}_i$ and $\tilde{u}_j$. They define:

(1) a grade of possibility of dominance (of $\tilde{u}_i$ over $\tilde{u}_j$),

$$\text{PD}(\tilde{u}_i / \tilde{u}_j) \triangleq \text{Poss}(\tilde{u}_i \geq \tilde{u}_j) = \sup_{x_i, x_j, x_i \geq x_j} \min[\mu_{\tilde{u}_i}(x_i), \mu_{\tilde{u}_j}(x_j)]$$

(2) a grade of possibility of strict dominance

$$\text{PSD}(\tilde{u}_i / \tilde{u}_j) \triangleq \text{Poss}(\tilde{u}_i > \tilde{u}_j) = \sup_{x_i, x_j, x_j \geq x_i} \inf \min[\mu_{\tilde{u}_i}(x_i), 1 - \mu_{\tilde{u}_j}(x_j)]$$

(3) a grade of necessity of dominance

$$\text{ND}(\tilde{u}_i / \tilde{u}_j) \triangleq \text{Nec}(\tilde{u}_i \geq \tilde{u}_j) = \inf_{x_i, x_j, x_j \geq x_i} \sup \max[1 - \mu_{\tilde{u}_i}(x_i), \mu_{\tilde{u}_j}(x_j)]$$

(4) a grade of necessity of strict dominance

$$\text{NSD}(\tilde{u}_i / \tilde{u}_j) \triangleq \text{Nec}(\tilde{u}_i > \tilde{u}_j) = 1 - \text{PD}(\tilde{u}_j / \tilde{u}_i)$$

Dubois and Prade's method behaves relatively better than other methods compared in Ref 3-40. In this study, PD and PSD will be used to assist comparison of the system performances.

3.6 Application of Fuzzy Logic to Barrier Framework

Demonstration of the fuzzy logic application to render the TOPS BF into a quantitative model is given in this section. The results of Lawrence Livermore

National Laboratory (LLNL)'s effort [Ref 3-37] in applying the TOPS BF to ten different (existing and proposed) reactor systems and their associated fuel cycles (excluding institutional barriers) were utilized for this purpose. The systems evaluated include HTGR (prismatic fuel high temperature gas cooled reactor), PBR (pebble bed reactor), STAR (small, transportable, autonomous reactor), LWR-OT-ThU (light water reactor-once through-thoria urania fuel), LWR-OT-HB (high burnup), LWR-OT-Th (thorium seed blanket core), LWR-OT, IFR/BREST (integral fast reactor/ Russian lead cooled fast reactor), LWR-MOX (mixed oxide fuel), and IRIS-MOX (international reactor innovative secure). Table 3-22 is one sample result for LWR-OT system from LLNL's work [Ref 3-37]. The results from this qualitative assessment were used as input for the application of fuzzy logic. The barrier levels estimated in the report were replaced by fuzzy numbers as defined in Figure 3-7.

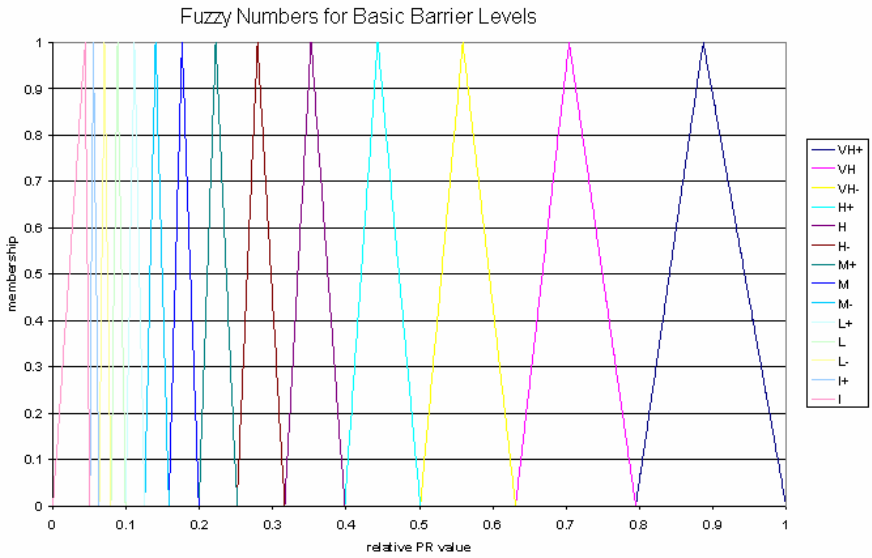

Figure 3-7 Assigned fuzzy numbers for basic barrier levels

MATLAB [Ref 3-33] was used for fuzzy number calculations. The fuzzy numbers for each fuel cycle stage were combined as described in section 3.4.3. Proliferation

resistance of the LWR-MOX fuel cycle as assessed by the proposed method is shown in Figure 3-8 (as example). The figure shows variations of proliferation resistance of LWR-MOX at different fuel cycle stages from mining (stage 1) to waste disposal (stage 35).

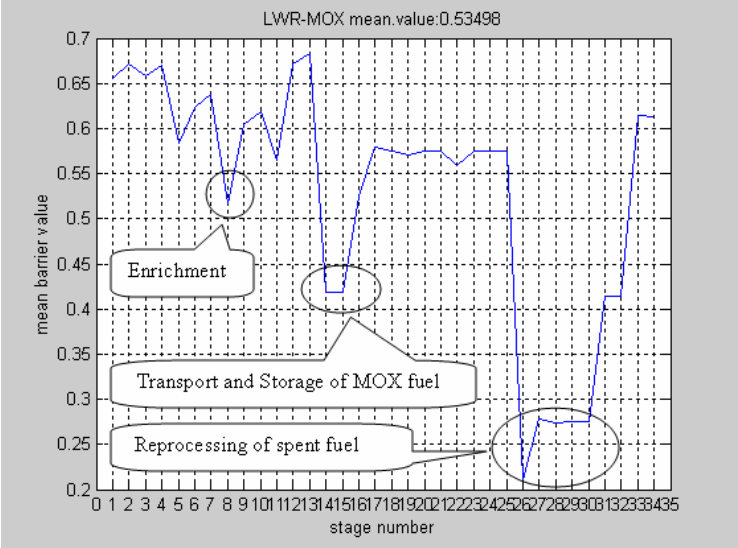

Figure 3-8 Mean proliferation resistance of each stage for LWR-MOX

Table 3-23 shows the summary comparisons of proliferation resistance of ten different reactor systems. Differences in proliferation resistance between “full fuel cycle” and “reactor system only” are also indicated. Here “full fuel cycle” means including all front end, reactor operation, and the back end. “Reactor system only” includes only the transport of fresh and spent fuel, the associated fuel storage, and the reactor operation. The numbers represent the mean relative fuzzy barrier value of each system.

The results indicated that if the LWR-OT is used as a reference system, HTGR, STAR, and PBR are better than the reference with respect to proliferation resistance. Comparison between “reactor system only” and “full fuel cycle” results

indicates that LWR-MOX and IRIS-MOX systems become much less proliferation resistant when the full fuel cycle is provided. This is mainly due to the wet reprocessing step involved - IFR/BREST was better with the use of pyroprocessing. The other three systems (LWR-OT-HB, LWR-OT-ThU, and LWR-OT-Th) show almost the same proliferation resistance as the reference system.

Table 3-22 Barriers framework applied to the once-through LWR cycle

	Material barriers					**Technical barriers**					
Stage of the fuel cycle	**Isotopic**	**Radiological**	**Chemical**	**Mass and bulk**	**Detectability**	**Facility unattractiveness**	**Facility access**	**Available mass**	**Facility detectability**	**Skills, knowledge, expertise**	**Time**
Beginning of the cycle											
Mining	VH	I	M	H	M	VH	I	I	I	VH	I
Transport	VH	I	M	H	M	VH	I	L-M	I	VH	M
Milling	VH	I	M	H	M	VH	I	I	I	VH	M
Transport	VH	I	M	H	M	VH	I	L-M	I	VH	M
Conversion	VH	I	L	H	M	VH	I	I	M	M	M
Storage	VH	I	L	H	M	VH	I	I	M	VH	M
Transport	VH	I	L	H	M	VH	I	L-M	M	VH	M
Uranium enrichment	VH	I	L	M	M	I-M	M-VH	I	VH	I	H
Storage	VH	I	L	M	M	VH	I	I	M	VH	VH
Transport	VH	I	L	M	M	VH	I	L-M	M	VH	VH
Fuel fabrication	VH	I	L	M	M	VH	I	I	M	M	H
Storage	VH	I	M	H	M	VH	I	I	M	VH	VH
Transport	VH	I	M	H	M	VH	I	L-M	M	VH	VH
Reactor operations											
Storage of fresh fuel	VH	I	M	VH	M	VH	I	I	VH	VH	VH
Fuel handling	VH	I	M	VH	M	VH	L	I	VH	VH	VH
Reactor irradiation	L	VH	VH	VH	VH	L-H	VH	I	VH	M	H
Spent-fuel handling	L	VH	VH	VH	VH	VH	M	I	VH	VH	VH
Storage of spent fuel	L	VH	VH	VH	VH	VH	M	I	VH	VH	M
On-site dry storage	L	H-VH	VH	VH	VH	VH	M	I	VH	VH	L-M
Back-end of the cycle											
Transport (of spent fuel)	L	H-VH	VH	VH	VH	VH	M	I	VH	VH	VH
Storage (of spent fuel)	L	H-VH	VH	VH	VH	VH	H	I	VH	VH	H
Once-through:											
Processing for direct disposal	L	H-VH	VH	VH	VH	H-VH	H	I	VH	H-VH	H
Transport	L	H-VH	VH	VH	VH	VH	M	I	VH	VH	VH
Pre-emplacement storage	L	H-VH	VH	VH	VH	VH	H	I	VH	VH	H
Repository emplacement	L	H-VH	VH	VH	VH	VH	VH	I	<VH-VH	VH	I

VH very high
H high
M medium
L low
I ineffective
NA not applicable

One of the strengths of the method is the qualitative interpretation of the results: Based on the definition of the fuzzy numbers, the result directly reflects qualitative effectiveness of the proliferation barrier of the system, as characterized in the TOPS report [Ref 3-30]. These qualitative interpretations are also given in Table 3-23. According to the results, the reference system, LWR-OT, presents a slightly high barrier against proliferation attempts. Fuzzy numbers that represent proliferation resistance of the entire fuel cycle system for ten systems are shown together in Figure 3-9 for full cycle consideration and in Figure 3-10 for reactor system only consideration. Figure 3-11 to Figure 3-30 show fuzzy numbers for each fuel cycle system under two different considerations. In both two different consideration scenarios, the fuzzy numbers overlap to each other in a relative large range. This explains that the mean values of the ten systems are very close, especially the first 7 systems. And the ten systems can only be classified into three levels and the first 7 (in full cycle consideration) and the ranking 2 to 7 systems (in reactor system only consideration) are in the same level with the slight difference among their mean system PR values.

Table 3-23 Comparison of overall proliferation resistance of different reactor systems and their fuel cycles (threat in a developing country, numbers are the centroid mean barrier value)

system	Full fuel cycle	Barrier effective-ness	Reactor system only	Barrier effective-ness
PBR	0.63	High -	0.65	High
HTGR	0.62	High -	0.64	High -
STAR	0.61	High -	0.65	High -
LWR-OT	0.60	High -	0.62	High -
LWR-OT-HB	0.60	High -	0.61	High -
LWR-OT-ThU	0.59	High -	0.60	High -
LWR-OT-Th	0.58	High -	0.59	High -
LWR-MOX	0.33	Low+	0.54	Medium+
IRIS-MOX	0.33	Low+	0.54	Medium+
IFR/BREST	0.44	Medium	0.50	Medium+

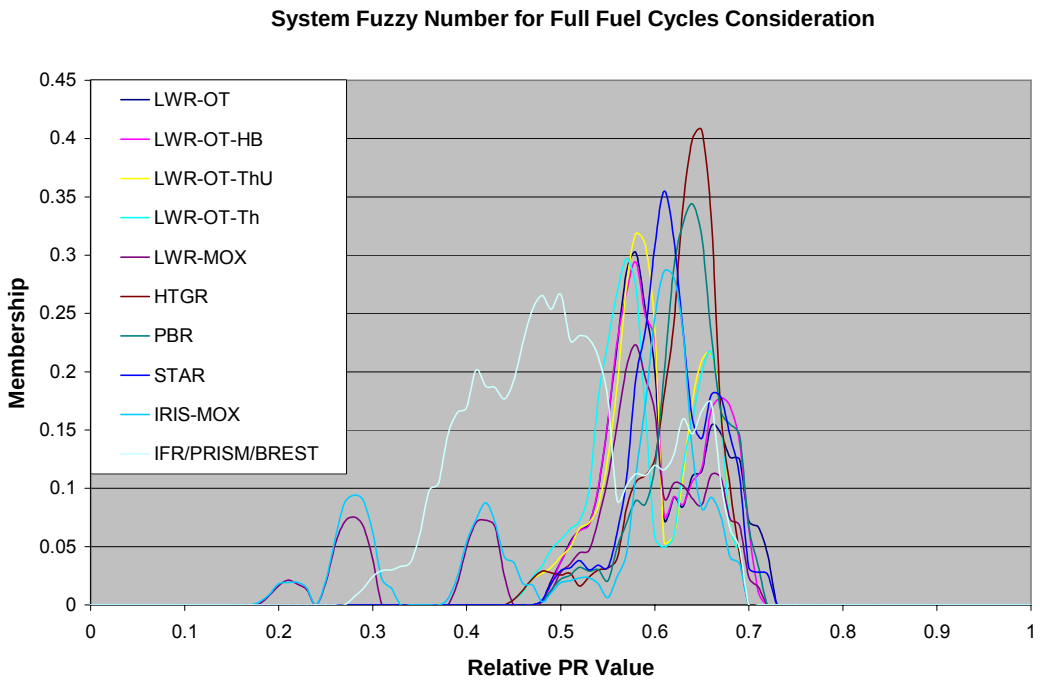

Figure 3-9 System fuzzy numbers for full cycle consideration (ALL)

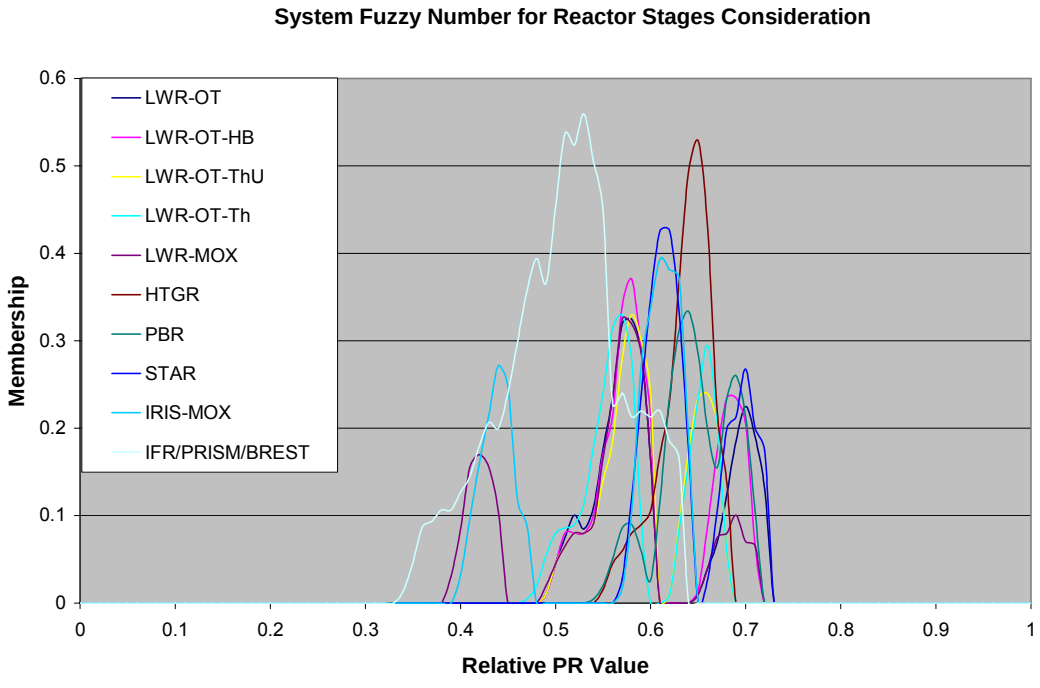

Figure 3-10 System fuzzy numbers for reactor operation only consideration (ALL)

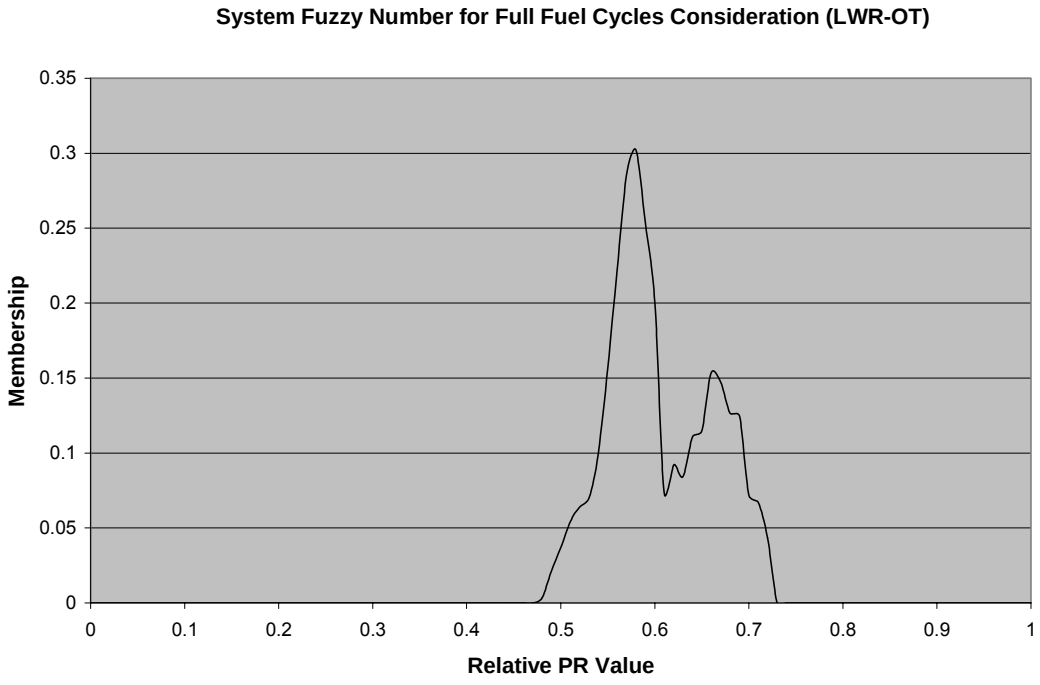

Figure 3-11 System fuzzy number for full cuel cycles consideration (LWR-OT)

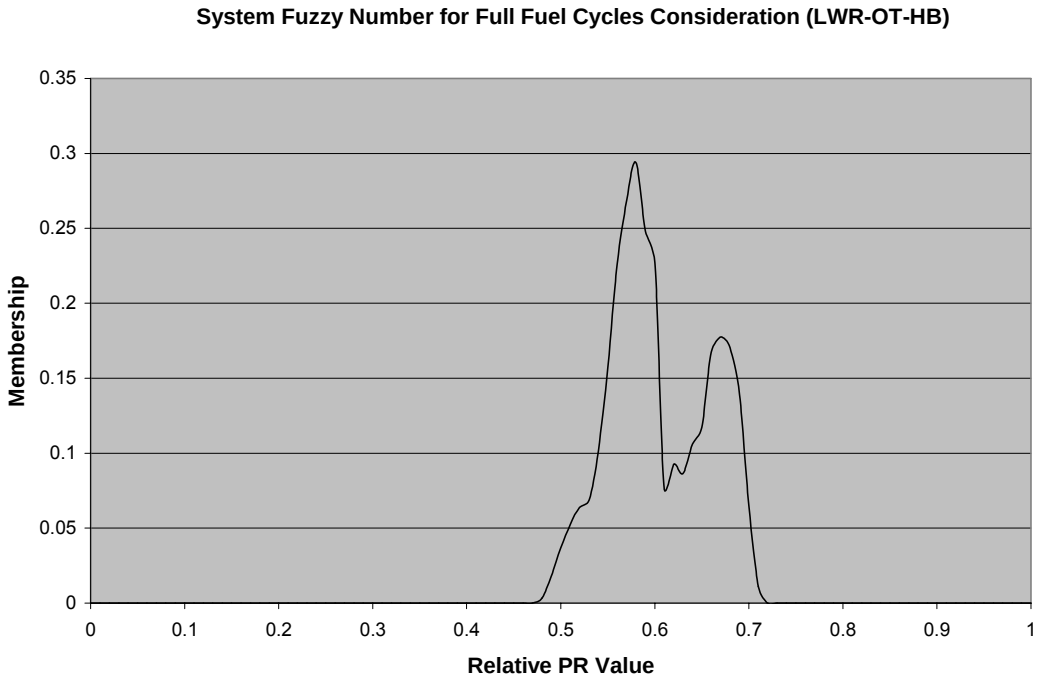

Figure 3-12 System fuzzy number for full cuel cycles consideration (LWR-OT-HB)

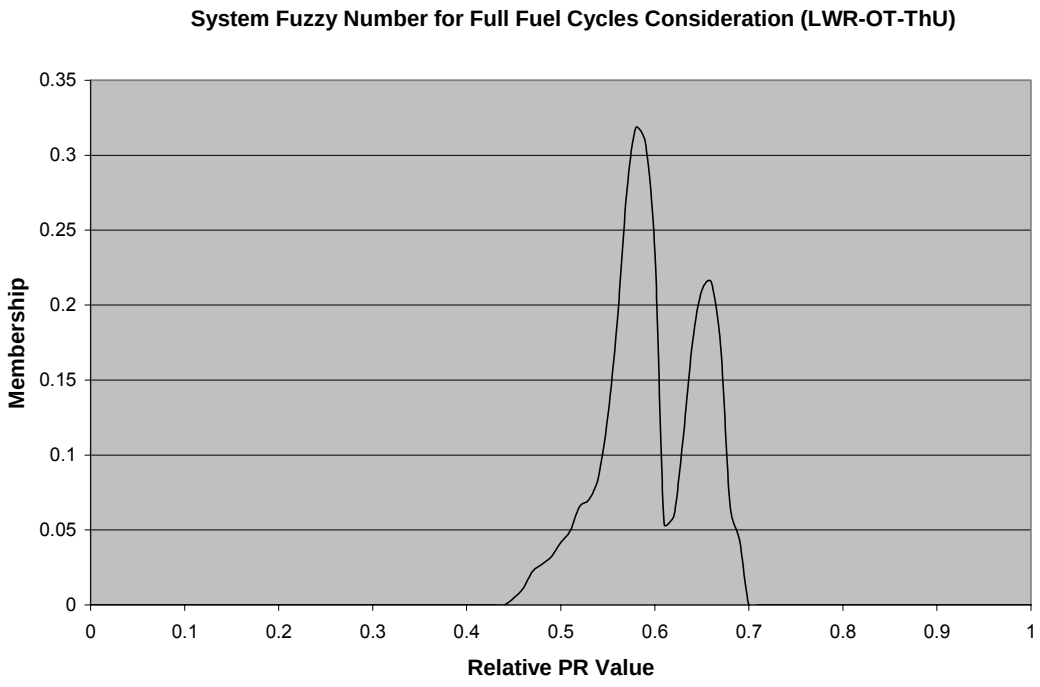

Figure 3-13 System fuzzy number for full cuel cycles consideration (LWR-OT-ThU)

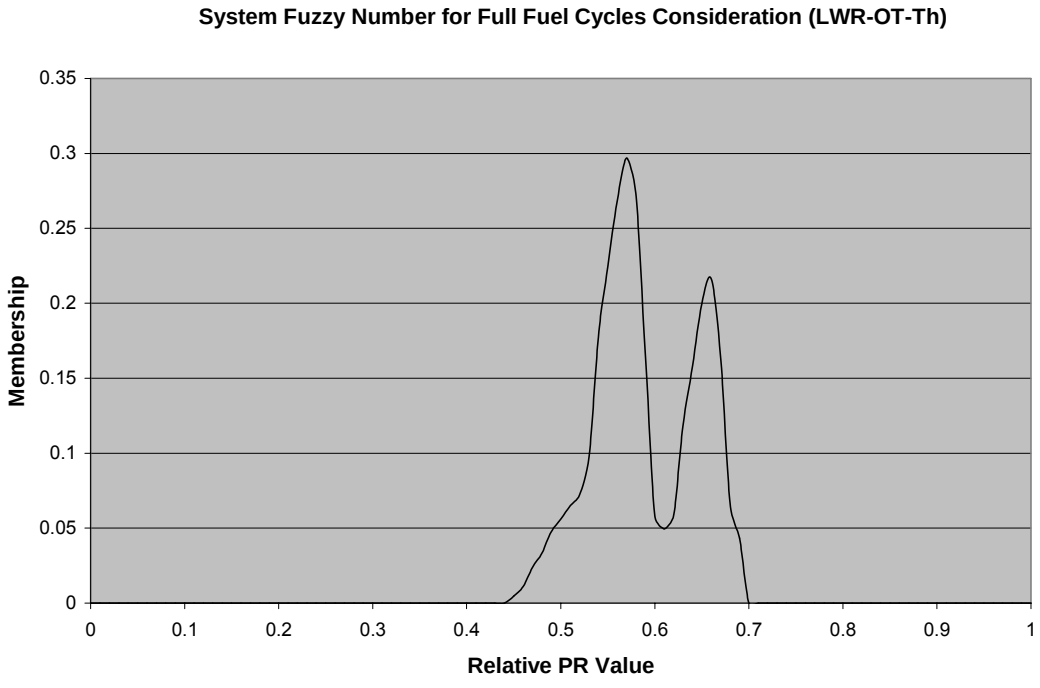

Figure 3-14 System fuzzy number for full cuel cycles consideration (LWR-OT-Th)

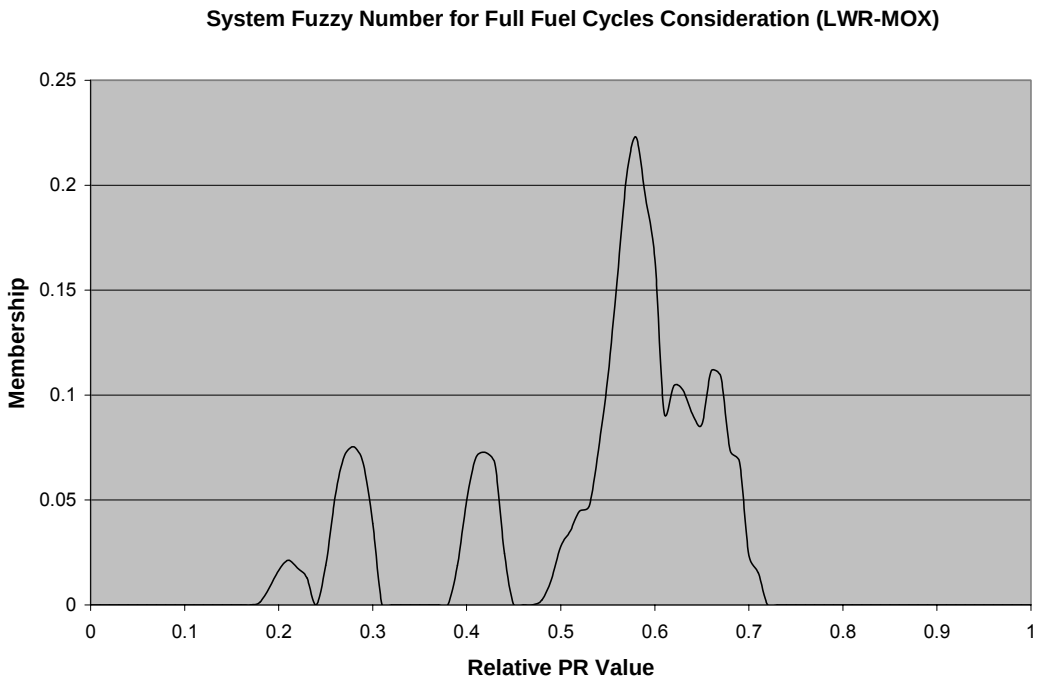

Figure 3-15 System fuzzy number for full cuel cycles consideration (LWR-MOX)

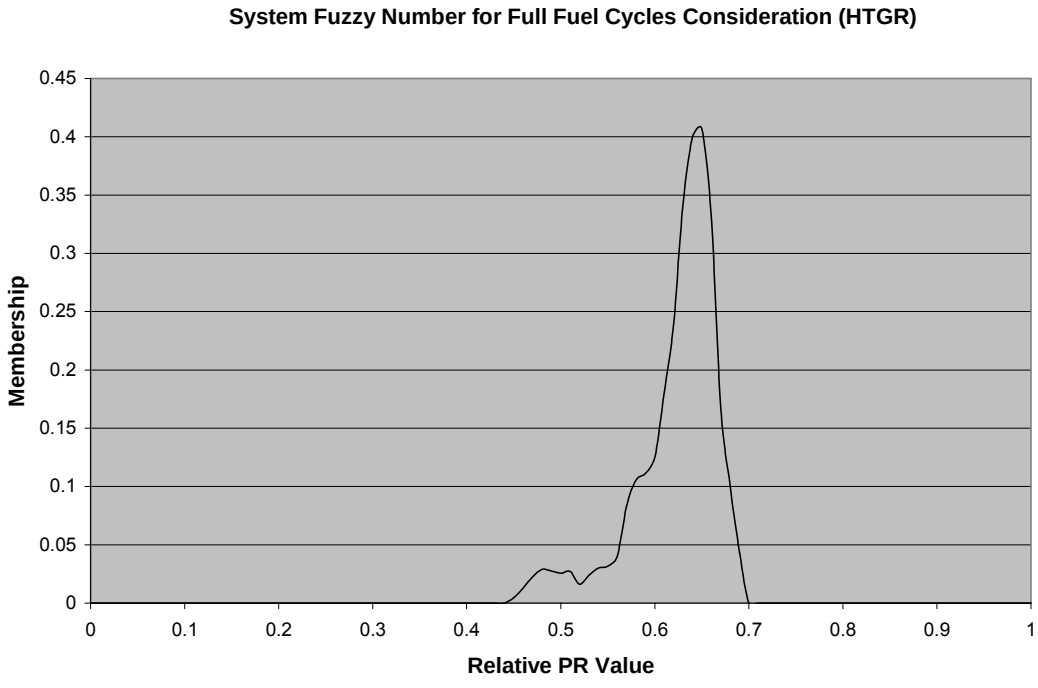

Figure 3-16 System fuzzy number for full cuel cycles consideration (HTGR)

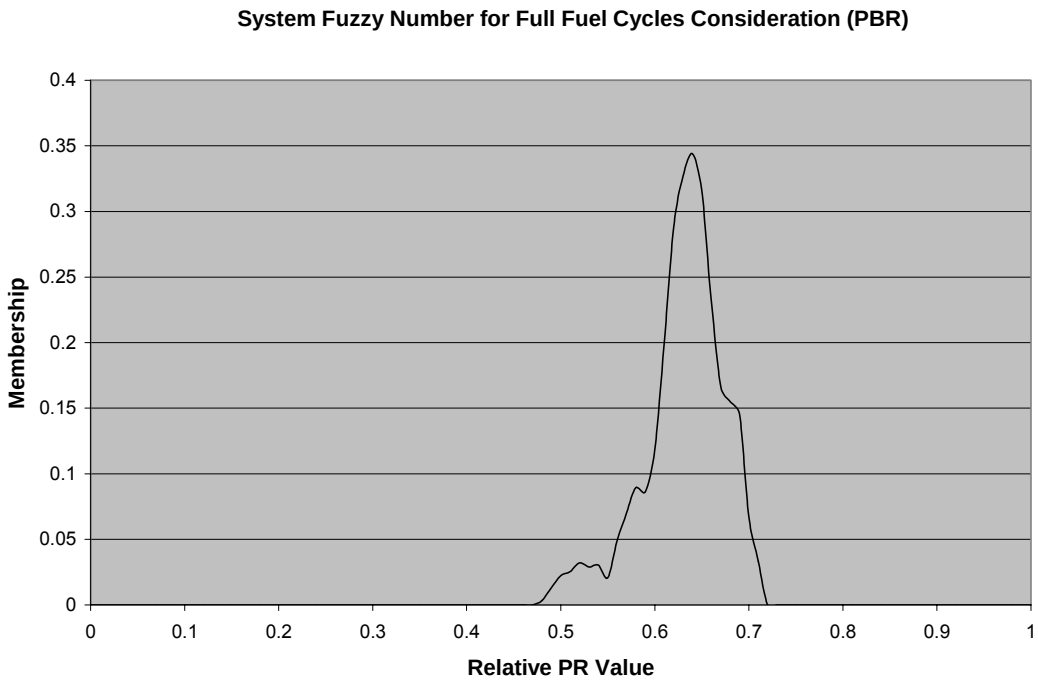

Figure 3-17 System fuzzy number for full cuel cycles consideration (PBR)

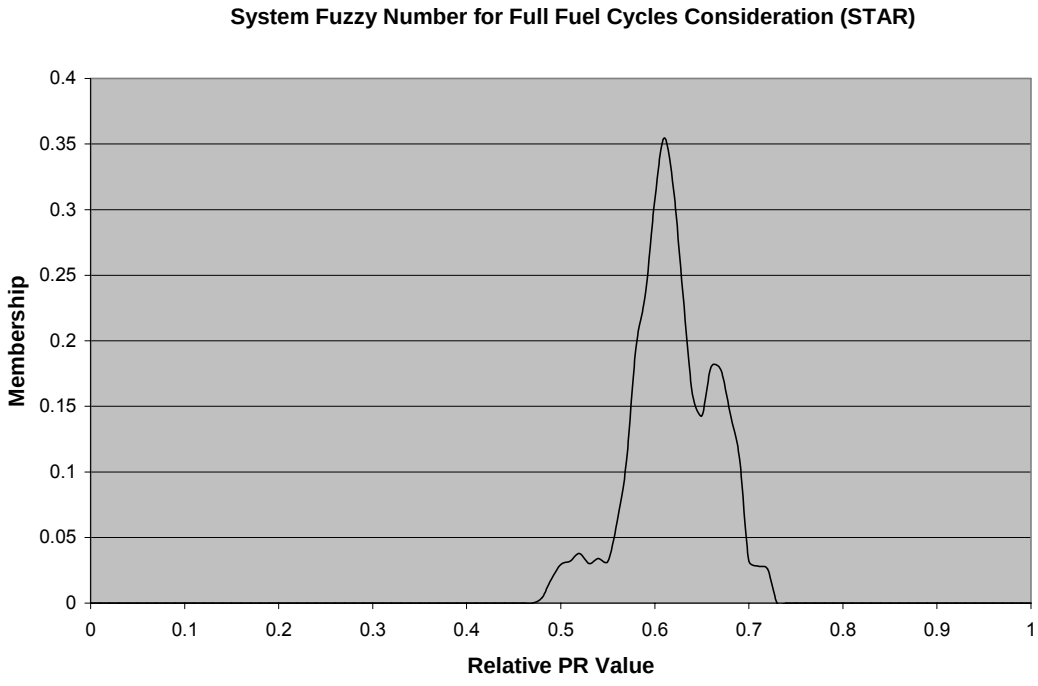

Figure 3-18 System fuzzy number for full cuel cycles consideration (STAR)

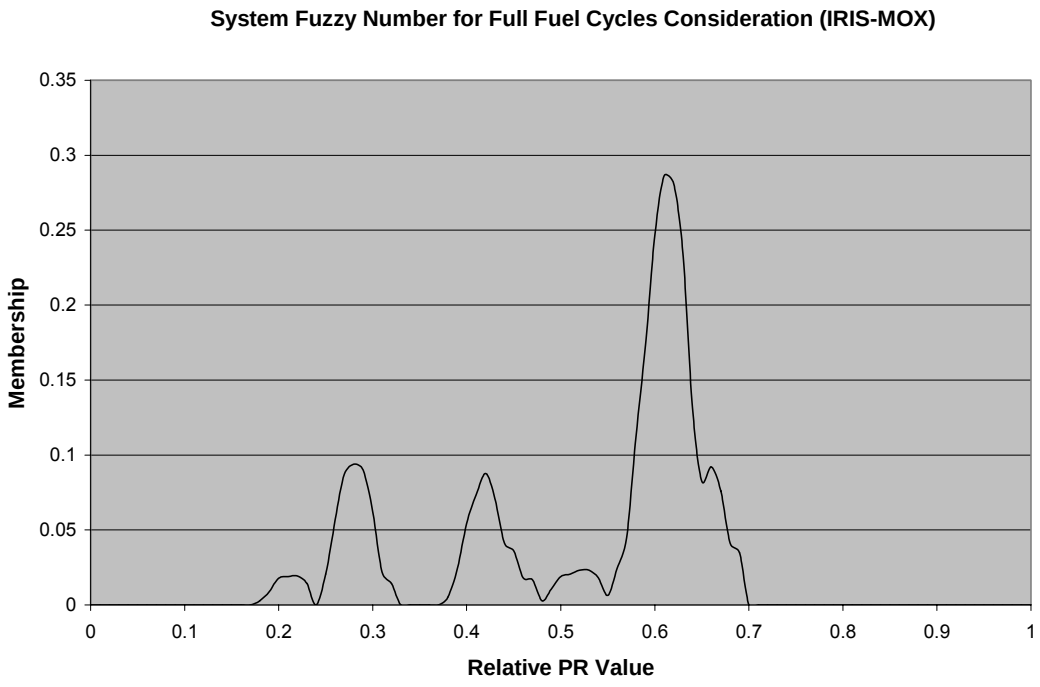

Figure 3-19 System fuzzy number for full cuel cycles consideration (IRIS-MOX)

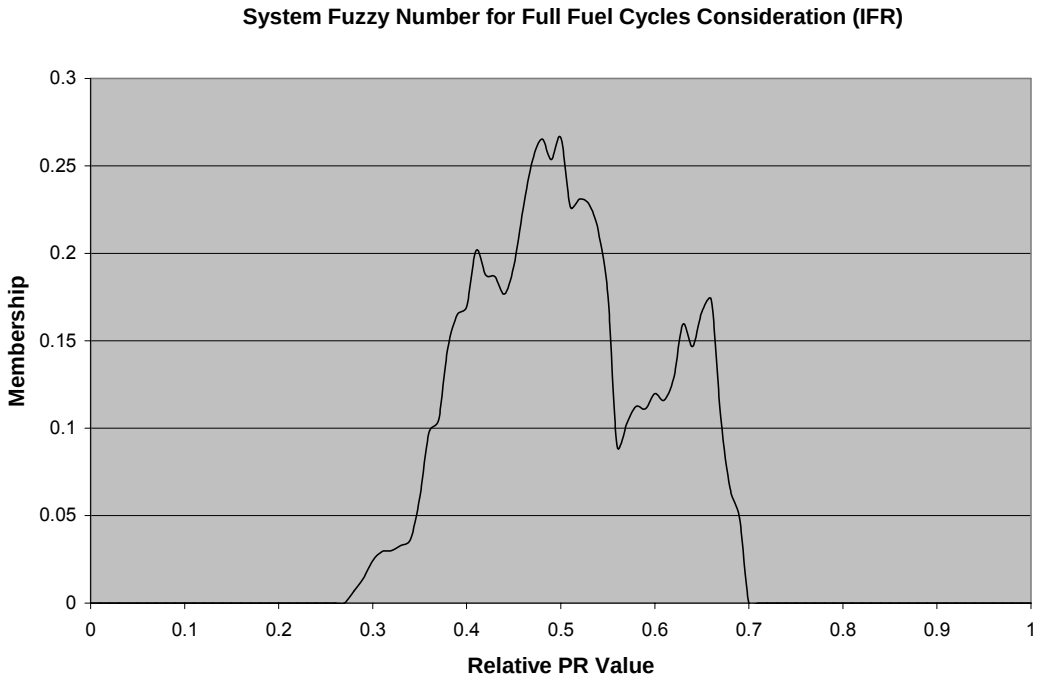

Figure 3-20 System fuzzy number for full cuel cycles consideration (IFR)

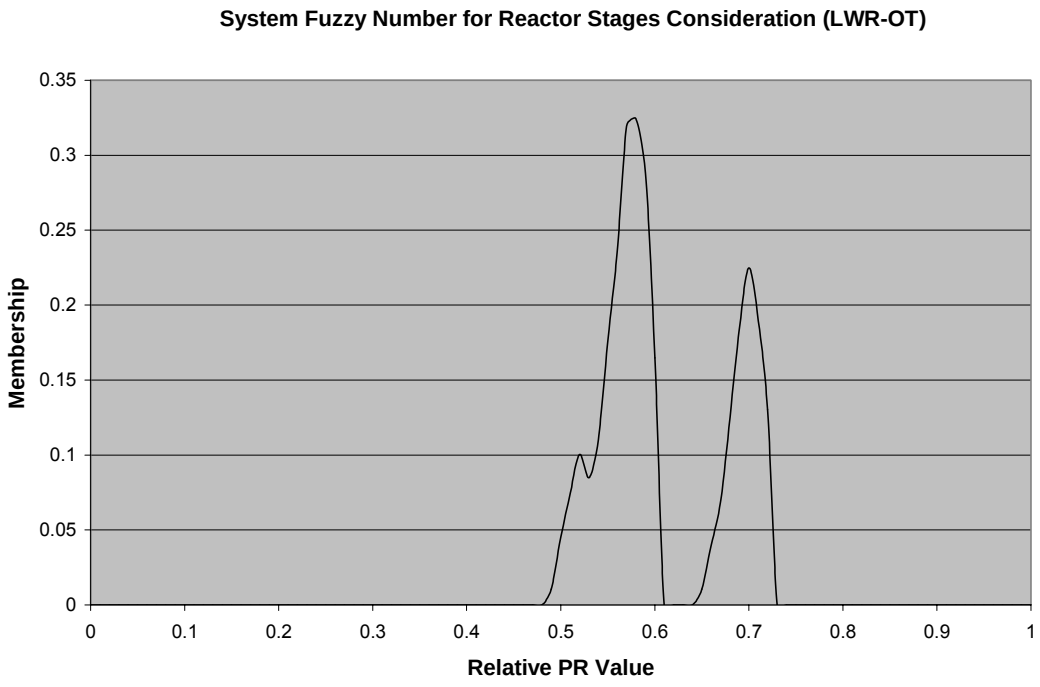

Figure 3-21 System fuzzy number for reactor stages consideration (LWR-OT)

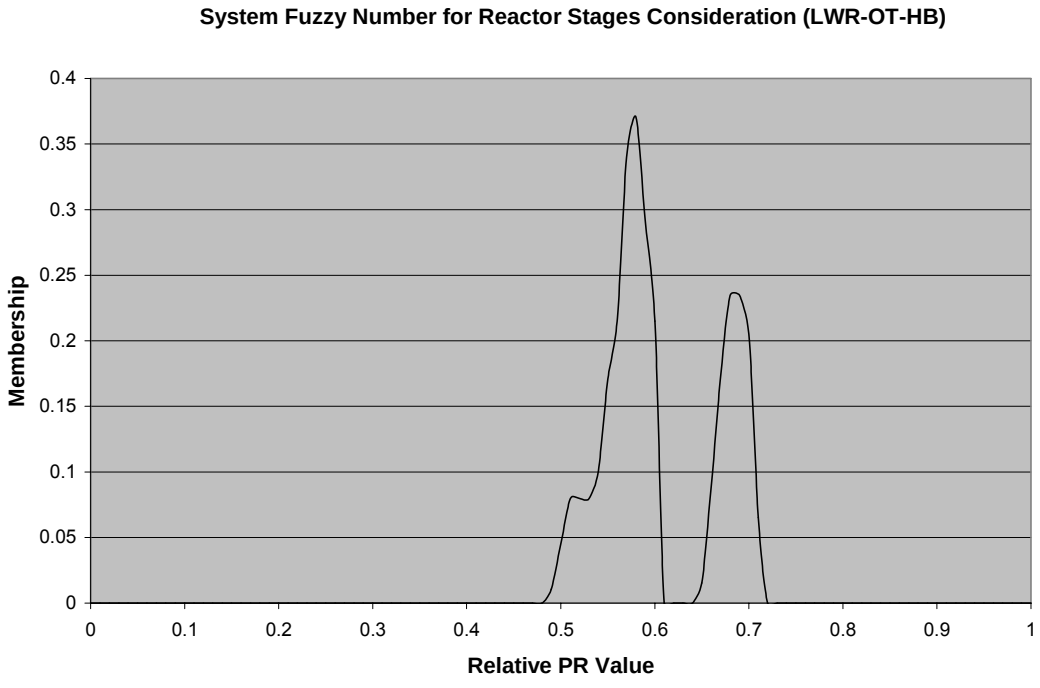

Figure 3-22 System fuzzy number for reactor stages consideration (LWR-OT-HB)

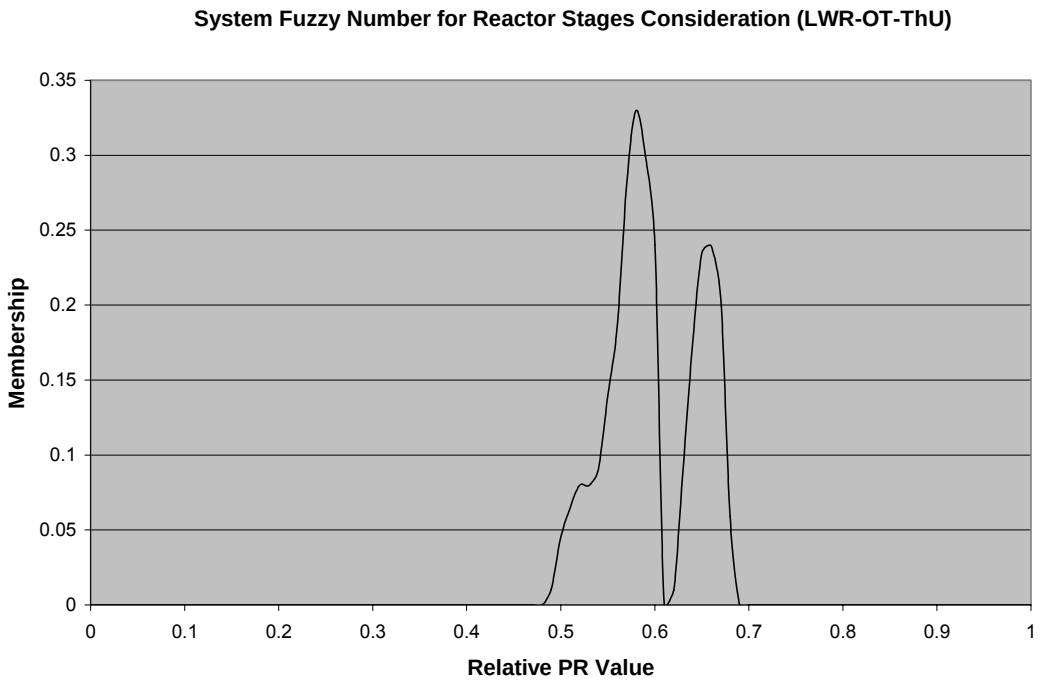

Figure 3-23 System fuzzy number for reactor stages consideration (LWR-OT-ThU)

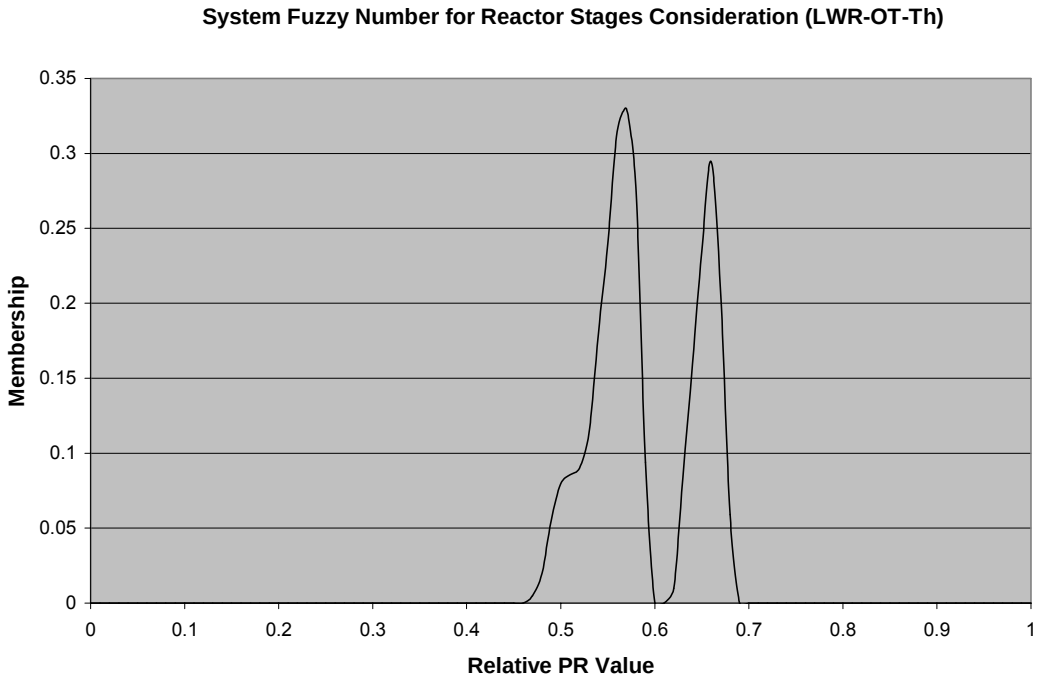

Figure 3-24 System fuzzy number for reactor stages consideration (LWR-OT-Th)

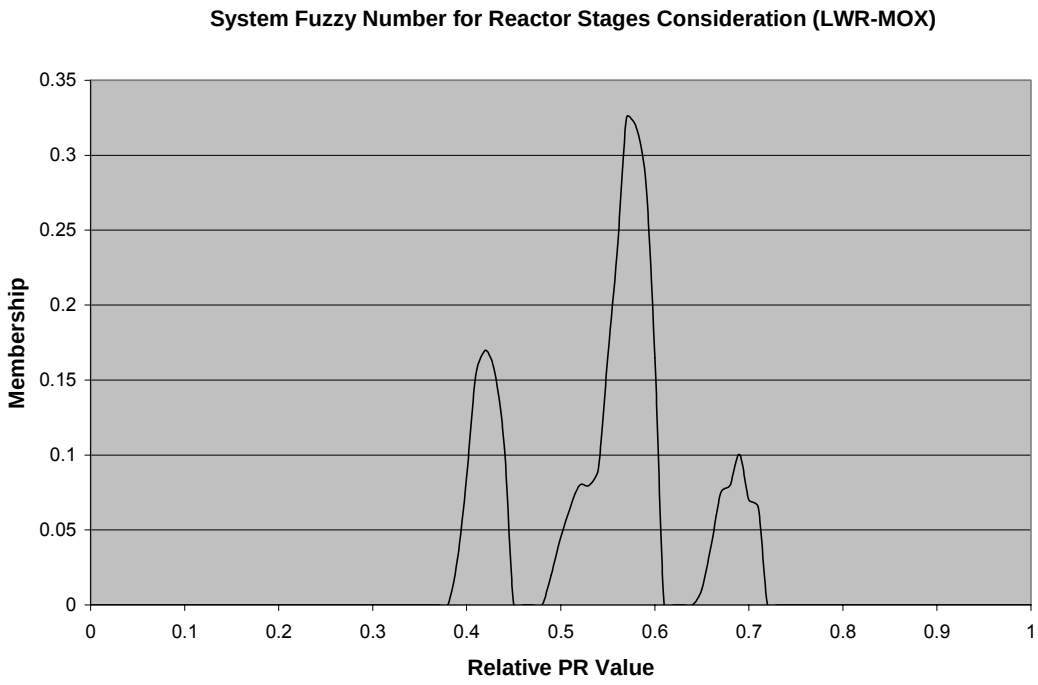

Figure 3-25 System fuzzy number for reactor stages consideration (LWR-MOX)

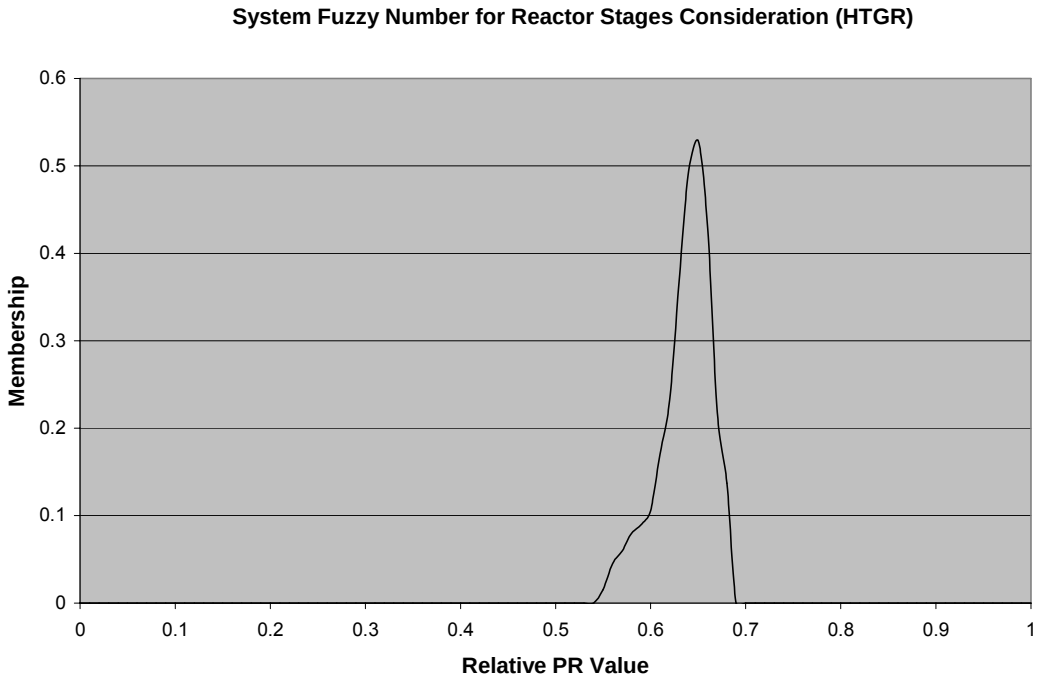

Figure 3-26 System fuzzy number for reactor stages consideration (HTGR)

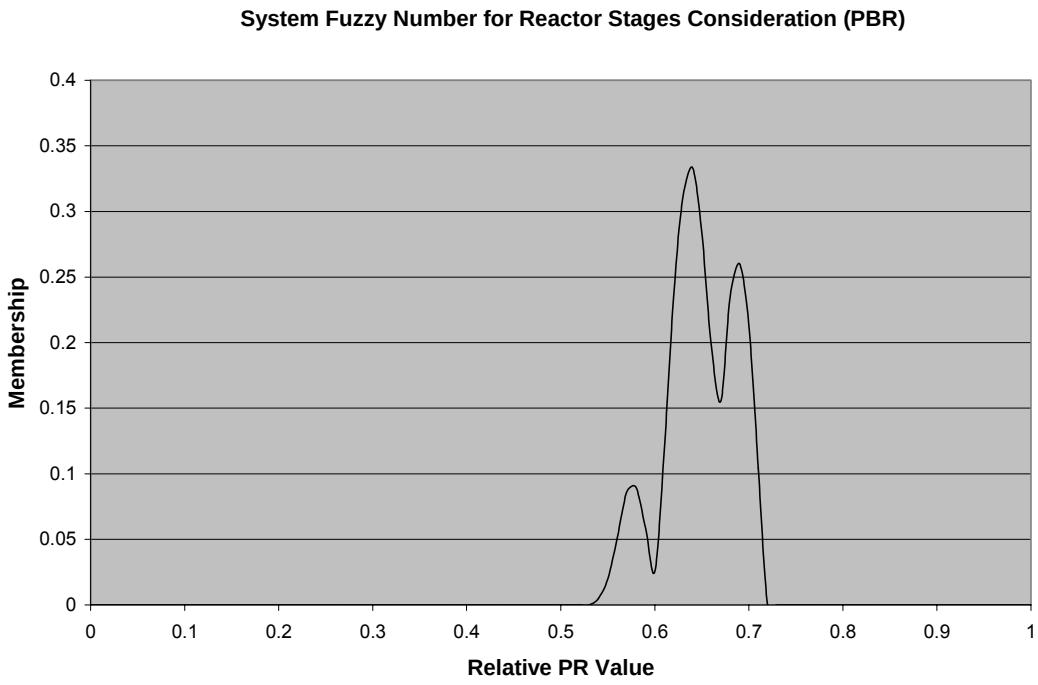

Figure 3-27 System fuzzy number for reactor stages consideration (PBR)

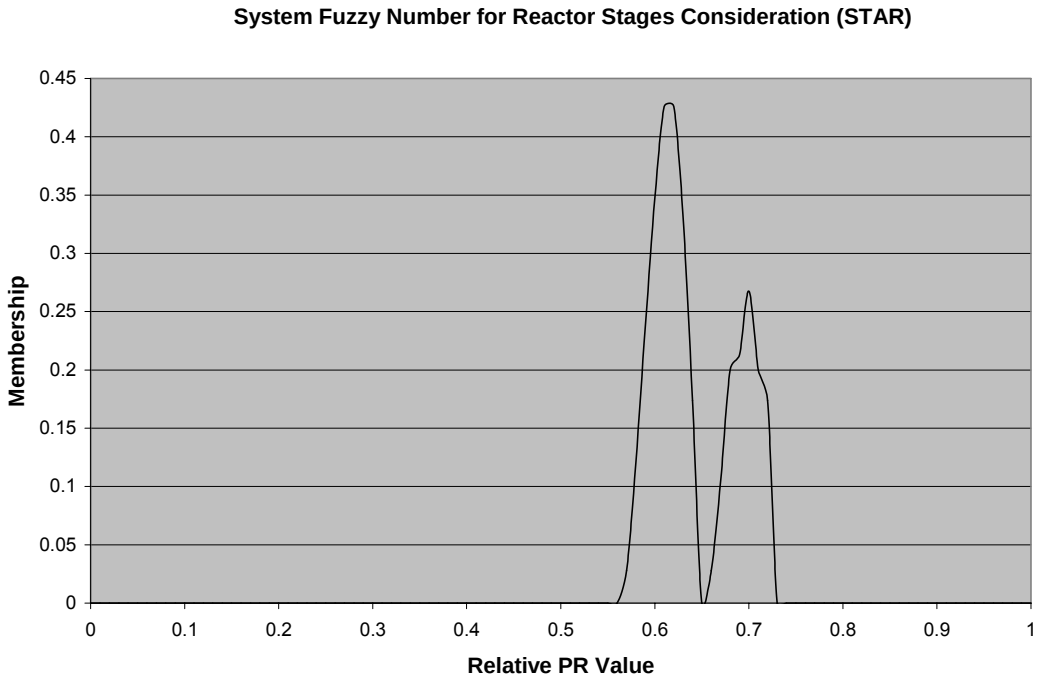

Figure 3-28 System fuzzy number for reactor stages consideration (STAR)

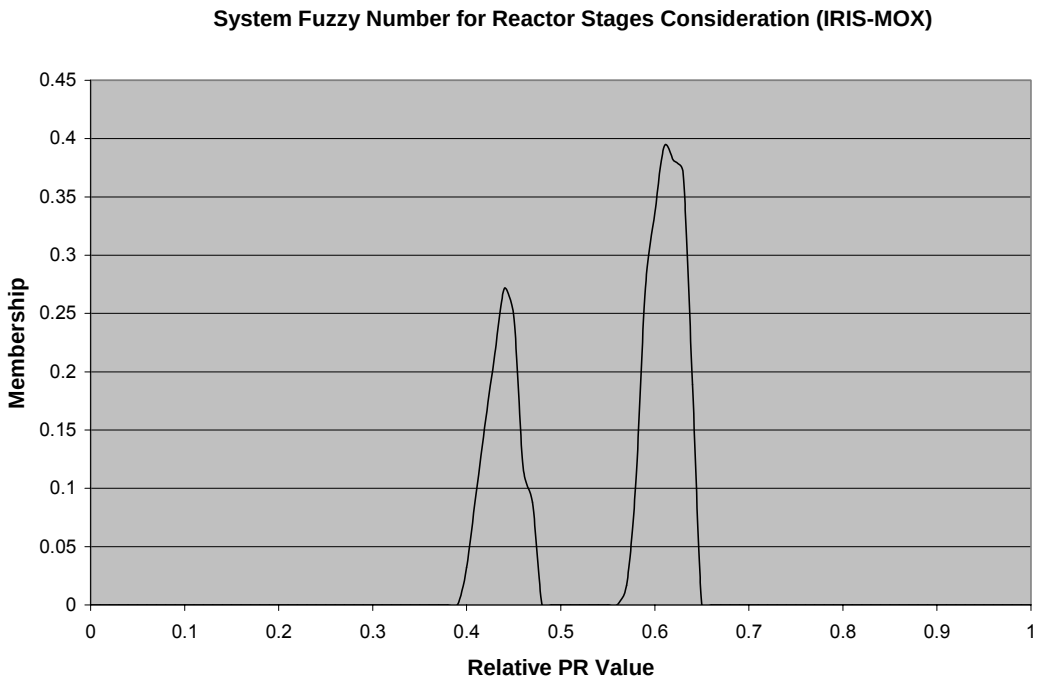

Figure 3-29 System fuzzy number for reactor stages consideration (IRIS-MOX)

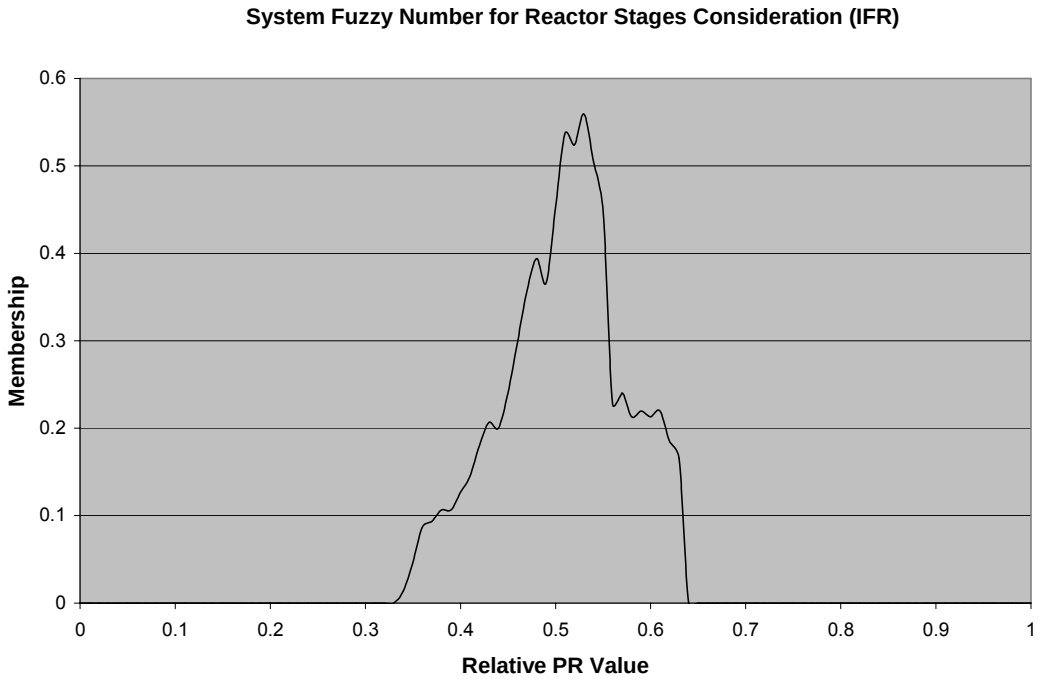

Figure 3-30 System fuzzy number for reactor stages consideration (IFR)

3.7 Validation of the New PR Method

Due to the abstract nature of the assessment, validation of any proliferation assessment method would be difficult. In this section, validation of the newly developed method is attempted by comparing the results of proliferation resistance assessments from the new method with the relevant available information from the literature.

Table 3-24 Comparison of PR values from two methods

Stage Name	The Newly Developed Method			Method from the literature [Ref 3-21]		
	PWR-OT	MOX	DUPIC	PWR-OT	MOX	DUPIC
Reprocessing		0.114 (L+)			0.25	0.44
fuel fabrication	0.496(VH-)	0.155(M-)	0.214(M+)	0.58	0.34	0.52
Reactor Operation	0.178(M)	0.239(M+)	0.137(M-)	0.9	0.9	0.78
Dry Storage	0.213(M+)	0.245(M+)	0.223(M+)	0.64	0.78	0.58
Disposal	0.202(M+)	0.246(M+)	0.224(M+)	0.6	0.58	0.54

First comparison, the PR analysis for three fuel cycle systems (details described in Chapter 5) by using the new developed method is compared with results from other method. The referenced method is a MAU based method that developed at the University of Texas in collaboration with Oak Ridge National Lab [Ref 3-20]. The results of proliferation assessment by using this method for the three fuel cycles as presented in a PNL report are used in this study [Ref 3-21]. Table 3-24 shows the PR values obtained by using the fuzzy logic-based barrier framework approach and MAU based method. In this table, a larger number means higher proliferation resistance. The fuzzy logic-based barrier framework approach also allows qualitative interpretation of the PR numbers as given in Table 3-24. The PR values

in Table 3-24 reflect the proliferation resistance of each fuel cycle stage by considering all intrinsic barriers, such as isotopic barrier, chemical barrier, radiological barrier, etc..

It can be observed that reprocessing & recycling of Pu in MOX fuel cycle are estimated to have the lowest PR values. But fuel processing & fabrication in DUPIC fuel cycle shows relatively high PR values. It can also be seen that MOX fuel fabrication represents relatively lower PR because of the existence of separated Pu. The biggest difference between two methods was for the reactor operation stage for all three fuel cycles where current method predicts medium PR values while the MAU based method predicts a very high PR value. Since Pu is produced during reactor operation stage and the Pu can potentially be diverted, the numbers predicted by current method appear more appropriate. The predicted PR values for the backend of fuel cycle seem to be in agreement between the methods. DUPIC is predicted to have lower PR values than MOX in the back-end stages except the fuel fabrication stage; but this difference was not significant in terms of the qualitative interpretation from current method. Current method and the MAU based method are comprehensive PR evaluation method considering the intrinsic barriers of a fuel cycle. The results from current method can be interpreted as high, medium, or low proliferation resistance as defined in the TOPS report [Ref 3-30] whereas the results from the MAU based method represent only relative differences. Two methods showed reasonably good agreement except for the reactor operation stage, in particular for the PWR-OT fuel cycle.

Table 3-25 Barrier levels determined from barrier effectiveness functions

Stage ID	Stage Name	Barrier ID										
		1	2	3	4	5	6	7	8	9	10	11
2	Conversion	VH	L	M	VH	M	VH+	I	M	VH+	H	M
3	Enrichment	VH	L-	M	VH	M	I	H	I	VH+	L	H
4	LEU Fuel Fabrication	VH	L	M	VH	M	VH	I	L	VH+	H	VH
5	PWR	L-	VH	VH	I	VH	L	VH+	I	VH+	M	H
6	AFR Storage	I+	VH	VH	L	VH	VH	H	I	VH+	H	I
7	Permanent Disposal	L+	VH	VH	I	VH	VH	VH	I	VH+	VH	I

Table 3-26 Barrier levels assigned from Ref 3-37

Stage ID	Stage Name	Barrier ID										
		1	2	3	4	5	6	7	8	9	10	11
1	Mining	VH	I	M	H	M	VH	I	I	I	VH	I
2	Conversion	VH	I	L	H	M	VH	I	I	M	M	M
3	Uranium enrichment	VH	I	L	M	M	I-M	M-VH	I	VH	I	H
4	Fuel fabrication	VH	I	L	M	M	VH	I	I	M	M	H
5	Reactor irradiation	L	VH	VH	VH	VH	L-H	VH	I	VH	M	H
6	Storage (of spent fuel)	L	H-VH	VH	VH	VH	VH	H	I	VH	VH	H
7	Repository emplacement	L	H-VH	VH	VH	VH	VH	VH	I	<VH-VH	VH	I

Second comparison is the qualitative result from current model with published study. Table 3-25 show the comparison of barrier levels table generated by the PR model based on defined barrier effectiveness functions and input important quantities values for PWR-OT system. Table 3-26 is extracted result from the study finished by Hassberger [Ref 3-37] for the same stages for LWR-OT system. Both tables cover results for 7 selected stages. 11 barriers are included for each stage and a barrier level is assigned for each barrier at each stage. For most of the

barriers for all 7 stages, the two tables show good match, except barrier number 4 which is Mass and Bulk Barrier. In the LLNL report, “VH” was assigned to this barrier at the later systems during/after fuel irradiation by only considering the consuming of ^{235}U during reactor irradiation. The building up of Pu which is another important fissile material during the reactor irradiation should be considered too. The effect of Pu building up is considered in the new PR model and shown in the Table 3-25.

3.8 References

Ref 3-1 MIT Nuclear Energy Study Advisory Committee, “The Future of Nuclear Power”, MIT, 2003

Ref 3-2 President Carter, “Statement by the President on nuclear power”, 7 April 1977

Ref 3-3 “Report from the Commission to the Council: International Nuclear Fuel Cycle Evaluation, Document COM (80) 316 Final”, 11 June 1980

Ref 3-4 DOE, “Nuclear Proliferation and Civilian Nuclear Power, Report of the Nonproliferation Alternative Systems Assessment Program”, United States Department of Energy, Washington DC, June 1980

Ref 3-5 Harold A. Feiveson, “Proliferation Resistant Nuclear Fuel Cycles”, Ann. Rev. Energy, 3:357-94, 1978

Ref 3-6 Papazoglou, I.A., Gyftopoulos, E.P., Miller, M.M., Rasmussen, N.C., Raiffa, H., “A Methodology for the Assessment of the Proliferation Resistance of Nuclear Power Systems”, MIT Report, MIT-EL 78-021, 1978

Ref 3-7 Papazoglou, I.A., Gyftopoulos, E.P., Miller, M.M., Rasmussen, N.C., Raiffa, H., “A Methodology for the Assessment of the Proliferation Resistance of Nuclear Power Systems”, MIT Report, MIT-EL 78-022, 1978

Ref 3-8 C. D. Heising, Isi Saragossi and P. Sharafi, “A Comparative Assessment of the Economics and Proliferation Resistance of Advanced Nuclear Energy Systems”, Energy Vol. 5, pp. 1131-1153, 1980

Ref 3-9 C. D. Heising, “Quantification of Nuclear diversion risks: promises and problems”, ENERGY POLICY, 1982

Ref 3-10 P. Silvennoinen, J. Vira, “An Approach to Quantitative Assessment of Relative Proliferation Risks from Nuclear Fuel Cycles“, The Journal of the Operational Research Society, Vol. 32, No. 6, pp. 457-466, Jun. 1981

Ref 3-11 P. Silvennoinen, J. Vira, “Quantifying Relative Proliferation Risks from Nuclear Fuel Cycles”, Progress in Nuclear Energy, Vol. 17, No. 3, pp. 231-243, 1986

Ref 3-12 T.L. Saaty, “A Scaling method for priorities in hierarchical structures”, J. Math. Psychol. 15, pp. 234-281, 1977

Ref 3-13 Shahid Ahmed, A.A. Husseiny, “Risk Assessment of Alternative Proliferation Routes”, Nuclear Technology, Vol. 56, Mar. 1982

Ref 3-14 James Dyer, “A Methodology for the Analysis and Selection of Alternatives for the Disposition of Surplus Plutonium”, Amarillo National Research Center for Plutonium, ANRCP-1999-23, August 1999

Ref 3-15 W. Ko, H. D. Kim, M. S. Yang, H. S. Park, “Electrical Circuit Model for Quantifying the Proliferation Resistance of Nuclear Fuel Cycles”, Annals of Nuclear Energy, 27 1399-1425, 2000

Ref 3-16 R.A. Krakowski, “A Multi-Attribute Utility Approach to Generating Proliferation Risk Metrics”, Los Alamos National Laboratory, LA-UR-96-3620, 1996

Ref 3-17 R.A. Krakowski, “Review of Approaches for Quantitative Assessment of the Risks of and Resistance to Nuclear Proliferation from the Civilian Fuel Cycle”, Los Alamos National Laboratory Report, LA-UR-01-169, Jan. 2001.

Ref 3-18 E. Kiriyama and S. Pickett, “Non-proliferation criteria for nuclear fuel cycle options”, Progress in Nuclear Energy, Vol. 37, No. 1-4, pp. 71-76, 2000

Ref 3-19 H. Matsuoka, Y. Nishiwaki, A. Ryjov and A. Belenki, “An evaluation method on the integrated safeguards based on fuzzy theory”, Information Sciences 142, pp. 131-150, 2002

Ref 3-20 Charlton, W. S., D. G. Ford, R. F. LeBouf, and C. Gariazzo, “Proliferation Resistance Assessments Methodology for Nuclear Fuel Cycles,” Proceedings of the 45th INMM Annual Meeting, Orlando, FL, July 16-22, 2004

Ref 3-21 P. Baron, C. Brown, B. Kaiser, B. Matthews, T. Mukaiyama, R. Omberg, L. Peddicord, M. Salvatores, A. Walter, “An Evaluation of the Proliferation Resistant Characteristics of Light Water Reactor Fuel with the Potential for Recycle in the United States”, Pacific Northwest National Laboratory, November 2004

Ref 3-22 US DOE Nuclear Energy Research Advisory Committee and the Generation IV International Forum, “A Technology Roadmap for Generation IV Nuclear Energy Systems”, GIF002-00, December 2002

Ref 3-23 US DOE Nuclear Energy Research Advisory Committee and the Generation IV International Forum, “Final System Screening Evaluation Methodology R&D Report”, GIF012-00, December 2002

Ref 3-24 US DOE Nuclear Energy Research Advisory Committee and the Generation IV International Forum, “Viability and Performance Evaluation Methodology Report”, GIF013-00, December 2002

Ref 3-25 US DOE Nuclear Energy Research Advisory Committee and the Generation IV International Forum, “Fuel Cycle Assessment Report”, GIF014-00, December 2002

Ref 3-26 J. Roglans, R. Bari, R. Nishimura, and S. Mladineo, “A proliferation resistance and physical protection assessment methodology for use at the nuclear system design stage”, Proceedings of the 7th International Conference on Facility Operations: Safeguards Interface, p 189-194, 2004

Ref 3-27 P. Peterson, J. Roglans, R. Bari, “Assessment methodology development for proliferation resistance and physical protection of generation IV systems”, Global 2003, p. 882-888, 2003

Ref 3-28 R.Nishimura, J. Roglans, R. Bari and P. Peterson, “Evaluation Methodology for Proliferation Resistance and Physical Protection of Generation IV Nuclear Energy Systems”, Proceedings of the Institute of Nuclear Materials Management, 46th Annual Meeting, July 10-14 2005

Ref 3-29 NERAC, “Technological Opportunities to Increase the Proliferation Resistance of Global Civilian Nuclear Power Systems (TOPS)”, 2001

Ref 3-30 NERAC, “Attributes of Proliferation Resistance for Civilian Nuclear Power Systems”, 2000

Ref 3-31 Stanley A. Erickson, “Economic and Technological Trends Affecting Nuclear Nonproliferation”, The Nonproliferation Review, summer 2001

Ref 3-32 G. S. Selvaduray, “Comparative Evaluation of Nuclear Fuel Reprocessing Techniques for Advances Fuel Cycle Concepts”, dissertation, Stanford University, 1978

Ref 3-33 MATLAB™, The Math Works Inc. <http://www.mathworks.com/>

Ref 3-34 A. G. Croff, “A User’s manual for the ORIGEN2 Computer Code”, ORNL/TM-7175, 1980.

Ref 3-35 J.F. BRIESMEISTER, ed., “MCNP – A General Monte Carlo N-particle Transport Code – Version 4B,” LA-12625-M, Los Alamos National Laboratory (1997).

Ref 3-36 Zadeh, L, “Fuzzy sets as a basis for a theory of possibility”, Fuzzy Sets System, 1, 3-28, 1965

Ref 3-37 J.A. Hassberger, “Application of Proliferation Resistance Barriers to Various Existing and Proposed Nuclear Fuel Cycles”, UCRL-ID-147001, 2001

Ref 3-38 “Microshield Version 3 Manual,” Grove Engineering, Inc., Rockville, MD, 1987

Ref 3-39 A.N. Chebeskov, V.I. Oussanov, V.V. Korobeynikov, S.V. Iougai, B.B. Tikhomirov, “An Approach to Evaluate Attractiveness of Plutonium of

Various Origin" , New Orleans, LA, Global 2003, pp. 1838-1846, November 2003

Ref 3-40 G. Bortolan, R. Degani, "A Review of Some Methods for Ranking Fuzzy Subsets", Fuzzy Sets and Systems 15, 1-19, 1985

Ref 3-41 D. Dubois, H. Prade, "Ranking Fuzzy Numbers in the Setting of Possibility Theory", Inform. Sci. 30, 183-224, 1983

Ref 3-42 D. Dubois, H. Prade, "Operations on Fuzzy numbers", Int. J. Systems Sci., Vol 9, No. 6, 613-626, 1978

Ref 3-43 R.R.YAGER, "Ranking fuzzy subsets over the unit interval", Proceedings of the 1978 CDC, P. 1435-1437, 1978

Ref 3-44 R.R.YAGER, "A procedure for ordering fuzzy subsets of the unit interval", Information Sciences 24, p. 143-161, 1981

4 Economic Analysis of Nuclear Fuel Cycle

4.1 Introduction

The basic cost components of a nuclear power system are capital cost, operation and maintenance cost, and fuel cycle cost. Capital cost includes investment and associated interest to construct nuclear power plant, heavy water inventory (if required) and dismantling. The operation and maintenance (O&M) cost includes required money to operate and decommission a nuclear power plant like the salaries for workers, materials, and supplies. The fuel cost is to handle fuel during the fuel cycle from the beginning (mining uranium ore) to the end (disposal of SNF) including the purchase of the uranium ore, its conversion, enrichment (if required), fuel fabrication, transportation, the storage of spent fuel, reprocessing (if undertaken) and waste disposal. Those costs vary for different countries, different economic conditions and for different geopolitical factors or decisions. For the US, the distribution of these costs in July of 1996 (for a total cost of 33.28 mil/kWh for a new PWR using a once through fuel cycle [Ref 4-14]) was approximately as follows.

Capital cost	55%
O&M cost	27%
Fuel cycle cost	19%

As cost is a key factor in selecting a technology, the cost of implementing different fuel cycle scheme will be considered in the study as part of the performance indicators. The nuclear fuel cycle covers the whole lifetime of nuclear fuel from the beginning of uranium ore mining, to the end of SNF/HLW disposal. The SNF/HLW

is treated as liability for nuclear industry. The nuclear fuel cycle is considered as three stages: front-end of the fuel cycle, fuel at reactor and back end of the fuel cycle. The front-end includes uranium mining and milling, conversion, enrichment and fuel fabrication until the reactor site. The back end includes transport and interim storage of spent fuel, reprocessing if used, waste treatment/package, and final waste disposal.

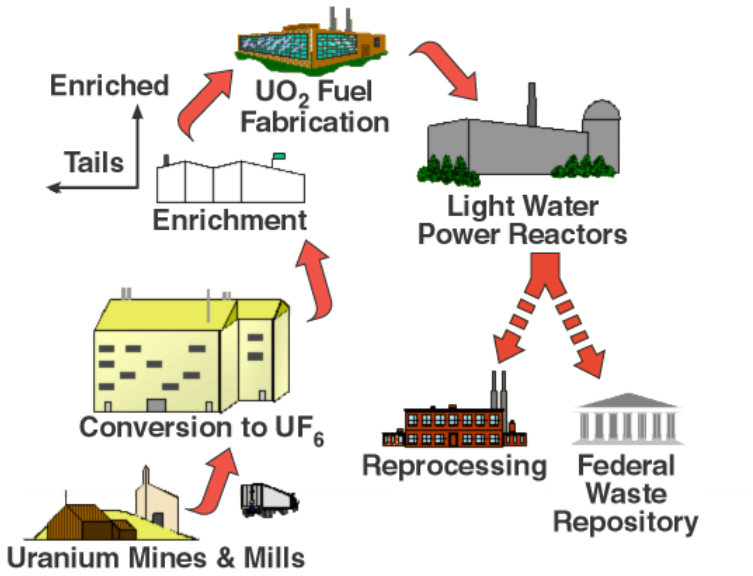

Figure 4-1 Nuclear fuel cycle example

Figure 4-1 [Ref 4-1] shows one example nuclear fuel cycle. Uranium ore is mined and milled in to yellowcake which contains U_3O_8. yellow cake is further refined into Uranium oxide (UO_2) and Uranium oxide is converted into uranium hexafluoride gas (UF_6). As a gas, it is easier to be enriched normally from ~0.72% ^{235}U to around 3-5% ^{235}U at enrichment facility. The enriched gas is turned back to solid Uranium oxide (UO_2) for assembly as fuel element. The fuel assembly is sent

to reactor for irradiation. The spent fuel will be sent to either reprocessing facility or repository for direct disposal.

Discounted levelized cost in constant money value terms is the basis of fuel cycle cost estimation which is the total cost of building and operation the station over its life divided by the net electrical output over the same period [Ref 4-2]. This cost reflects the minimum charge needed for the sale of electricity to cover all costs associated to generate the electricity. All money is converted to the money at a selected time point; normally it is when the first fresh fuel is inserted into the reactor core. First, cost at each facility/component is calculated. And then all costs are discounted to a selected base date and summed up to get a total fuel cycle cost in present value terms. Levelized fuel cycle cost is calculated by dividing the total discounted fuel cycle cost by the total discounted electricity generated. Discrete discount method is commonly used (compounded 1/year) while continuous discounting method can be employed for both electricity discount and the cost discount. The discount rate used for discounting is a matter of policy and might be different between countries and between government and private utilities. It generally counts the effect of tax and rate of return of funds. This method has been used in a series of studies by OECD to compare the projected cost of generating electricity from different sources including nuclear, coal, natural gas and others [Ref 4-12 - Ref 4-16].

In 1994 OECD study [Ref 4-3], average levelized fuel cycle costs were studied for PWR fuel cycle as well as CANDU and Advanced Thermal Reactor (ATR). Discrete discounting was used for cost discount. Electricity is discounted by

applying continuous discounting method. The study has investigated two different back end options for PWR fuel cycle: direct disposal and reprocessing. In the reprocessing option, Pu and U in the SNF are recycled. Indifference method was adopted from 1985 OECD study [Ref 4-2] to calculate the plutonium credit. Indifference method is based on assumption that the back-end costs for UO_2 fuel are the same as for MOX fuel and the value of plutonium is calculated from the difference of front-ends costs. The recovered uranium value is calculated in different ways according the recovered form of uranium [Ref 4-4].

During fuel irradiation, the isotopic composition in a batch changes dramatically with time/burnup, in turn, the value of fuel changes dramatically too. To capture this economic effect during fuel irradiation for fuel/fuel loading optimization, there is desire to know the time/burnup dependent present worth of the fuel. Several nuclear fuel cycle cost analysis codes are available for such purpose [Ref 4-8]; they are usually coupled with reactor simulation tools. The neutronic data provided by the reactor simulation tools is used along with the other economic data to determine the time/burnup dependent fuel value. CINCAS [Ref 4-7] is a nuclear fuel cycle cost code developed through cooperation of the Commonwealth Edison Company, Iowa-Illinois Gas and Electric Company, Northern States Power Company, Consumers Power Company, Arthur Anderson and Company, and Sargent and Lundy, Engineers. CINCAS calculates the fuel cost at each month of a period, normally from the arrival of a fuel batch at the reactor site to the withdrawal of the batch from the reactor. Pre-irradiation costs for uranium and fabrication are represented as progress payment by the utility prior to irradiation. The interest is counted for those

payments before the fuel begins to produce power. All costs incurred by a batch are given to one ore more cost categories. Six direct cost categories are used: uranium, plutonium credit, fabrication, shipping, reprocessing, and re-conversion. Four inventory cost categories are used, uranium, plutonium, fabrication, and post-irradiation, to cover the return on investment of the utility. All costs are discounted (compounded 1/month) and levelized over electricity generated for each batch. Levelized fuel cycle cost for a cycle and for the planning horizon are further calculated. OCEON-P [Ref 4-9] is another fuel cycle cost code developed at North Carolina State University, Electric Power Research Center. It uses a carrying charge model based on the method used by the CINCAS code to evaluate the levelized fuel cycle cost. The objective of the OCEON-P fuel cycle cost model is to rank alternative fuel cycling schemes instead of to predict accurate levelized fuel cycle cost in an absolute sense. Other codes are available like REFCO [Ref 4-10] and PACTOLUS [Ref 4-11].

ORCA [Ref 4-5, Ref 4-6] is an economic analysis model for LWR fuel cycle developed at Cornell. Levelized fuel cycle cost is obtained and the result is a linear function of the unit cost at each component and of the quantities obtained from the material balance of the fuel cycle. Continuous discounting method is used for all costs involved at different components. A sinking fund is used to pay all back end costs. The sinking fund is risk-free fund and earns at a user-specifiable rate which is much lower than the discount rate.

A simpler version of fuel cycle economics model was used in the MIT Future of Nuclear Energy study [Ref 4-17, Ref 4-18]. This simpler model uses discrete

discounting method (compounded 1/yr). The back end costs were assumed to be paid at the end of fuel irradiation to avoid the situation that the back end costs become trivial because of the discounting on the long time period between fuel irradiation and final spent fuel disposal.

This simple FCC model estimated the fuel cycle cost of MOX cycle as 22.4 mills/kWh(e) under the U.S. conditions. This figure was approximately 4.5 times higher than the cost for once-through UOX cycle (5.15 mills/kWh(e)). This result is significantly different from the finding of the OECD study in 1994 [Ref 4-3] where the cost of once-through option is about 15% lower. The OECD model is more detailed and the methodology for dealing with carrying charges is more involved. And difference assumptions about the workings of the fuel cycle like the credit of recovered uranium are used in OECD. Also the OECD study used costs that are much more favorable to the reprocessing option. When OECD assumptions were applied in the simpler FCC model, it generated closer costs to OECD study for both cycles (6.43 mills/kWh for Once-through and 6.80 mills/kWh for MOX).

The simple model in the MIT approach is easy to use and was considered appropriate for comparison of different fuel cycles at system level. Accordingly, this simple model is adopted in this study to represent fuel cycle economics as one of the system performance measures to compare fuel cycles.

4.2 Fuel Cycle Cost Model

The simplified fuel cycle cost model utilized in this study is described in this section. To evaluate and compare different fuel cycles in system level, it is assumed the system design is in best shape, that is, the configuration of the system is setup

and optimized. A simple expression for the fuel cycle cost is used [Ref 4-17, Ref 4-18]:

$$FCC = \sum_i M_i \bullet C_i + \sum_i M_i \bullet C_i \bullet \phi \bullet \Delta T_i \quad [\$]$$

where:

FCC = Fuel Cycle Cost [$]

M_i = mass processed at stage i [kg or kg SWU]

C_i = unit cost at stage i [$/kg or $/kg SWU]

ϕ = carrying charge factor [yr^{-1}]

ΔT_i = delay between the investment for stage i and the midpoint of the irradiation of the fuel (yr)

The assumptions of the model are as follows:

- All batches of fuel are considered equilibrium batches, having equal in-core residence time and equal charge and discharge enrichment (i.e., neglecting startup and shutdown batches).
- The revenue and depreciation charges for each batch are represented by single payments at the middle of the irradiation interval.
- Depreciation is a linear function of time (~ burnup).
- In-core fuel cycle operation and maintenance costs are negligible.
- The revenues received from the sale of energy generated by a batch of fuel exactly compensate for all the costs and credits associated with all steps of the fuel cycle, as well as the appreciate carrying charges for these steps.

Carrying charge factor:

$$\phi = \frac{x}{1-\tau}$$

where: ϕ = carrying charge factor [yr^{-1}]

x = discount rate [yr^{-1}]

τ = equivalent tax fraction

Discount rate:

$$x = (1-\tau)\, f_b\, r_b + f_s\, r_s$$

where: f_b = debt fraction

f_s = equity fraction = 1 – f_b

r_b = rate of return to bond holders

r_s = rate of return to stock holders

The separative work per unit of enriched product can be obtained as:

$$\frac{kgSWU}{kg\ \mathrm{Pr}oduct} = (2x_p - 1) \bullet \ln(\frac{x_p}{1-x_p}) + \frac{x_p - x_f}{x_f - x_t} \bullet (2x_t - 1) \bullet \ln(\frac{x_t}{1-x_t}) -$$

$$\frac{x_p - x_t}{x_f - x_t} \bullet (2x_f - 1) \bullet \ln(\frac{x_f}{1-x_f})$$

where:

x_p = product enrichment

x_f = feed material enrichment

x_t = tails assay

4.3 Electricity Generation Cost

In addition to estimating fuel cycle cost, this study envisions the use of total electricity generation cost for fuel cycle comparisons. Estimation of the total cost of electricity generation is described in this section.

The total cost of electricity, c_{elec} can be expressed as:

$$c_{elec} = c_{cap} + c_{om} + \text{FCC}$$

where c_{cap} is the capital cost

c_{om} is the operations and maintenance cost

FCC is the fuel cycle cost.

Capital cost is the biggest contributor to the total cost and it can be changed by the investment source, payment schedule, interest rate, depreciation schedule, tax and insurance policy and other factors. It includes

Capital cost c_{cap} ($/kW$_e$h) can be defined as [Ref 4-19-Ref 4-20]:

$$c_{cap} = \frac{C_{cap}}{8766\eta} F_{cr}$$

Where C_{cap} is the total construction cost, in dollars per kilowatt of installed net electrical capacity ($/kW$_e$), η is the capacity factor (the total amount of electricity produced in a year divided by the total amount that would be produced from continuous operation at full power), 8766 is the average number of hours in a year. The "fixed charge rate," F_{cr} (y^{-1}), is the fraction of the initial investment that must be collected each year to repay the initial costs, including interest or return on investment.

Operations and maintenance costs are continuing costs of running a plant that do not relate to its fuel—such as worker salaries and routine plant maintenance. Most of these costs do not depend on the amount of electricity produced by the plant, and so most calculations, including this one, assume a fixed annual expense. Provisions placed into a fund for eventual decommissioning of the plant are also included in most estimates of operations and maintenance costs. O&M cost has increased its importance in total cost of nuclear plant in recent years while the importance of fuel cost has declined [Ref 4-22]. The contribution of these expenses to the cost of electricity is given by [Ref 4-21]

$$c_{om} = \frac{C_{om} + C_{dd} F_{dd}}{8766\eta}$$

Where c_{om} is the annual non-fuel operations and maintenance cost ($/kW$_e$y), C_{dd} is the cost to dismantle and decommission the plant at the end of its operating life ($/kW$_e$), and F_{dd} (y^{-1}) is the annual annuity factor, given by

$$F_{dd} = \frac{i_{dd}}{(1+i_{dd})^N - 1}$$

Where i_{dd} is the annual rate of return on the funds invested and N is the length of time the annuity is paid (usually the same as the period over which the construction costs are repaid). For example, if the rate of return is 3 percent per year and the annuity is paid over 30 years, F_{dd} = 0.021; if C_{om} = $80/kW$_e$y, C_{dd} = $150/kW$_e$, and η = 0.85, then c_{om} = $0.0112/kW$_e$h.

4.4 Examples of Fuel Cycle Estimation

Examples of fuel cycle cost comparisons are given in Chapter 5.

4.5 References

Ref 4-1 NRC website, “Storage of the Nuclear Fuel Cycle”, Nov. 29th, 2005, <http://www.nrc.gov/materials/fuel-cycle-fac/stages-fuel-cycle.html>

Ref 4-2 “The Economics of the Nuclear Fuel Cycle”, NEA, OECD, 1985

Ref 4-3 “The Economics of the Nuclear Fuel Cycle”, NEA, OECD, 1994

Ref 4-4 “Plutonium fuel: an assessment (report by an expert group)”, OECD, 1989

Ref 4-5 K.B.CADY, E.A. SCHNEIDER, J.C. GUAIS and R.F. ORTEGA. "ORCA: A Model for the Economic Analysis of the Nuclear Fuel Cycle". Trans. Am. Nucl. Soc., 83:47, 2000

Ref 4-6 E.A. Schneider, “A Physical and Economic Model of the Nuclear Fuel Cycle”, dissertation, Cornell University, 2002

Ref 4-7 T.W.Craig et al., “CINCAS, A Nuclear Fuel Cycle Engineering Economy and Accounting Forecasting Code”, Argonne Code Center Abstract 354, Argonne, Illionis, 1968

Ref 4-8 B.E. Prince, J.P. Peerenboom and J.G. Delene, “A Survey of Nuclear Fuel Cycle Economics: 1970-1985”, ORNL/TM-5703, Oak Ridge National Lab., 1977

Ref 4-9 “OCEON-P User’s Manual, Version 2.0.0”, North Carolina State University, 1998

Ref 4-10 J.G. Delene and O.W. Hermann, “REFCO-83 User’s Manual”, NUREG/CR-3800, (ORNL-TM-9186), Oak Ridge National Lab., 1984

Ref 4-11 C. H. Bloomster, J. H. Nail and D. R. Haffner, “PACTOLUS, A Code for Computing Nuclear Power Costs”, BNWL-1169, 1970

Ref 4-12 “The costs of Generating Electricity in Nuclear and Coal Fired Power Stations”, NEA, OECD, 1983

Ref 4-13 “Projected Costs of Generating Electricity: from nuclear and coal-fired power stations for commissioning in 1995”, NEA, OECD, 1986

Ref 4-14 “Projected Costs of Generating Electricity”, NEA, OECD, 1989

Ref 4-15 “Projected Costs of Generating Electricity: Update 1992”, NEA, OECD, 1992

Ref 4-16 “Projected Costs of Generating Electricity: Update 1998”, NEA, OECD, 1998

Ref 4-17 M.A. Malik, “A Long Term Perspective of the LWR Fuel Cycle”, dissertation, MIT, 1984

Ref 4-18 “The Future of Nuclear Power: an interdisciplinary MIT study”, MIT, July, 2003

Ref 4-19 Paul J. Turinsky, “Lecture for Nuclear Fuel Cycles”, 2003

Ref 4-20 Carolyn D. Heising, Isi Saragossi, Pirooz Sharafi, “A Comparative Assessment of the Economics and Proliferation Resistance of Advanced Nuclear Energy Systems”, Energy, Vol. 5, Issue 11, p1131-1153, 1980

Ref 4-21 M. Bunn, S. Fetter, J. P. Holdren, B. V. D. Zwaan, “ The Economics of Reprocessing vs. Direct Disposal of Spent Nuclear Fuel”, Harvard University, 2003

Ref 4-22 NEA, “Methods of Projecting Operations and Maintenance costs for Nuclear Power Plants”, NEA, OECD, 1995

5 Case Study

5.1 Candidate Systems

Three systems are chosen in the case study: PWR-OT, MOX, and DUPIC. PWR-OT is chosen as reference system as it represents the most common fuel cycle concept in the U.S. MOX (Mixed Oxide) system is used because of its importance in reducing plutonium stockpile. DUPIC is a very interesting design and maximizes the usage of nuclear fuel without separation of plutonium and other actinides (Figure 5-1) [Ref 5-1].

(PWR-OT)

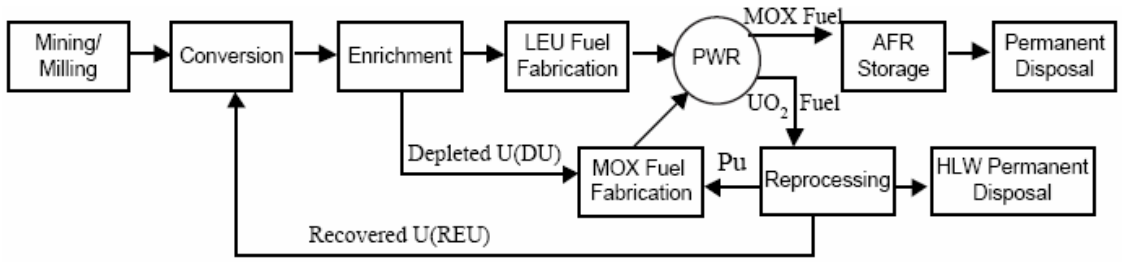

(MOX)

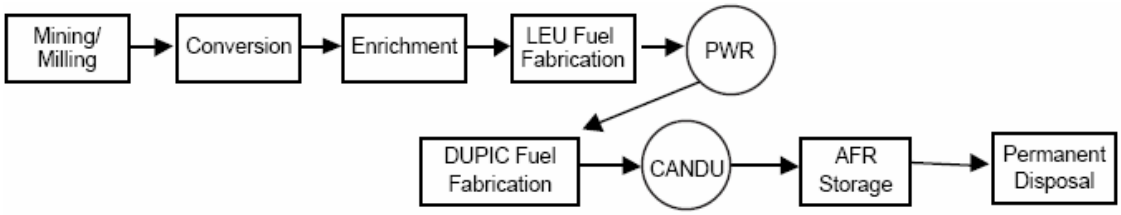

(DUPIC)

Figure 5-1 Candidate systems in case study

In this study, [Ref 5-1], the PWR fuels and MOX fuels were assumed to be burnt to 35,000 MWD/MTU. The initial enrichment of PWR fuel was assumed to be low enriched uranium (LEU), is 3.5% In MOX cycle, it was assumed that LEU and MOX fuels are loaded in the PWR reactor, and burnt up to 35,000 MWD/MTU, and all plutonium are recycled and made into MOX fuel and all MOX spent fuel will go to repository for final disposal. And in DUPIC cycle, LEU is firstly burnt up to 35,000 MWD/MTU, then the PWR spent fuel is made into CANDU fuel and is burnt in CANDU reactor to 15,400 MWD/MTHM [Ref 5-1]. The system characteristics are listed in Table 5-1.

Table 5-1 Characteristics of reference reactors [Ref 5-1]

Reactor parameters	PWR	CANDU
Electric power (MWe)	950	713
Thermal efficiency (%)	34	33
Thermal power (MWt)	2,794	2,161
Specific power (MWt/t U)	40.2	25.5
Load factor	0.8	0.9
Cycle length (Full Power Day)	290	—
Number of fuel assemblies or bundles per core	157	4,560
Number of batches for PWR	3	—
Loading per core (MTU)	69.5	84.7

5.2 Fuel Cycle Mass Balance

Isotopic mass balance of the fuel materials is the key component of fuel cycle systems modeling. In this work, fuel material isotopic mass balance was estimated based on the characteristics of reference reactors and ORIGEN2.2 is used for reactor simulation.

Annual requirement = $\frac{P \times 365 \times C}{\varepsilon \times BU}$, where *P*, *C* and *BU* are the electric power (MWe), the capacity factor (%) and burnup (MWd/MTHM), respectively [Ref 5-1].

Required fuel amount to generate 1 GWe-yr electricity = $\frac{1000}{P} \times$ Annual requirement, it is 24.54 MTU for PWR reactor and 64.64 MTU for CANDU reactor with DUPIC fuel. The fuel characteristics are listed in Table 5-2.

Table 5-2 Fuel characteristic parameters [Ref 5-1]

	PWR with LEU fuel	PWR with LEU and MOX fuel	CANDU with DUPIC fuel
per core (MTU)	69.5	69.5	84.7
fuel requirement (MTU)	23.31	23.31	46.09
Fuel Form	UO2	5%Puf MOX + 95% UO2	PWR SF
Initial enrichment	3.50%	5%Puf MOX +LEU (3.5%)	PWR SF
Number of fuel rods per assembly	264	264	43
Discharge burnup (MWd/kgHM)	35	35	15.4
Required fuel amount for 1 GWe-yr (MTU or MTHM)	24.54	24.54	64.64

5.2.1 MOX Fuel

Table 5-3 Pu inventory in PWR spent fuel

Pu Inventory after discharged from PWR reactor (35,000MWD/MTHM) [gram]						
Time	discharge	0.5YR	1.0YR	2.0YR	5.0YR	10.0YR
PU236	9.95E-04	8.87E-04	7.85E-04	6.16E-04	2.97E-04	8.80E-05
PU237	1.84E-04	1.15E-05	7.16E-07	2.78E-09	1.62E-16	1.43E-28
PU238	1.50E+02	1.56E+02	1.58E+02	1.59E+02	1.56E+02	1.50E+02
PU239	5.24E+03	5.34E+03	5.34E+03	5.34E+03	5.34E+03	5.34E+03
PU240	2.21E+03	2.21E+03	2.21E+03	2.21E+03	2.21E+03	2.21E+03
PU241	1.22E+03	1.19E+03	1.17E+03	1.11E+03	9.61E+02	7.55E+02
PU242	4.60E+02	4.60E+02	4.60E+02	4.60E+02	4.60E+02	4.60E+02
PU243	1.40E-01	3.68E-14	3.68E-14	3.68E-14	3.68E-14	3.68E-14
PU244	2.61E-02	2.61E-02	2.61E-02	2.61E-02	2.61E-02	2.61E-02
PU245	6.12E-07	0.00E+00	0.00E+00	0.00E+00	0.00E+00	0.00E+00
PU246	5.20E-09	4.46E-14	4.98E-19	1.16E-19	1.16E-19	1.16E-19
Total	9.28E+03	9.35E+03	9.33E+03	9.27E+03	9.12E+03	8.91E+03

It is assumed that PWR SF is cooled for 10 years before reprocessing or DUPIC fuel fabrication. It is assumed that the loss factors are 0.5% for conversion and for CANDU fuel fabrication, 1% for PWR, DUPIC and MOX fuel fabrication and for reprocessing plant. An equilibrium state is reached when all spent PWR fuels are reprocessed to make needed MOX fuels. The inventory of Pu in PWR spent fuel is estimated from ORIGEN2.2 as listed in Table 5-3.

One MTHM PWR spent fuel contains 8.91 Kg Pu after 10 years cooling. After 1% loss in reprocessing and MOX fuel fabrication, 8.73 Kg Pu remains in the new MOX fuel, which means 174.65 Kg MOX fuel (5% Pu + depleted U) can be made. Assume f as mass fraction of PWR fuel in the core, and the other 1-f is MOX, in equilibrium state: $(1\text{-}f) \times Mass_{core} = f \times Mass_{core} \times 174.65/1000 \Rightarrow f = 0.8513$

So in the annual required fuel 24.54 MTHM for 1 GWe-yr for PWR-MOX, there is 20.89 MTHM of PWR LEU (85.13% of all in term of mass) and 3.65 MTHM MOX fuel (Table 5-5). In this state, the plutonium is self-sustaining in the cycle. Depleted U here means 0.3% enrichment of U235, tails from enrichment facility.

5.2.2 DUPIC FUEL

In DUPIC scenario, in order to use all PWR SF to make DUPIC fuel, there is a equilibrium core ratio between PWRs and CANDUs. It is assumed that 1% for DUPIC fuel fabrication. PWR SF is cooled for 10 years and then fabricated into DUPIC fuel. For 1 GWe-yr, assume r as core ratio between PWRs and CANDUs, Wp is HM in the core for PWR. Then $rWp \times 99\%$ is HM can be used in the core for the following CANDU, to make it equal to Wc which is HM in one core for CANDU:

$rWp \times 0.99 = Wc \Rightarrow$

#ofPWR/#ofCANDU = r = Wc/0.99Wp = 46.09/(0.99×23.31) = 1.997

Electricity generation portion of PWR will be [Ref 5-1]:

$$\frac{P_{PWR}r}{P_{PWR}r + P_{CANDU}}$$

where P_{PWR} and P_{CANDU} are electricity powers of PWR and CANDU respectively.

It can be calculated that the electricity generation portions of PWR and CANDU are 72.68% and 27.32% respectively.

Table 5-4 DUPIC characteristics

	PWR	CANDU
Ratio of core #	1.997	1
Electric power per core (MWe)	950	713
Electricity generation portion (%)	72.68	27.32
Electricity generated (MWe)	726.8	273.2
Thermal efficiency (%)	34	33
Load factor	0.8	0.9
Discharge burnup (MWd/kgHM)	35	15.4

5.2.3 Loaded Fuels for All Scenarios

Table 5-5 Required fuels for the three fuel cycle options (Based on 1GWe-yr)

Fuel types	Nuclear fuel cycles (MTHM)		
	PWR-OT	PWR-MOX	DUPIC
PWR	24.54	20.89	17.83
MOX	—	3.65	—
DUPIC	—	—	(17.66)*
Total Input	24.54	24.54	17.83
* made with PWR SF from previous stages			

Table 5-6 Fresh fuel characteristics

Fuel types	Description
PWR	UO2, 3.5% U235
MOX	5%PuO2, Pu reprocessed from PWR SF with 35,000 GWD/MTHM, 95% UO2, Depleted U with 0.3% U235
DUPIC	DUPIC fuel, made from 35,000 GWD/MTHM, PWR SF

To generate 1 GWe-yr electricity, the required fuel amounts for three cycles are calculated and summarized in Table 5-5. And the fresh fuel characteristics are summarized in Table 5-6.

Table 5-7, Table 5-8, and Table 5-9 list the required material flow in the three cycles to generate 1 GWe-yr respectively.

Table 5-7 Material flow of PWR-OT based on 1Gwe-yr scenario

Stage Name	Product Material	Input Material (MTHM)	Input Material (MT)
Mining/Milling	(WORLD AVERAGE ORE GRADE (% U3O8): 0.15%) ore is processed locally, yellowcake is produced, which contains 80% U3O8, enrichment 0.72%	189.75	171890.21
Conversion	U3O8 is purified and converted into uranium hexafluoride through the process: U3O8 - UO2 - UF4 - UF6, 0.5% loss.0.72%	189.75	322.3
Enrichment	U235 are enriched in the step. Two large commercial scale facilities: centrifuge and gas diffusion techniques. Assume tail 0.3% and product 3.5%	188.8	279.32
LEU Fuel Fabrication	UF6 is converted into UO2 and then the powder is pressed to form a right circular cylindrical pellet. The pellet is further ground into required size and then properly cupped at the ends. The dry fuel pellets are loaded into zircaloy tubes. The fuel rods are assembled together (17×17). pellet o.d. 7.4 mm, assembly length is 3.7 m. 1% loss. 3.5%	24.79	28.12
PWR	PWR fresh fuel (3.5% UO2) is burned up to 35,000 GWD/MTHM. SF with ~0.8%	24.54	27.84
AFR Storage	PWR SF	24.54	27.84
Permanent Disposal	PWR SF	24.54	27.84

Table 5-8 Material flow of DUPIC based on 1Gwe-yr scenario

Stage Name	Product Material	Input Material (MTHM)	Input Material (MT)
Mining/Milling	(WORLD AVERAGE ORE GRADE (% U3O8): 0.15%) ore is processed locally, yellowcake is produced, which contains 80% U3O8, enrichment 0.72%	137.91	124893.21
Conversion	U3O8 is purified and converted into uranium hexafluoride through the process: U3O8 - UO2 - UF4 - UF6, 0.5% loss.0.72%	137.91	234.18
Enrichment	U235 are enriched in the step. Two large commercial scale facilities: centrifuge and gas diffusion techniques. Assume tail 0.3% and product 3.5%	137.22	202.95
LEU Fuel Fabrication	UF6 is converted into UO2 and then the powder is pressed to form a right circular cylindrical pellet. The pellet is further ground into required size and then properly cupped at the ends. The dry fuel pellets are loaded into zircaloy tubes. The fuel rods are assembled together (17×17). pellet o.d. 7.4 mm, assembly length is 3.7 m. 1% loss. 3.5%	18.01	20.43
PWR	PWR fresh fuel (3.5% UO2) is burned up to 35,000 GWD/MTHM. SF with ~0.8%	17.83	20.23
Storage	PWR SF	17.83	20.23
DUPIC Fuel Fabrication	PWR SF is processed after 10 yr cooling. 1% loss during DUPIC fuel fabrication, ratio of PWR core # to CANDU core # is 1.997	17.83	20.23
CANDU	DUPIC fuel is burned up to 15,400 GWD/MTHM.	17.66	20.23
AFR Storage	DUPIC SF	17.66	20.23
Permanent Disposal	DUPIC SF	17.66	20.23

Table 5-9 Material flow of PWR-MOX based on 1Gwe-yr scenario

Stage Name	Product Material	Input Material (MTHM)	Input Material (MT)
Mining/Milling	(WORLD AVERAGE ORE GRADE (% U3O8): 0.15%) ore is processed locally, yellowcake is produced, which contains 80% U3O8, enrichment 0.72%	141.78	128435.28
Conversion	U3O8 is purified and converted into uranium hexafluoride through the process: U3O8 - UO2 - UF4 - UF6, 0.5% loss. 0.72%	161.51 (141.78 from milling + recovered U 19.73)	274.33
Enrichment	U235 are enriched in the step. Two large commercial scale facilities: centrifuge and gas diffusion techniques. Assume tail 0.3% and product 3.5%	162.33 (141.23 tail + 21.1 product)	237.74
LEU Fuel Fabrication	UF6 is converted into UO2 and then the powder is pressed to form a right circular cylindrical pellet. The pellet is further ground into required size and then properly cupped at the ends. The dry fuel pellets are loaded into zircaloy tubes. The fuel rods are assembled together (17×17). pellet o.d. 7.4 mm, assembly length is 3.7 m. 1% loss. 3.5%	21.1	23.94
MOX Fuel Fabrication	5% Pu recovered from PWR SF + 95% Depleted U (0.3% enrichment, tail from enrichment facility) 1% loss.	3.69 (0.18 Pu + 3.51U)	4.19
PWR-MOX	85.13% LEU (3.5% UO2) + 14.87% MOX (5% Pu + 95% Depleted U) is burned up to 35,000 GWD/MTHM.	24.54 (20.89 LEU + 3.65 MOX)	27.84
AFR Storage	MOX SF	3.65	4.14
PWR SF Reprocessing	PWR SF is reprocessed after 10 years cooling. 99% Pu (0.891wt% in SF) is recovered to make MOX fuel. 99% U (95.4 wt%, U235 0.85%) is recovered and sent to conversion facility, the rest is treated as HLW	20.89 (0.98 HLW+0.18 Pu + 19.73 recovered U))	23.7
Permanent Disposal	MOX SF + HLW	4.63	5.23

5.3 System Performances

Fuel cycle system performances were investigated for the selected cases by using the models developed in this study. No attempt is made in this section to combine the calculated performance metrics of repository impact, proliferation resistance, and economics. Combining these metrics using a cost-based integration scheme is described in the next sections (5.4&5.5).

5.3.1 Repository Performance

Table 5-10 summarizes the repository performance of three scenarios. As shown in Figure 5-2, decay heat from MOX spent fuel is much higher than the other two types of spent fuels in 100,000 years and due to the temperature limits at repository, very limited MOX spent fuel can be loaded in the repository. This is because there are more actinides left in MOX spent fuel and they are main contributors for long term decay heat (Table 5-11). In all three scenarios, the maximum loading is limited by the temperature limit at midway between drifts. The repository can host more DUPIC spent fuel than the other two types of spent fuel. The projected dose rates from the full loaded repository in three scenarios are shown in Figure 5-3.

Table 5-10 Repository performance of three scenarios
(assume only one type of spent fuel filling the capacity limit)

	DUPIC	PWRMOX	PWROT
Total Area[acre]	1165.8	1165.8	1165.8
Total Buried Waste [MTU]	113730.6	19660.6	87391
Repository AML [MTU/acre]	97.6	16.9	75
WP Density [MTU/WP]	12.09	2.09	9.29
Maximum Drift-wall Temperature [°C]	166.7	113.5	139.9
At time [yr]	69.3	162.1	77.3
Maximum Midway Temperature [°C]	95.5	91.5	95.7
At time_[yr]	474.2	657.5	657.5

The result shows more inventory results more the projected dose rate. The waste package will not fail until 90,000 years.

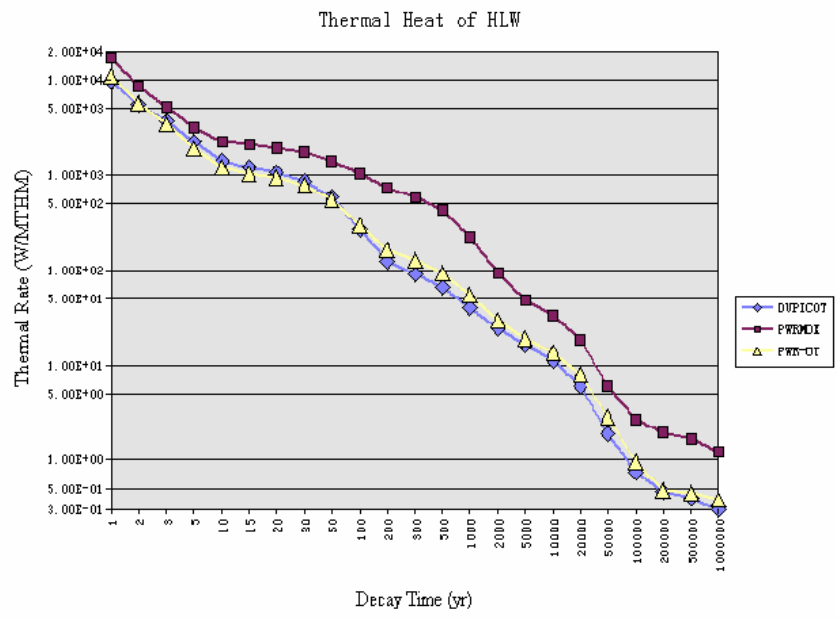

Figure 5-2 Decay heat of the nuclear waste

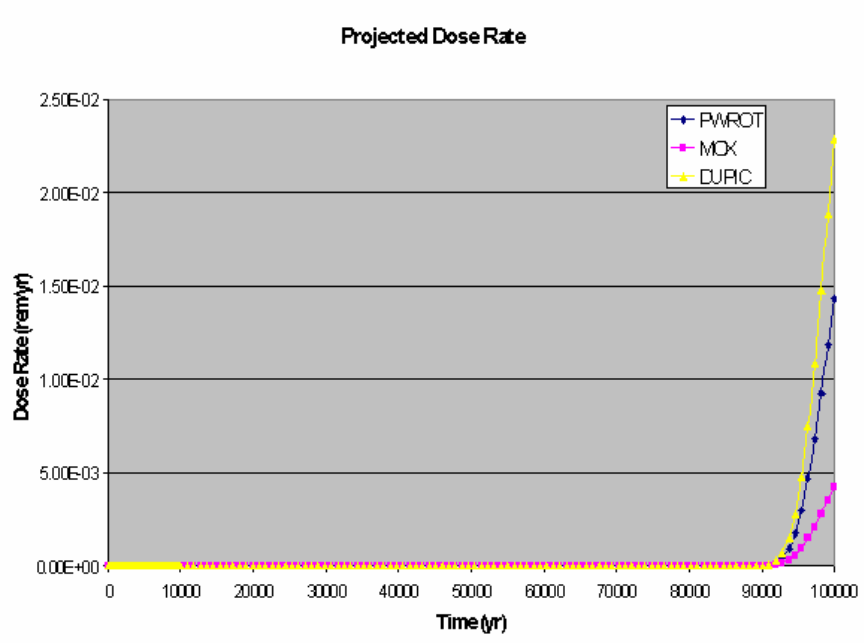

Figure 5-3 Projected dose rate from full loaded repository

Table 5-11 Isotopes inventory in spent fuel

	halflife	PWR-OT	**MOX**	DUPIC
	[yr]	Inventory [Ci/MTU]		
Cm246	**4.73E+03**	3.47E-02	**4.01E-01**	1.89E-01
Cm245	**8.50E+03**	1.66E-01	**2.24E+00**	1.20E-01
Cm244	**1.81E+01**	1.52E+03	**2.10E+04**	3.33E+03
Cm243	**2.85E+01**	1.23E+01	**1.26E+02**	5.10E+01
Am243	**7.38E+03**	1.83E+01	**2.44E+02**	3.04E+01
Pu242	**3.87E+05**	1.76E+00	**1.84E+01**	3.93E+00
Am242m	**1.52E+02**	1.16E+01	**1.64E+02**	1.38E+00
Pu241	**1.44E+01**	7.80E+04	**3.92E+05**	4.64E+04
Am241	**4.32E+02**	1.70E+03	**9.32E+03**	1.04E+03
Pu240	**6.54E+03**	5.04E+02	**1.50E+03**	5.46E+02
Pu239	**2.41E+04**	3.32E+02	**4.96E+02**	1.87E+02
U238	**4.47E+09**	3.17E-01	**3.14E-01**	3.15E-01
Pu238	**8.77E+01**	2.53E+03	**1.19E+04**	3.07E+03
Np237	**2.14E+06**	3.69E-01	**6.35E-02**	2.63E-01
U236	**2.34E+07**	2.82E-01	**1.79E-02**	3.06E-01
U235	**7.04E+08**	1.75E-02	**2.83E-03**	7.39E-04
U234	**2.45E+05**	8.34E-02	**4.18E-01**	1.13E-01
U233	**1.59E+05**	1.88E-05	**2.84E-06**	1.28E-05
U232	**7.20E+01**	2.11E-02	**2.65E-03**	4.28E-03
Pa231	**3.28E+04**	4.52E-06	**9.27E-07**	1.13E-06
Th230	**7.70E+04**	4.26E-06	**2.28E-05**	7.41E-06
Th229	**7.34E+03**	3.42E-08	**4.85E-09**	4.74E-07
Ac227	**2.18E+01**	7.80E-07	**1.82E-07**	3.41E-07
Ra226	**1.60E+03**	6.99E-09	**3.98E-08**	1.86E-08
Pb210	**2.23E+01**	9.52E-10	**3.53E-09**	2.82E-09
Sm151	**9.00E+01**	3.71E+02	**5.35E+02**	9.10E+01
Cs137	**3.00E+01**	8.83E+04	**9.10E+04**	1.08E+05
Cs135	**2.30E+06**	3.81E-01	**6.19E-01**	8.08E-01
I129	**1.57E+07**	3.30E-02	**4.19E-02**	4.05E-02
Sn126	**1.00E+05**	7.93E-01	**9.58E-01**	1.05E+00
Sn121m	**5.00E+01**	1.86E-01	**2.86E-01**	2.55E-01
Ag108m	**4.18E+02**	2.76E-05	**6.22E-05**	1.12E-04
Pd107	**6.50E+06**	1.14E-01	**3.10E-01**	1.85E-01
Tc99	**2.13E+05**	1.40E+01	**1.46E+01**	1.84E+01
Nb94	**2.03E+04**	1.43E-04	**2.74E-04**	2.26E-04
Mo93	**3.50E+03**	1.00E-30	**1.00E-30**	1.00E-30
Zr93	**1.53E+06**	1.95E+00	**1.33E+00**	2.69E+00
Sr90	**2.91E+01**	6.28E+04	**2.97E+04**	6.92E+04
Se79	**1.10E+06**	4.36E-01	**3.30E-01**	5.95E-01
Ni63	**9.20E+01**	1.00E-30	**1.00E-30**	1.00E-30
Ni59	**8.00E+04**	1.00E-30	**1.00E-30**	1.00E-30
Cl36	**3.01E+05**	1.00E-30	**1.00E-30**	1.00E-30
C14	**5.73E+03**	1.25E-04	**1.23E-04**	1.80E-04

5.3.2 Proliferation Resistance

Isotopic actinides inventory is generated by using ORIGEN2.2 for spent fuels from three scenarios (Table 5-12 - Table 5-14).

Table 5-12 Isotopic actinides inventory for PWROT

PWROT						
	SF		10.0YR		50.0YR	
U235	8.09E+03	0.84%	8.09E+03	0.84%	8.10E+03	0.85%
U238	9.41E+05	98.19%	9.41E+05	98.23%	9.41E+05	98.30%
PU238	1.48E+02	0.02%	1.48E+02	0.02%	1.08E+02	0.01%
PU239	5.24E+03	0.55%	5.34E+03	0.56%	5.33E+03	0.56%
PU240	2.21E+03	0.23%	2.21E+03	0.23%	2.22E+03	0.23%
PU241	1.22E+03	0.13%	7.57E+02	0.08%	1.10E+02	0.01%
PU242	4.60E+02	0.05%	4.60E+02	0.05%	4.60E+02	0.05%
Total	9.59E+05	100.00%	9.58E+05	100.00%	9.58E+05	100.00%

Table 5-13 Isotopic actinides inventory for MOX

MOX						
	SF		10.0YR		50.0YR	
U235	1.30E+03	0.14%	1.31E+03	0.14%	1.32E+03	0.14%
U238	9.35E+05	97.16%	9.35E+05	97.38%	9.35E+05	97.71%
PU238	6.41E+02	0.07%	6.96E+02	0.07%	5.09E+02	0.05%
PU239	7.90E+03	0.82%	7.97E+03	0.83%	7.97E+03	0.83%
PU240	6.49E+03	0.67%	6.60E+03	0.69%	6.77E+03	0.71%
PU241	6.15E+03	0.64%	3.80E+03	0.40%	5.54E+02	0.06%
PU242	4.82E+03	0.50%	4.82E+03	0.50%	4.82E+03	0.50%
Total	9.62E+05	100.00%	9.60E+05	100.00%	9.57E+05	100.00%

Table 5-14 Isotopic actinides inventory for DUPIC

DUPIC						
	SF		10.0YR		50.0YR	
U235	3.41E+02	0.04%	3.42E+02	0.04%	3.45E+02	0.04%
U238	9.35E+05	99.20%	9.35E+05	99.21%	9.35E+05	99.26%
PU238	1.57E+02	0.02%	1.79E+02	0.02%	1.31E+02	0.01%
PU239	2.92E+03	0.31%	3.01E+03	0.32%	3.00E+03	0.32%
PU240	2.38E+03	0.25%	2.40E+03	0.25%	2.42E+03	0.26%
PU241	7.28E+02	0.08%	4.50E+02	0.05%	6.56E+01	0.01%
PU242	1.03E+03	0.11%	1.03E+03	0.11%	1.03E+03	0.11%
Total	9.43E+05	100.00%	9.43E+05	100.00%	9.42E+05	100.00%

Table 5-15 Stages involved in three scenarios

Stage Number	PWR-OT	PWR-MOX	DUPIC-OT
1	Mining/Milling	Mining/Milling	Mining/Milling
2	Conversion	Conversion	Conversion
3	Enrichment	Enrichment	Enrichment
4	LEU Fuel Fabrication	LEU Fuel Fabrication	LEU Fuel Fabrication
5	PWR irradiation	MOX Fuel Fabrication	PWR irradiation
6	AFR Storage	PWR irradiation	DUPIC Fuel Fabrication
7	Permanent Disposal	AFR Storage	CANDU irradiation
8		PWR SF Reprocessing	AFR Storage
9		Permanent Disposal	Permanent Disposal

In PWR-OT scenario, the spent fuel at AFR storage stage is treated as 10 year old spent fuel and Disposal stage has 50 years old spent fuel. Similar assumption is applied for MOX scenario. In DUPIC scenario, DUPIC Fuel is the same as 10 year old PWR-OT spent fuel and the DUPIC spent fuel at AFR storage stage is treated as 10 year old DUPIC spent fuel and Disposal stage has 50 years old DUPIC spent fuel.

Use total mass at each stage (Table 5-7-Table 5-9) and the mass fraction (Table 5-12-Table 5-14), and the basic information list in Table 3-3, 15 quantities at each stage are calculated (Table 5-16-Table 5-18).

The market natural uranium metal price is around $200/kg (from internet), this value is assumed as the reprocessing cost for single compounds including oxides because the “yellow cake” is very cheap as around $15/lb, and the main cost of natural uranium metal should be the separation cost from oxide. For spent fuel, it is assumed as 3000 $/Kg and 100 $/kg is assumed for MOX fuel since the separated Pu appears.

If there is no fission products exist, the dose rate is assigned as 0.001 mrem/hr/kg, otherwise, the value is assigned as 100 mrem/hr/kg [Ref 5-1].

If there is no fission products exist, then detectability level is assigned as 3, otherwise, detectability level is assigned as 5 [Ref 3-30]. The other values are assumed by the author.

Table 5-15 shows the stages involved in the three scenarios and Figure 5-4 shows the proliferation resistance changes along the stages from the beginning to the end of a fuel cycle. PWR-OT shows relative high proliferation resistance during the whole cycle. And DUPIC has a low point at stage 7, which is CANDU reactor operation. The low proliferation resistance at this stage is mainly due to the online refueling characteristic which makes the system is assessable to proliferators in much higher chance compared to PWR reactor operation. In MOX system, there are two relative lower points in the cycle, stage 5 and stage 8 are MOX fuel fabrication and PWR spent fuel reprocessing respectively. These two low points are due to the separated Pu. The reprocessing technology at stage 8 may be used directly by the proliferator for other purpose, this makes stage 8 has even lower proliferation resistance. The weighted system PRs are shown in Table 5-19. Based on the mean values, PWR-OT can be ranged to HIGH proliferation resistance level and both MOX and DUPIC belong to HIGH-MINUS level. But based on min stage mean values, PWR-OT will be grouped into M+ level, MOX into L+ level and DUPIC into M- level.

Table 5-16 Important Quantities for PWR-OT

Stage Number	1	2	3	4	5	6	7
Weight	7.948E-04	4.239E-01	2.366E+00	3.086E+00	3.159E+00	3.206E+00	3.206E+00
Critical Mass (kg)	3.375E+05	3.375E+05	1.886E+04	1.886E+04	1.000E+01	1.000E+01	1.000E+01
Equivalent Enrichment	7.200E-01	7.200E-01	3.500E+00	3.500E+00	4.725E+01	4.875E+01	5.091E+01
SFN (neutron/sec/kg)	1.260E+01	1.260E+01	1.226E+01	1.226E+01	3.327E+03	3.333E+03	3.231E+03
Heat (W/kg)	8.877E-06	8.877E-06	1.021E-05	1.021E-05	1.227E-01	1.197E-01	9.185E-02
Gamma rate (MeV/s/kg)	1.039E-01	1.039E-01	4.482E-01	4.482E-01	2.123E+02	2.053E+02	1.536E+02
SeparationCost ($/Kg)	200	200	200	200	3000	3000	3000
DoseRate (mrem/hr/kg)	0.001	0.001	0.001	0.001	100	100	100
Concentration (1/kg)	3.271E-09	1.744E-06	3.583E-05	4.673E-05	8.815E-02	8.815E-02	8.815E-02
Detectability	3	3	3	3	5	5	5
FacilityModificationTime (week)	100	100	0.1	100	1	100	100
FrequencyofAccess (day/yr)	365	365	180	365	10	180	100
AvailableMass (# of CM)	0.56	0.56	10.01	1.31	65.00	24.54	24.54
UncertaintyofMeasurement (#ofCM/yr)	0.01	0.01	0.01	0.01	0	0	0
Knowledge (yr)	10	10	0.1	10	2	10	10
Time (yr)	2	2	1	0.5	3	10	50

Table 5-17 Important quantities for MOX

Stage Number	1	2	3	4	5	6	7	8	9
Weight	7.95E-04	4.24E-01	2.39E+00	3.08E+00	2.46E+00	3.74E+00	3.78E+00	9.00E-01	8.85E-01
Critical Mass (kg)	3.37E+05	3.37E+05	1.89E+04	1.89E+04	1.00E+01	1.00E+01	1.00E+01	1.00E+01	1.00E+01
Equivalent Enrichment	7.20E-01	7.20E-01	3.50E+00	3.50E+00	4.72E+01	3.58E+01	3.71E+01	4.72E+01	3.94E+01
SFN (neutron/sec/kg)	1.26E+01	1.26E+01	1.23E+01	1.23E+01	3.31E+03	1.64E+04	1.67E+04	3.31E+03	1.64E+04
Heat (W/kg)	8.88E-06	8.88E-06	1.02E-05	1.02E-05	1.23E-01	4.83E-01	5.02E-01	1.23E-01	3.73E-01
Gamma rate (MeV/s/kg)	1.04E-01	1.04E-01	4.48E-01	4.48E-01	2.12E+02	8.66E+02	8.91E+02	2.12E+02	6.51E+02
SeparationCost ($/Kg)	200	200	200	200	100	3000	3000	100	3000
DoseRate (mrem/hr/kg)	0.001	0.001	0.001	0.001	100	100	100	100	100
Concentration (1/kg)	3.27E-09	1.74E-06	3.62E-05	4.67E-05	9.00E-02	8.81E-02	8.82E-02	9.00E-02	8.85E-02
Detectability	3	3	3	3	3	5	5	1	5
FacilityModificationTime (week)	100	100	0.1	100	100	100	100	1	100
FrequencyofAccess (day/yr)	365	365	180	365	365	10	180	365	100
AvailableMass (# of CM)	0.42	0.48	8.60	1.12	0.18	65	3.65	0.18	4.63
UncertaintyofMeasurement (#ofCM/yr)	0.01	0.01	0.01	0.01	0.01	0	0	0.01	0
Knowledge (yr)	10	10	0.1	10	10	10	10	0.1	10
Time (yr)	2	2	1	0.5	1	3	10	2	50

Table 5-18 Important quantities for DUPIC

Stage Number	1	2	3	4	5	6	7	8	9
Weight	7.95E-04	4.24E-01	2.37E+00	3.09E+00	3.16E+00	3.16E+00	1.38E+00	1.42E+00	1.42E+00
Critical Mass (kg)	3.37E+05	3.37E+05	1.89E+04	1.89E+04	1.00E+01	1.00E+01	1.00E+01	1.00E+01	1.00E+01
Equivalent Enrichment	7.20E-01	7.20E-01	3.50E+00	3.50E+00	4.72E+01	4.72E+01	4.02E+01	4.11E+01	4.23E+01
SFN (neutron/sec/kg)	1.26E+01	1.26E+01	1.23E+01	1.23E+01	3.33E+03	3.33E+03	4.59E+03	4.67E+03	4.56E+03
Heat (W/kg)	8.88E-06	8.88E-06	1.02E-05	1.02E-05	1.23E-01	1.23E-01	1.23E-01	1.35E-01	1.04E-01
Gamma rate (MeV/s/kg)	1.04E-01	1.04E-01	4.48E-01	4.48E-01	2.12E+02	2.12E+02	2.16E+02	2.37E+02	1.79E+02
SeparationCost ($/Kg)	200	200	200	200	3000	3000	3000	3000	3000
DoseRate (mrem/hr/kg)	0.001	0.001	0.001	0.001	100	100	100	100	100
Concentration (1/kg)	3.27E-09	1.74E-06	3.58E-05	4.67E-05	8.81E-02	8.81E-02	8.73E-02	8.73E-02	8.73E-02
Detectability	3	3	3	3	5	5	5	5	5
FacilityModificationTime (week)	100	100	0.1	100	1	100	1	100	100
FrequencyofAccess (day/yr)	365	365	180	365	10	365	365	180	100
AvailableMass (# of CM)	0.41	0.41	7.27	0.95	65	17.83	85	17.66	17.66
UncertaintyofMeasurement (#ofCM/yr)	0.01	0.01	0.01	0.01	0.01	0.01	0.01	0	0
Knowledge (yr)	10	10	0.1	10	2	10	10	10	10
Time (yr)	2	2	1	0.5	3	0.5	3	10	50

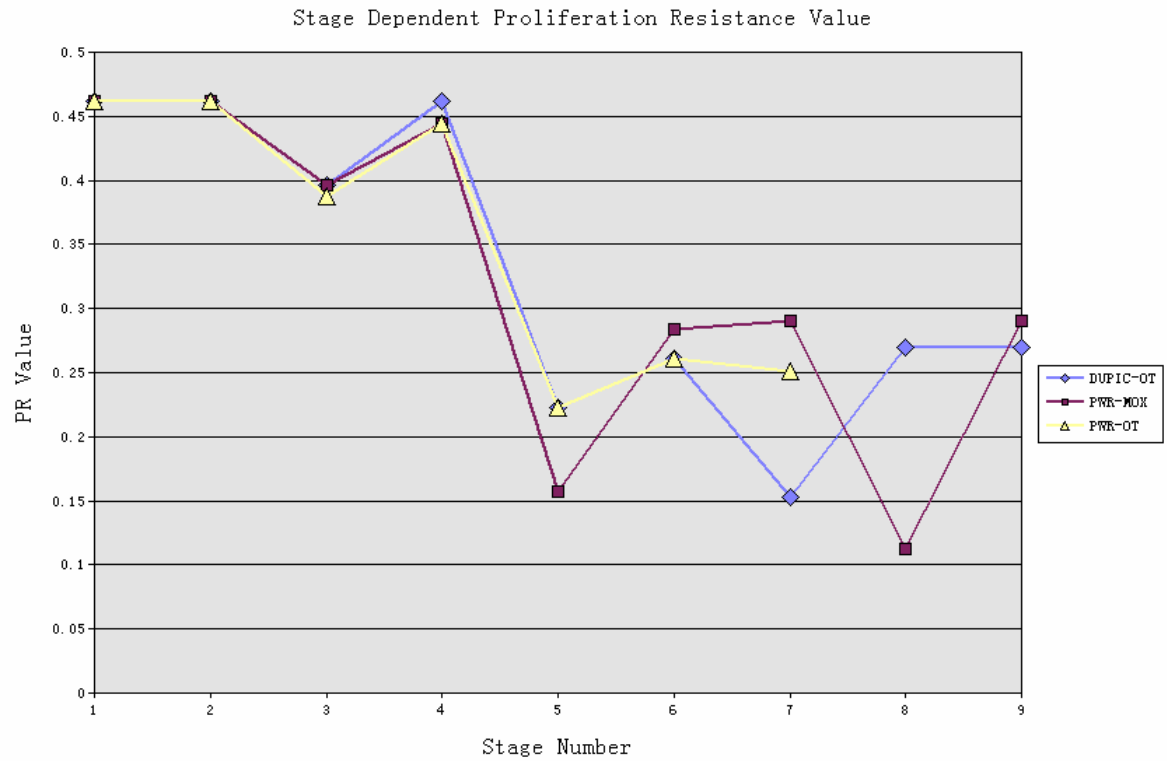

Figure 5-4 Stage mean proliferation of systems

Table 5-19 System PRs

System Name	System Mean PR	System Level indicated by System Mean PR	Min Stage Mean PR	System Level indicated by Min Stage Mean PR
PWR-OT	0.3285	H	0.2232	M+
PWR-MOX	0.2938	H-	0.1129	L+
DUPIC-OT	0.3033	H-	0.1533	M-

5.3.3 Fuel Cycle Cost

For case (private owner [Ref 5-2]):

τ = 38% f_b = 30%

r_b = 9% r_s = 16%

$\Rightarrow$

x = 0.13

ϕ = 0.21

Table 5-20 Unit price used in fuel cycle cost

Cost Component	**OECD Estimate***	
Ore Purchase	30 ± 10	$/kgHM
Conversion	5 ± 2	$/kgSWU
Enrichment	80 ± 30	$/kgHM
UOX Fabrication	250 ± 50	$/kgHM
SF Storage and Disposal	420 ± 100	$/kgHM
Reprocessing	800 ± 100	$/kgHM
HLW Storage and Disposal	46 ± 5.75	$/kgHM
MOX Fabrication	1100 ± 200	$/kgHM
DUPIC Fabrication[Ref 5-4]	623 ± 125	$/kgHM

* In 2000 dollars, escalation rate of 3% [Ref 5-3]

Assumptions:

1. Fuel irradiation time: 3 yrs
2. enrichment tails assay: 0.3%
3. natural U enrichment: 0.72%
4. fresh PWR fuel enrichment: 3.5%
5. losses are neglected
6. carrying charge factor: ϕ = 0.21 per year
7. the cost of waste storage and disposal is paid at the end of irradiation
8. lead time or lag time (Lead time is the term referring to the date at which materials are obtained, services are performed and payments for front-end components occur, prior and relative to the date of loading fuel into the reactor. Lag time is the date at which a payment for the back-end occurs, after and relative to the fuel discharge date):

Table 5-21 Lead time of all components

Component	**Lead Time (yr)**
ore purchase	2
conversion	2
enrichment	1
PWR fuel fabrication	0.5
DUPIC fuel fabrication	0.5
MOX fuel fabrication	1
reprocessing	2
storage of HLW from reprocessing	1

Based on the assumptions and the material flow (Table 5-7-Table 5-9) and assumption that the disposal cost is charged by price per unit mass, the fuel cycle costs for three scenarios were calculated. The details of the calculations are listed in Table 5-22, Table 5-23 and Table 5-24. All costs are in 2000 dollars, unless otherwise noted. PWR-OT provides the lowest FCC as 0.460 cents/kwhe and PWR-MOX provides the highest FCC as 0.764 cents/kwhe while DUPIC provides FCC as 0.512 cents/kwhe.

Table 5-22 PWR-OT fuel cycle cost to generate 1GWe-yr

						Direct Cost ($)	Carrying Charge ($)
	Mi		Ci		ΔTi (yr)	Mi.Ci	Mi.Ci.φ.ΔTi
ore purchase	189.75	MTHM	30	$/KgHM	3.5	5692500	4183987.5
conversion	189.75	MTHM	5	$/KgHM	3.5	948750	697331.25
enrichment	106.37	MT SWU	80	$/kg SWU	2.5	8509483.112	4467478.634
PWR fuel fabrication	24.54	MTHM	250	$/KgHM	2	6135000	2576700
storage and disposal	24.54	MTHM	420	$/KgHM	-1.5	10306800	-3246642
					Total ($)	31592533.11	8678855.384
				Grand Total ($)		40271388.5	
				fuel cycle cost		(cents/kWhe)	0.460

Table 5-23 PWR-MOX fuel cycle cost to generate 1GWe-yr

						Direct Cost ($)	Carrying Charge ($)
	Mi		Ci		ΔTi (yr)	Mi.Ci	Mi.Ci.φ.ΔTi
ore purchase	141.78	MTHM	30	$/KgHM	3.5	4253400	3126249
conversion	141.78	MTHM	5	$/KgHM	3.5	708900	521041.5
enrichment	90.54	MT SWU	80	$/kg SWU	2.5	7242843.633	3802492.907
PWR fuel fabrication	21.1	MTHM	250	$/KgHM	2	5275000	2215500
reprocessing	20.89	MTHM	800	$/KgHM	4.5	16712000	15792840
MOX Fabrication	3.69	MTHM	1100	$/KgHM	2.5	4059000	2130975
storage and disposal of HLW	0.98	MTHM	46	$/KgHM	2.5	45080	23667
storage and disposal of MOX SF	3.65	MTHM	420	$/KgHM	-1.5	1533000	-482895
					Total ($)	39829223.63	27129870.41
				Grand Total ($)		66959094.04	
				fuel cycle cost		(cents/kWhe)	0.764

For DUPIC system, it is assumed that spent fuel from PWR is storied without charge and ready for DUPCI fuel fabrication. PWR and CANDU reactors are operated at the same time with the same irradiation time.

Table 5-24 DUPIC-OT fuel cycle cost to generate 1GWe-yr

						Direct Cost ($)	Carrying Charge ($)
	Mi		Ci		ΔTi (yr)	Mi.Ci	Mi.Ci.φ.ΔTi
ore purchase	137.91	MTHM	30	$/KgHM	3.5	4137300	3040915.5
conversion	137.91	MTHM	5	$/KgHM	3.5	689550	506819.25
enrichment	77.28	MT SWU	80	$/kg SWU	2.5	6182161.793	3245634.941
PWR fuel fabrication	17.83	MTHM	250	$/KgHM	2	4457500	1872150
DUPIC fuel fabrication	17.66	MTHM	623	$/KgHM	2	11002180	4620915.6
storage and disposal of DUPIC SF	17.66	MTHM	420	$/KgHM	-1.5	7417200	-2336418
					Total ($)	33885891.79	10950017.29
				Grand Total ($)		44835909.08	
				fuel cycle cost		(cents/kWhe)	0.512

5.4 Integration of Performance Measures

To effectively aid the decision making process for fuel cycle selections, a systematic integration of performance metrics is desirable. An integrated system performance index which includes all important system performance measures can help decision maker to screening candidate systems quicker and easier. The integrated system performance index also can be used easily in optimal system searching model.

Table 5-25 shows the performance summary. Due to the temperature limits, repository has different maximum loading for the three cycles. Even though repository can host the least MOX spent fuel, the total electricity generated from the loaded MOX waste in repository is more than the one from the loaded PWR-OT spent fuel. The repository with full loaded waste in DUPIC scenario can generate the most electricity which is 80% more in PWR-OT scenario. This is because fissile materials from PWR-OT spent fuel are recycled partially in both MOX and DUPIC scenarios. This means the same repository is maximally used in DUPIC scenarios. But PWR-OT has lowest system mean and stage minimum proliferation resistance.

Table 5-25 Performance summary

	PWR-OT	MOX	DUPIC
SF generated from 1 Gwe-yr electricity (MTHM)	24.54	4.63	17.66
Maximum loading in Yucca M. according to temperature limits (MTHM)	87391	19661	113731
total electricity generated from the max loading repository (Gwe-yr)	3561	4246	6440
Fuel Cycle Cost (cents/kwhe)	0.460	0.819	0.498
Mean Proliferation Resistance Value in all stages	0.328	0.294	0.303
Minimum Proliferation Resistance Value in all stages	0.223	0.113	0.153

5.4.1 Cost Benefit of Repository Capacity Expansion

Repository performance study shows the same repository like YUCCA Mountain has different capacity for different type of spent fuel, under the temperature limit at driftwall and midway between drifts (Table 5-10). Assume the disposal cost 420$/kgHM is for reference design of YUCCA Mountain for PWR-OT spent fuel. And the disposal cost will change with the capacity change when different spent fuel is loaded. To keep the total charge of all waste unchanged, the unit price of unit mass waste changes inverse to the total capacity (Table 5-26).

Table 5-26 Different disposal cost for three scenarios

Storage and Disposal for PWR-OT	420
Storage and Disposal of HLW for MOX	204.47
Storage and Disposal of MOX SF	1866.89
Storage and Disposal of DUPIC SF	322.73

The comparison of these two different calculation methods is shown in Table 5-27. FCC of MOX becomes higher because the more charge for final disposal. DUPIC FCC decreases slightly due to the decreasing disposal cost.

Table 5-27 FCCs of all cycles

	PWR-OT	MOX	DUPIC
Disposal Cost=420 $/kgHM	0.460	0.764	0.512
Different disposal cost	0.460	0.808	0.498
Disposal Charge per cask	0.460	0.819	0.498

In this study, it is assumed that the repository will be loaded fully in all scenarios, so the disposal cost should be charged by unit price per cask. The unit price per cask is calculated as: total disposal cost (total loading PWR waste 87391 MTHM multiples disposal cost 420 $/MTHM) divided by the total casks (9407 casks in this case), turns out to be 3.902 M$/cask. The result is very comparable to the result

with adjusted disposal cost (Table 5-27). The FCC calculated based on disposal charge per cask will be used in the rest of this report.

Table 5-28, Table 5-29 and Table 5-30 shows the contribution from each stage to the final FCC for all three cycles. Enrichment stage always costs a lot and even the most in PWR-OT cycle. Reprocessing costs the most in MOX cycle and DUPIC fuel fabrication costs most in DUPIC compared with other stages.

Table 5-28 Contribution of all stages to PWR-OT FCC

PWR-OT FCC		
Stage	cents/kwhe	percentage
ore purchase	0.113	25%
conversion	0.019	4%
enrichment	0.148	32%
PWR fuel fabrication	0.099	22%
storage and disposal	0.081	18%
TOTAL	0.46	100%

Table 5-29 Contribution of all stages to MOX FCC

MOX FCC		
Stage	cents/kwhe	percentage
ore purchase	0.084	10%
conversion	0.014	2%
enrichment	0.126	15%
PWR fuel fabrication	0.086	10%
reprocessing	0.371	45%
MOX Fabrication	0.071	9%
storage and disposal of MOX SF	0.068	8%
TOTAL	0.819	100%

Table 5-30 Contribution of all stages to DUPIC FCC

DUPIC FCC		
Stage	cents/kwhe	percentage
ore purchase	0.082	16%
conversion	0.014	3%
enrichment	0.108	22%
PWR fuel fabrication	0.072	14%
DUPIC fuel fabrication	0.178	36%
storage and disposal of DUPIC SF	0.045	9%
TOTAL	0.498	100%

5.4.2 Cost Benefit of Proliferation Resistance

Based on FCC with benefit of repository capacity expansion, further consider penalty to the different proliferation resistance performance, PWR-OT is used as reference. A nonproliferation resistance charge is assumed to be 15% of the FCC. If the system mean proliferation resistance of a system is lower than that of PWR-OT, then a higher nonproliferation resistance charge will be incurred. Table 5-31 shows the comparison of FCC with nonproliferation charge for all scenarios in this study. PWR-OT still behaviors best in term of FCC and DUPIC is very close (8.9% more). FCC of MOX is highest one which is 70% more than that of PWR-OT. This adjusted FCC is the result of considering benefit/penalty from both repository capacity change and proliferation resistance difference.

Table 5-31 FCC with non proliferation charge

fuel cycle cost (cents/kWhe)			
	PWR-OT	MOX	DUPIC
FCC (Table 5-27)	0.460	0.819	0.498
Mean PR	0.328	0.294	0.303
NonProliferation Charge	0.069	0.077	0.075
Adjusted FCC*	0.529	0.896	0.573

* Proliferation resistance cost assumes to be 15% of base FCC for PWR-OT

5.5 Comparisons of Fuel Cycles Based on Electricity Generation Cost

Comparison of fuel cycles can be made by comparing the total electricity generation cost of the same amount of electricity under the condition with one repository. With the same one repository condition, DUPIC scenario generates the most electricity (Table 5-25). The electricity gap between the other scenarios to

DUPIC scenario is assumed to be fulfilled by other type of energy resources (coal and natural gas by assumption). In this manner, for the same one repository and the same amount of electricity, total electricity generation cost which is from nuclear resource and/or other traditional resources can be obtained.

Use the Lowest the pre-tax levelized cost of electricity (LCOE) 31$/MWh in 2003 dollars for new design given in Table 9-7 in "The Economic Future of Nuclear Power", University of Chicago, 2004 [Ref 5-10], which considers 18 $/MWh 8-year production tax credits and 20% investment tax credits. Assume the same Capital Cost and O&M Cost for all scenarios, which is 25.56 $/MWh (31 $/MWh total cost minus 5.44 $/MWh FCC from the report), 23.39 $/MWh in 2000 dollars (3% escalation rate). FCCs for PWR-OT, MOX, DUPIC are 5.29, 8.96, and 5.73 $/MWh (adjusted FCC from Table 5-31) respectively. The electricity gap between any waste forms to dupic spent fuel is calculated and is assumed to be compensated by using energy resource coal and gas. The reference LCOE for other energy sources (coal+gas) is combination of lowest LCOEs of coal and gas (Table 5-32) [Ref 5-10] weighted by the contribution of these two energy sources (Table 5-33) and converted to 2000 dollars: 30.7 $/MWh under current environmental polices and 69.9 $/MWh under greenhouse policy.

Table 5-32 Fossil LCOEs with and without greenhouse policies, $ per MWh, 2003 dollars

	Under Current Environmental Policies	Under Greenhouse Policy
Coal-Fired	33 to 41	83 to 91
Gas-Fired	35 to 45	58 to 68

Table 5-33 Shares of total U.S. electricity generation, by type of generation, 2003

Energy Source	Net Generation, Percent
Coal	50.1
Nuclear	20.2
Natural Gas	17.9
Hydroelectric	6.6
Petroleum	2.5
Non-hydro Renewables	2.3
Other Sources	0.4
Total	100

Under current environmental polices, to generate the same amount of electricity with one repository, the total cost for MOX is highest. And DUPIC shows the lowest cost which is slightly lower than PWROT (1%, Table 5-34). This is because the cost of combination of coal and gas is higher than both total cost in PWROT and DUPIC scenarios, and the benefit of lower total electricity cost in PWROT to DUPIC is overcome by the benefit of more electricity generated under the same one repository in DUPIC to PWROT. Under greenhouse policy, due to higher total electricity cost of traditional resources, the benefit of more electricity generated under the same one repository becomes more obvious and DUPIC shows the lowest cost which is lower than PWROT by 60% (Table 5-35). Even MOX becomes a better choice than PWROT.

Table 5-34 Total cost comparison under current environmental policies

	PWROT	MOX	DUPIC
Total Electricity Cost ($/MWh)	28.68	32.35	29.12
total electricity generated from the max loading repository (Gwe-yr)	3561	4246	6440
Electricity Gap with DUPIC (Gwe-yr)	2879	2194	0
Cost for electricity from nuclear fuel cycle for max loading repository ($)	8.95E+11	1.20E+12	1.64E+12
Cost for electricity from other source to meet the gap ($)	7.74E+11	5.90E+11	0.00E+00
Total cost to generate the same amount of electricity with one repository ($)	1.67E+12	1.79E+12	1.64E+12

Table 5-35 Total cost comparison under greenhouse policy

	PWROT	MOX	DUPIC
Total Electricity Cost ($/MWh)	28.68	32.35	29.12
total electricity generated from the max loading repository (Gwe-yr)	3561	4246	6440
Electricity Gap with DUPIC (Gwe-yr)	2879	2194	0
Cost for electricity from nuclear fuel cycle for max loading repository ($)	8.95E+11	1.20E+12	1.64E+12
Cost for electricity from other source to meet the gap ($)	1.76E+12	1.34E+12	0.00E+00
Total cost to generate the same amount of electricity with one repository ($)	2.66E+12	2.55E+12	1.64E+12

FCC is only around 20% of total electricity cost, nonproliferation defined based on FCC can only show limited influence to total electricity cost. Nonproliferation charge can also be defined based on total electricity cost. 15% of total electricity cost in PWROT is assumed as the nonproliferation charge for PWROT. For others:

nonproliferation charge = Mean PR of PWROT $\times$ nonproliferation charge of PWROT / Mean PR of current scenario

Table 5-36 Nuclear electricity cost (15% Nonproliferation Charge)

	PWROT	MOX	DUPIC
FCC without Nonproliferation Charge ($/MWh)	4.60	8.19	4.98
Total Electricity Cost ($/MWh)	27.99	31.58	28.37
Mean PR	0.328	0.294	0.303
NonProliferation Charge*	4.20	4.68	4.55
PR adjusted Total Cost	32.19	36.27	32.92

Table 5-37 Total cost comparison under current policies (15% Nonproliferation Charge)

	PWROT	MOX	DUPIC
Total Electricity Cost ($/MWh)	32.19	36.27	32.92
total electricity generated from the max loading repository (Gwe-yr)	3561.00	4246.00	6440.00
Electricity Gap with DUPIC (Gwe-yr)	2879.00	2194.00	0.00
Cost for electricity from nuclear fuel cycle for max loading repository ($)	1.00E+12	1.35E+12	1.86E+12
Cost for electricity from other source to meet the gap ($)	8.46E+11	6.44E+11	0.00E+00
Total cost to generate the same amount of electricity with one repository ($)	1.85E+12	1.99E+12	1.86E+12

Table 5-38 Total cost comparison under greenhouse policy (15% Nonproliferation Charge)

	PWROT	MOX	DUPIC
Total Electricity Cost ($/MWh)	32.19	36.27	32.92
total electricity generated from the max loading repository (Gwe-yr)	3561.00	4246.00	6440.00
Electricity Gap with DUPIC (Gwe-yr)	2879.00	2194.00	0.00
Cost for electricity from nuclear fuel cycle for max loading repository ($)	1.00E+12	1.35E+12	1.86E+12
Cost for electricity from other source to meet the gap ($)	1.93E+12	1.47E+12	0.00E+00
Total cost to generate the same amount of electricity with one repository ($)	2.93E+12	2.82E+12	1.86E+12

Table 5-36 shows the adjusted total cost based on PR values. The adjusted total costs are used to recalculate the total cost to generate the same amount of electricity with one repository. The results under two different policies are shown in

Table 5-37 and Table 5-38. Compare Table 5-34 and

Table 5-37, the difference of impacts from two different nonproliferation charge methods appears. When nonproliferation charge is assumed to be 15% of FCC, under current policies, DUPIC is cheaper than PWROT. If nonproliferation charge is assumed as 15% of total electricity cost, under the same policies, PWROT becomes better choice because of its lower mean system PR. Under greenhouse policies, DUPIC becomes better choice again because the benefit of more generated electricity overcomes the benefit of higher PR.

5.6 Uncertainty and Sensitivity Study

For repository performance, proliferation performance, economics performance and integrated adjusted FCC, the uncertainty and sensitivity study is executed in a similar procedure. First, important parameters with uncertainty are identified and distributions of parameters are collected. @Risk [Ref 5-11] is linked with

performance models to do Monte Carole simulation and @Risk can also give statistics information and sensitivity information.

@RISK is the Risk Analysis and Simulation add-in for Microsoft Excel or Lotus 1-2-3. As an add-in, @RISK becomes seamlessly integrated - via a new toolbar and functions -- with spreadsheet, adding Risk Analysis to existing models. @RISK uses a technique known as Monte Carlo simulation to take all possible outcomes into account. Simply replace uncertain values in spreadsheet with @RISK functions which represent a range of possible values. Select cells as outputs, and start a simulation. @RISK recalculates spreadsheet hundreds or even thousands of times, each time selecting random numbers from the @RISK functions you entered. The result: distributions of possible outcomes and the probabilities of getting those results.

The probability density function (PDF) generated from @Risk is extended into a fuzzy number for all scenarios. In each case, for three scenarios, three PDFs are obtained. The maximum of three PDFs p(x) defined as $\max p$ is available. The associated fuzzy number is generated in this matter:

$$\mu(x) = p(x) / \max p$$

PD and PSD index defined by Dubois and Prade are used to compare the ranking of these three fuzzy numbers. The result is used to assistant the comparison.

5.6.1 Uncertainty of Repository Performance

The parameters with uncertainties are listed in Table 5-39.

Table 5-39 Stochastic parameters for projected dose model

Parameter	Distribution Type	Distribution Statistics	Reference
Bulk Density at SZ (g/ml)	Normal	Mean = 1.91, SD = 0.078	[Ref 5-5]
Effective Porosity at SZ	Beta	α1 = 17.76, α2 = 58.41	[Ref 5-6]
Aquifer Flow (m/yr)	Normal	Mean = 0.6, SD = 0.012	[Ref 5-7]
Longitudinal Dispersivity (m)	Log Normal	Mean = 100, SD = 5.66	[Ref 5-7]
Effective Porosity (layer 1)	Beta	α1 = 21.14, α2 = 178.13	[Ref 5-6]
Effective Porosity (layer 2)	Beta	α1 = 21.66, α2 = 228.12	[Ref 5-6]
Effective Porosity (layer 3)	Beta	α1 = 18.54, α2 = 72.51	[Ref 5-6]
Effective Porosity (layer 4)	Beta	α1 = 13.34, α2 = 19.64	[Ref 5-6]
Net Water Percolation Rate (m/yr)	Uniform	[0.004, 0.013]	[Ref 5-9]
Dilution Volume (m^3)	Uniform	[6203533.78, 17921319.82]	[Ref 5-9]
Water Usage(l/yr)	Normal	Mean = 730, SD = 36.5	[Ref 5-8]
SZ = Saturated Zone, SD = Standard Deviation			

Table 5-40 shows the accumulated dose in 100,000 yrs from the repository. The uncertainty is large, around 62% for PWR-OT, 56% for MOX and 58% for DUPIC. DUPIC projects highest dose in terms of mean value and 95% percentile and it dues to the highest loading. Table 5-41 and Table 5-42 list the PDs and PSDs. Those fuzzy number ranking values shows the vague ranking of the three cycles. Figure 5-5 shows the CDF of accumulated dose for three cycles. This figure shows clearly the ranking of three cycles at any probability level the same as the ranking shown in Table 5-40.

Figure 5-6-Figure 5-8 shows the correlation for accumulated dose of three cycles. A significant relation is indicated by a ranking order coefficient with value more than 0.1 indicates. Higher absolute ranking order coefficient shows stronger relationship. In all three scenarios, the four important parameters are Aquifer Flow, Dilution Volume, and Effective Porosity at layer 4 and Longitudinal.

Table 5-43 to Table 5-45 show similar ranking for peak dose rate in 100,000 yr compared with the accumulated dose. Figure 5-10 to Figure 5-12 show that the

correlation of parameters to the peak dose rate of the three cycles is very similar to the correlation of parameters to the accumulated dose of the three cycles respectively.

Table 5-40 Accumulated dose in 100,000 yrs statistics

Accumulated Dose in 100,000 yrs (rem)			
	PWR-OT	MOX	DUPIC
Minimum	3.66	0.69	5.82
Maximum	125.96	47.27	164.59
Mean	26.78	9.34	42.40
Std Deviation	16.56	5.20	24.61
95% Percentile	58.49	18.60	91.24

Table 5-41 Ranking of accumulated dose in 100,000 yrs for three scenarios

	PWROT	MOX	DUPIC
PD	0.61	0.51	0.61
PSD	0.41	0.15	0.58

Table 5-42 Ranking of accumulated dose in 100,000 yrs for PWR-OT and MOX

	PWROT	MOX
PD	0.90	0.90
PSD	0.81	0.15

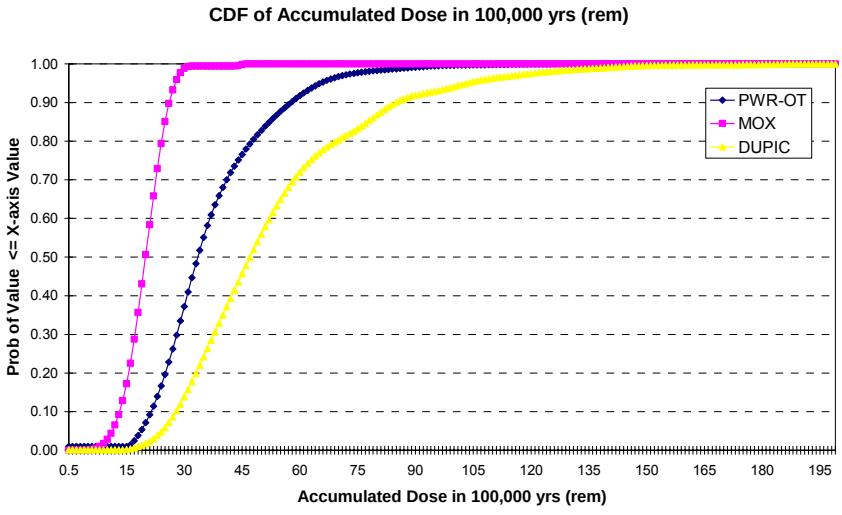

Figure 5-5 CDF of accumulated dose in 100,000 yrs (rem)

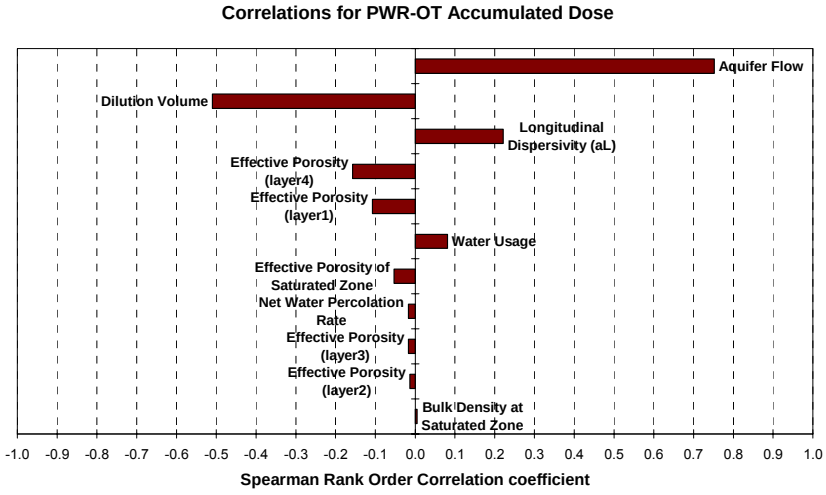

Figure 5-6 Correlations for PWR-OT accumulated dose

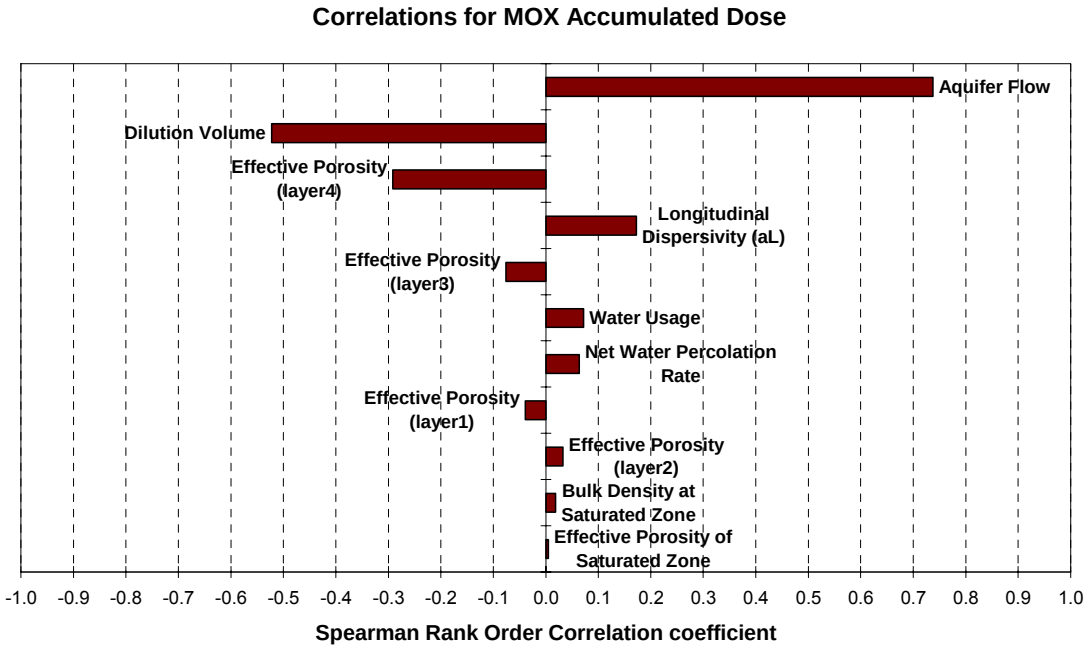

Figure 5-7 Correlations for MOX accumulated dose

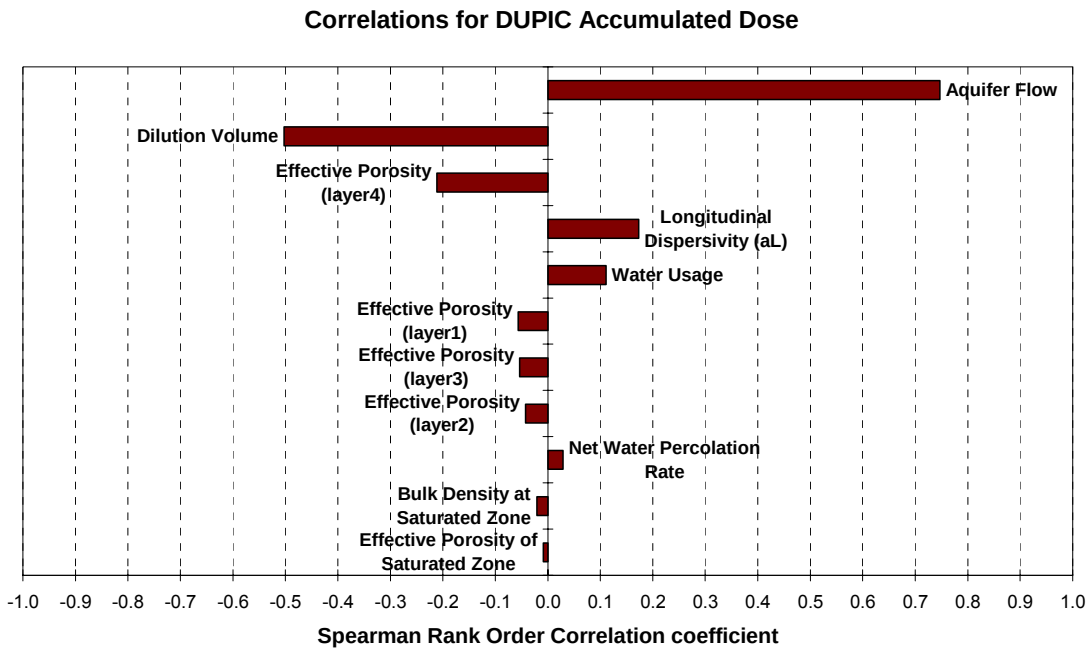

Figure 5-8 Correlations for DUPIC accumulated dose

Table 5-43 Peak dose rate statistics

Peak Dose Rate (rem/yr)			
	PWR-OT	MOX	DUPIC
Minimum	2.63E-03	5.10E-04	4.16E-03
Maximum	6.94E-02	2.59E-02	9.06E-02
Mean	1.63E-02	5.49E-03	2.58E-02
Std Deviation	9.21E-03	2.84E-03	1.38E-02
95% Percentile	3.44E-02	1.05E-02	5.26E-02

Table 5-44 Ranking of peak dose rate for three scenarios

	PWROT	MOX	DUPIC
PD	0.57	0.50	0.57
PSD	0.45	0.12	0.55

Table 5-45 Ranking of peak dose rate for PWR-OT and MOX

	PWROT	MOX
PD	0.91	0.91
PSD	0.85	0.12

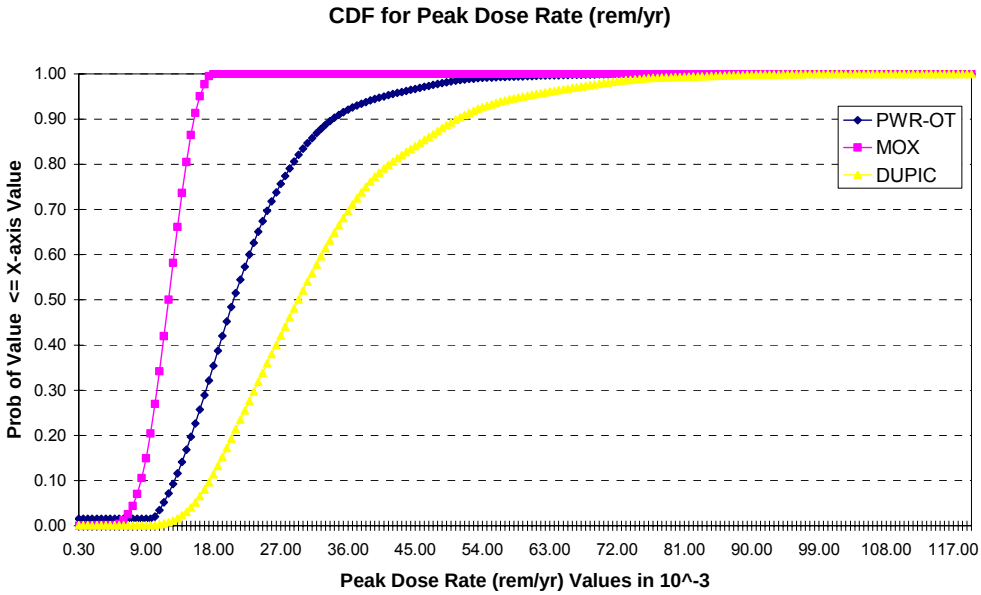

Figure 5-9 CDF for peak dose rate

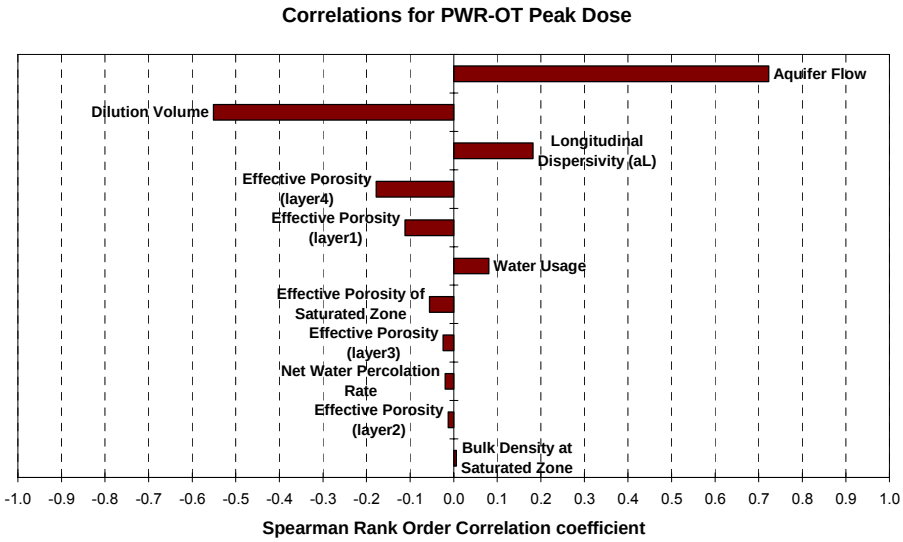

Figure 5-10 Correlations for PWR-OT peak dose rate

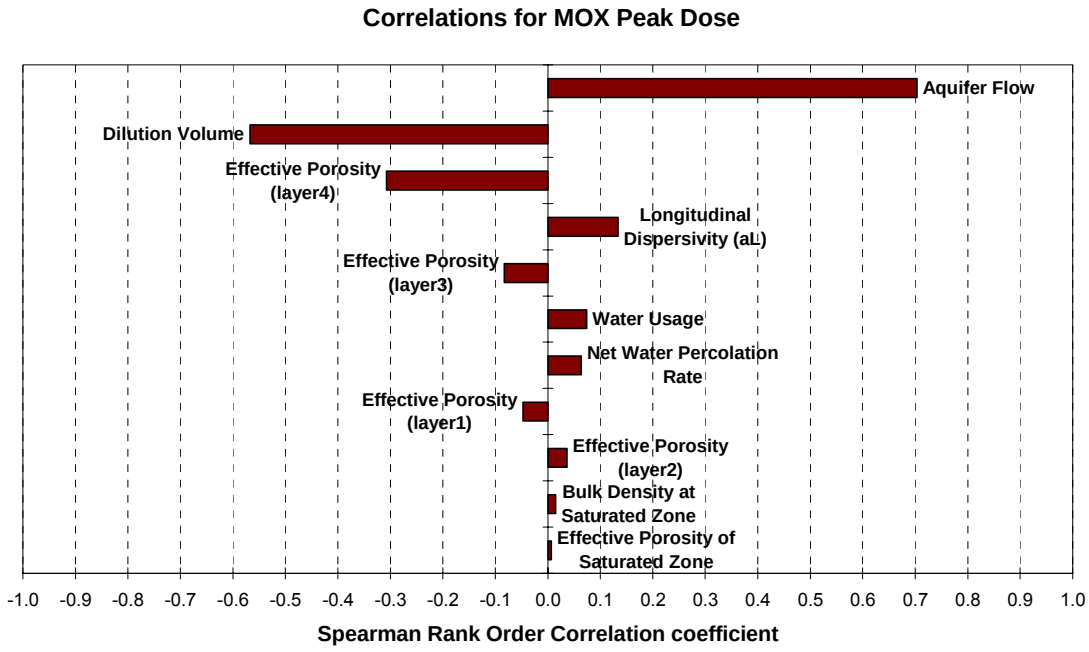

Figure 5-11 Correlations for MOX peak dose rate

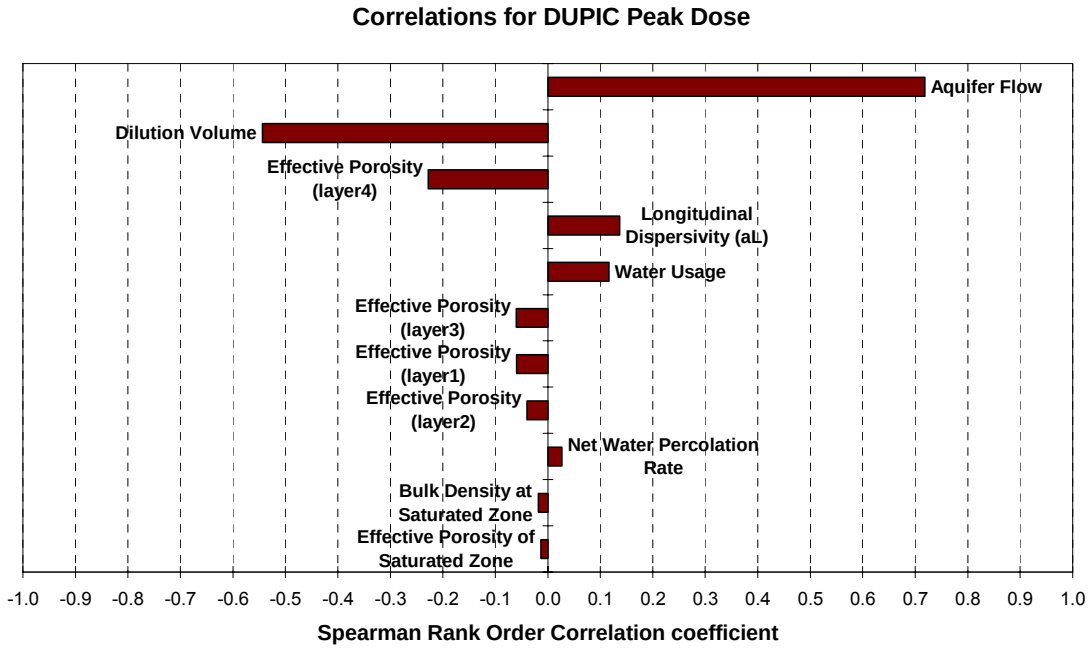

Figure 5-12 Correlations for DUPIC peak dose rate

5.6.2 Uncertainty of Proliferation Resistance

Table 5-46 Stochastic parameters for proliferation resistance model

Parameter	Distribution Type	Distribution Statistics
Isotopic Barrier Weight	Uniform	[130, 200]
Chemical Barrier Weight	Uniform	[20, 55]
Radiological Barrier Weight	Uniform	[5, 9]
Other Barrier Weight	Log Normal	SD/Mean = 50%
All Measurable Variables	Normal	SD/Mean = 20%
SD = Standard Deviation		

By given uncertainty in Table 5-46, the system mean proliferation resistance is listed in Table 5-47. The standard deviation is small, and PWR-OT has clearly highest proliferation resistance in terms of mean value and 95% percentile, which can also be observed from Figure 5-13 and Figure 5-14. DUPIC has very close proliferation resistance to MOX. The similar relationship can be indicated by the ranking number PD, PSD in Table 5-48 and Table 5-49 too. The assumed uncertainties from parameters hide the PR difference of MOX and DUPIC. It suggests more investigation is needed to compare these two systems.

Figure 5-15 to Figure 5-17 shows the parameters which have strong correlation with the system mean proliferation resistance. Barrier weight for Available Mass barrier shows strongest effect to the system mean proliferation resistance in all three scenarios because of its relevant higher importance compared with other barrier weights and the large uncertainty of its value (log normal distribution with 50% relative SD, Table 5-46). Same reason makes barrier weight of Facility Unattractiveness barrier having strong influence to system mean PR. Stage-weight also plays an important role because it directly affect the importance of PR at each

stage to final system mean PR. More investigation should be made to reduce the uncertainty from those important parameters.

Table 5-50 to Table 5-42 and Figure 5-18 to Figure 5-22 show the statistical information of minimum stage mean proliferation resistance of each cycle. The important parameters to minimum stage mean proliferation resistance are different from those to system mean proliferation resistance. The importance of stage-weight decreases reasonably, since the minimum stage mean PR is PR of one stage. Parameters related with the lower PR stage like CANDU reactor operation in DUPCI scenario, reprocessing facility in PWR-MOX scenario and reactor operation in PWR-OT scenario show strong effect.

Table 5-47 System mean proliferation resistance statistics

System Mean Proliferation Resistance			
	PWR-OT	MOX	DUPIC
Minimum	0.220	0.209	0.195
Maximum	0.389	0.350	0.352
Mean	0.320	0.284	0.284
Std Deviation	0.027	0.021	0.023
95% Percentile	0.360	0.318	0.320

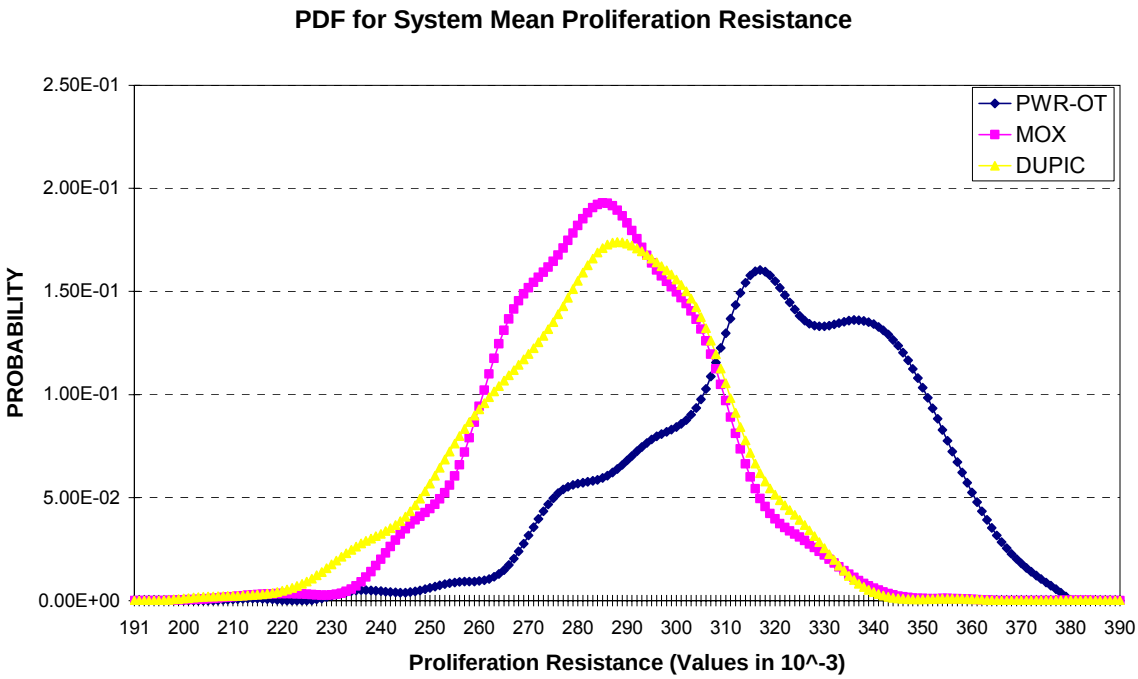

Figure 5-13 PDF for system mean proliferation resistance

Table 5-48 Ranking of system mean proliferation resistance for three scenarios

	PWROT	MOX	DUPIC
PD	0.83	0.58	0.60
PSD	0.76	0.20	0.23

Table 5-49 Ranking of system mean proliferation resistance for MOX and DUPIC

	MOX	DUPIC
PD	0.90	0.90
PSD	0.46	0.51

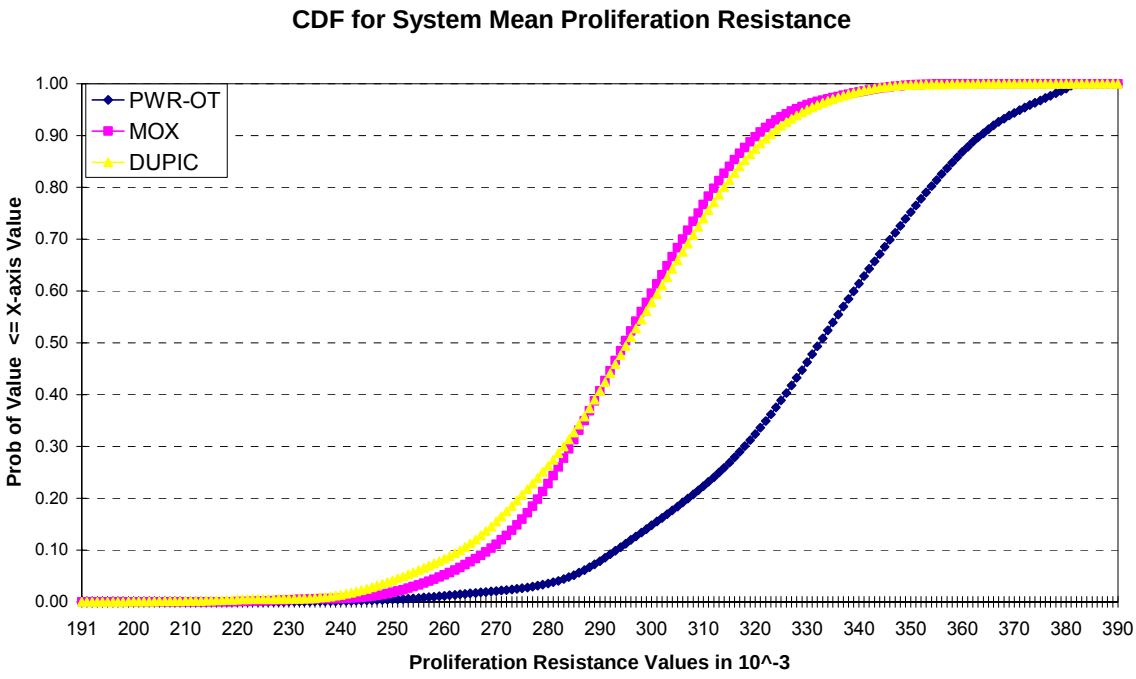

Figure 5-14 CDF for system mean proliferation resistance

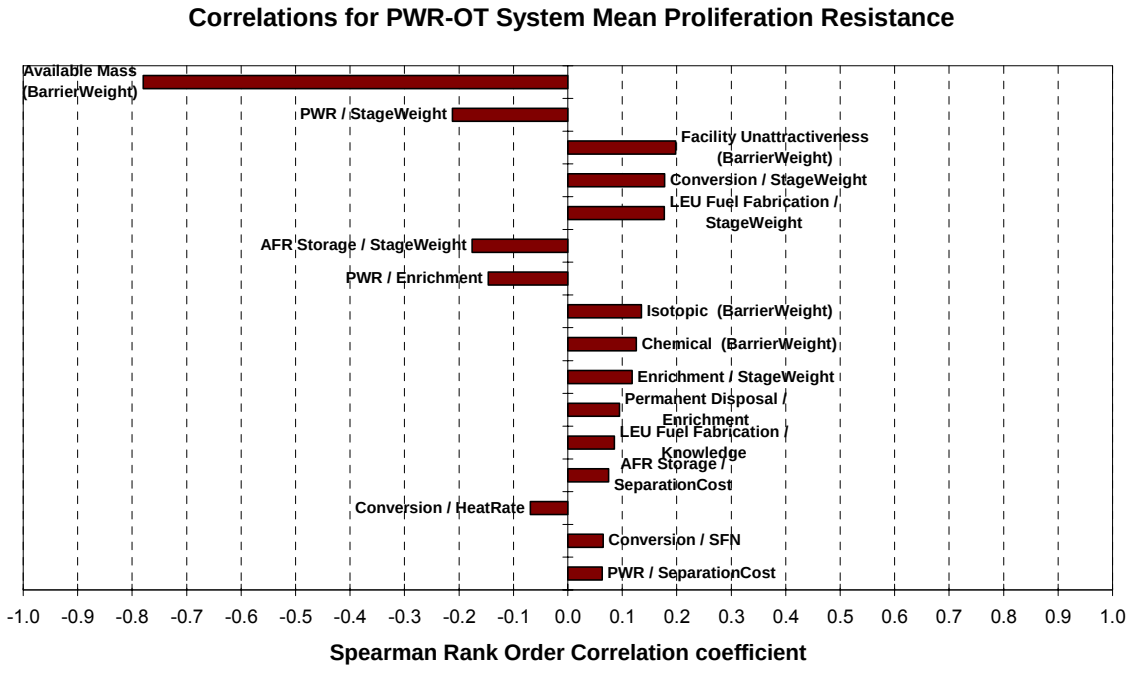

Figure 5-15 Correlations for PWR-OT system mean proliferation resistance

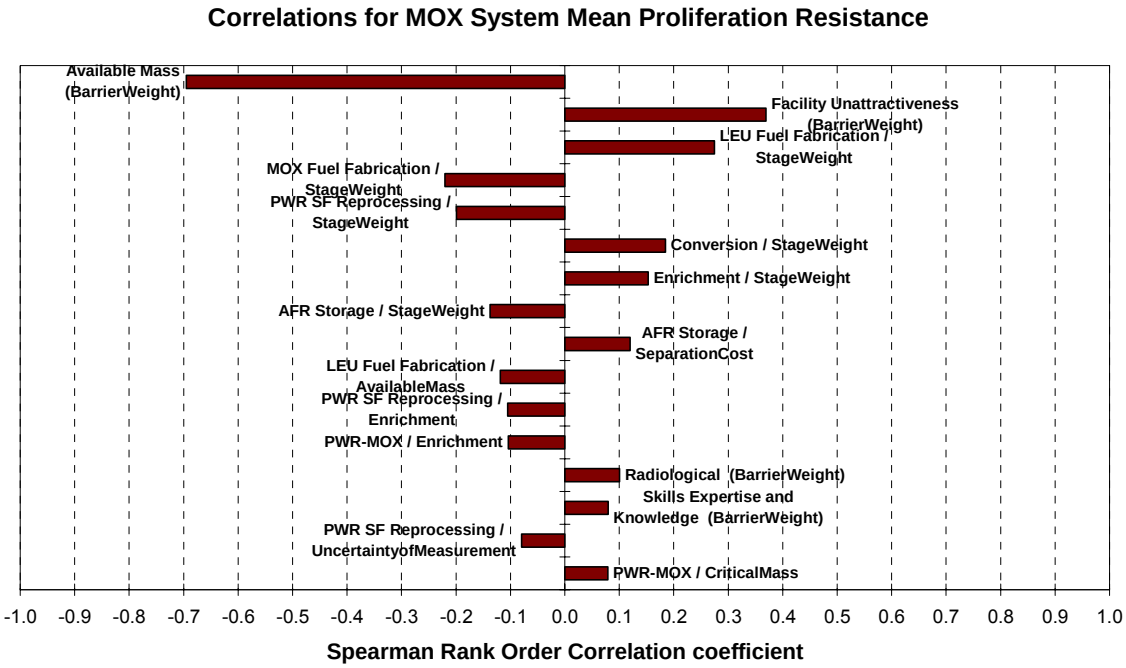

Figure 5-16 Correlations for MOX system mean proliferation resistance

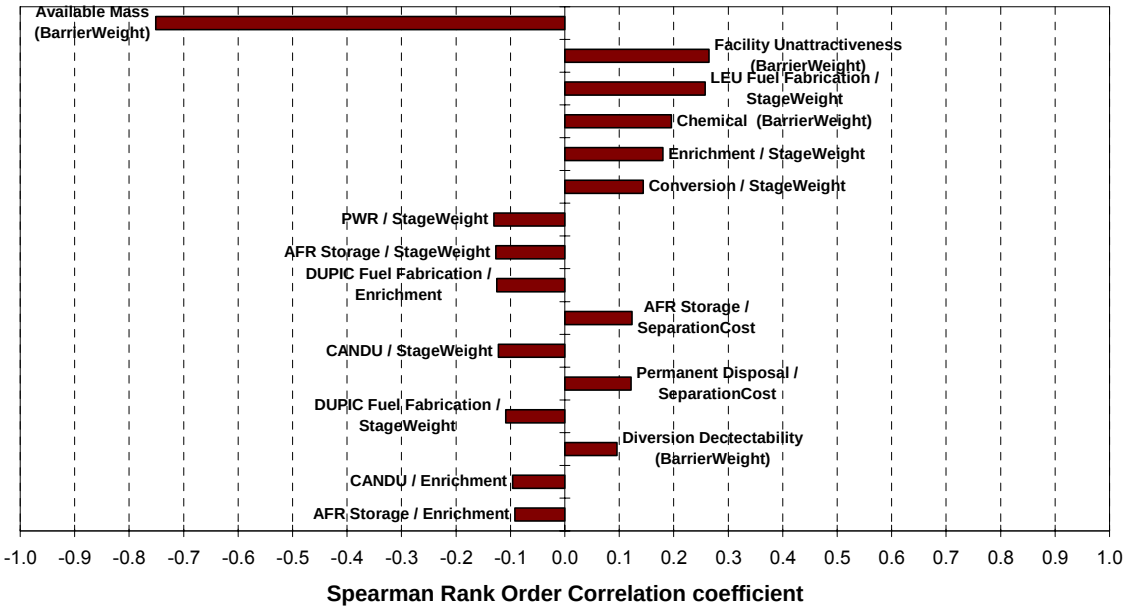

Figure 5-17 Correlations for DUPIC system mean proliferation resistance

Table 5-50 Minimum stage mean proliferation resistance statistics

Minimum Stage Mean Proliferation Resistance			
	PWR-OT	MOX	DUPIC
Minimum	0.096	0.080	0.084
Maximum	0.250	0.168	0.198
Mean	0.161	0.115	0.132
Std Deviation	0.027	0.016	0.020
95% Percentile	0.207	0.142	0.164

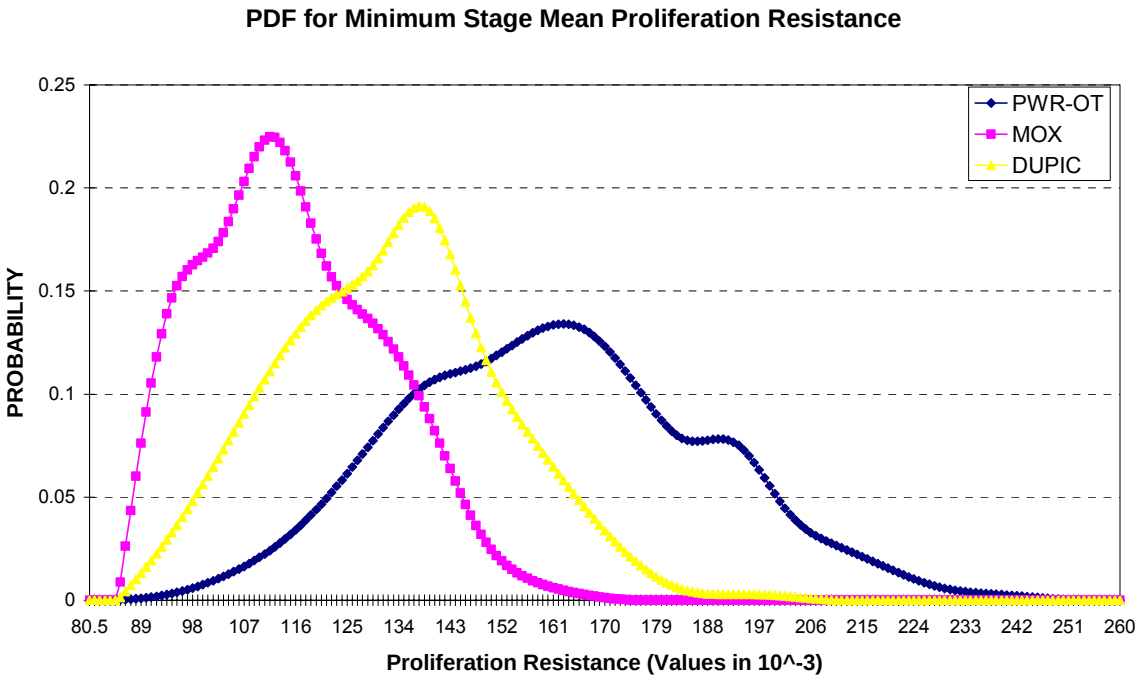

Figure 5-18 PDF for minimum stage mean proliferation resistance

Table 5-51 Ranking of minimum stage mean proliferation resistance for three scenarios

	PWROT	MOX	DUPIC
PD	0.60	0.45	0.51
PSD	0.60	0.26	0.40

Table 5-52 Ranking of minimum stage mean proliferation resistance for PWROT and MOX

	PWROT	MOX
PD	0.60	0.45
PSD	0.60	0.40

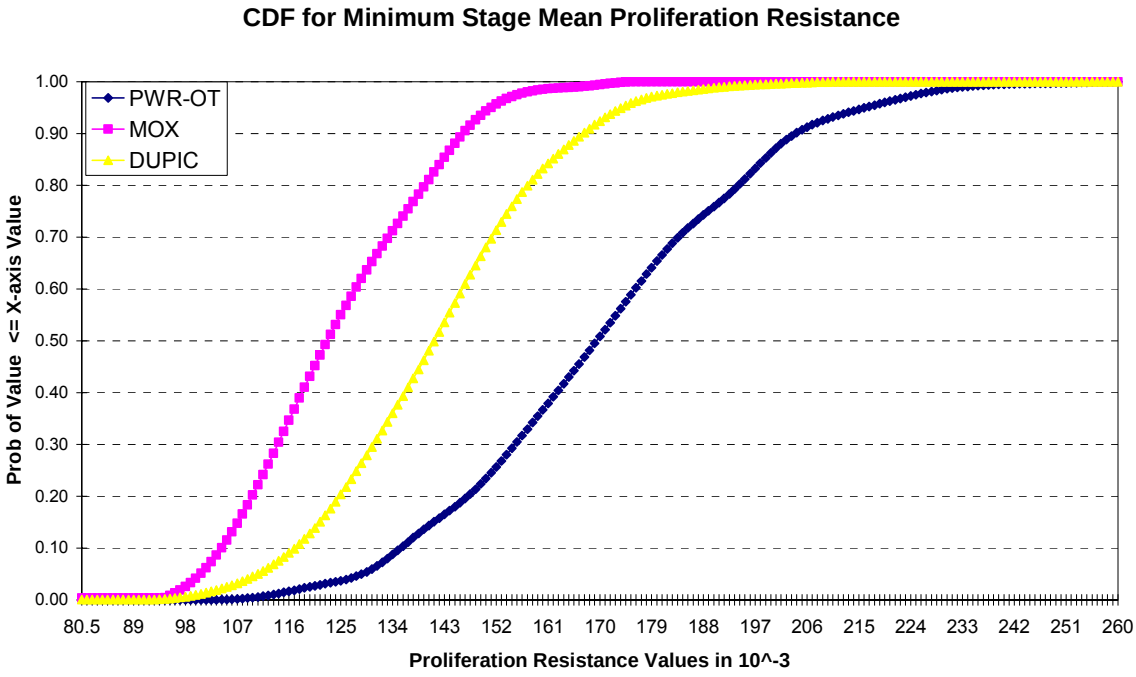

Figure 5-19 CDF for minimum stage mean proliferation resistance

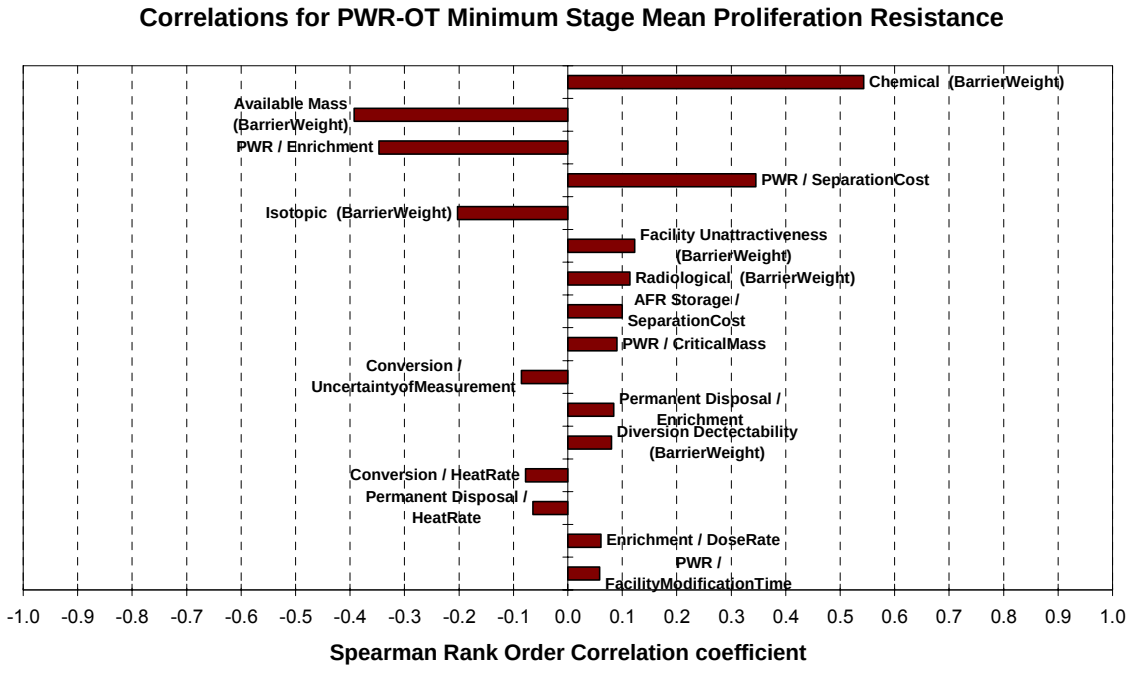

Figure 5-20 Correlations for PWR-OT minimum stage mean proliferation resistance

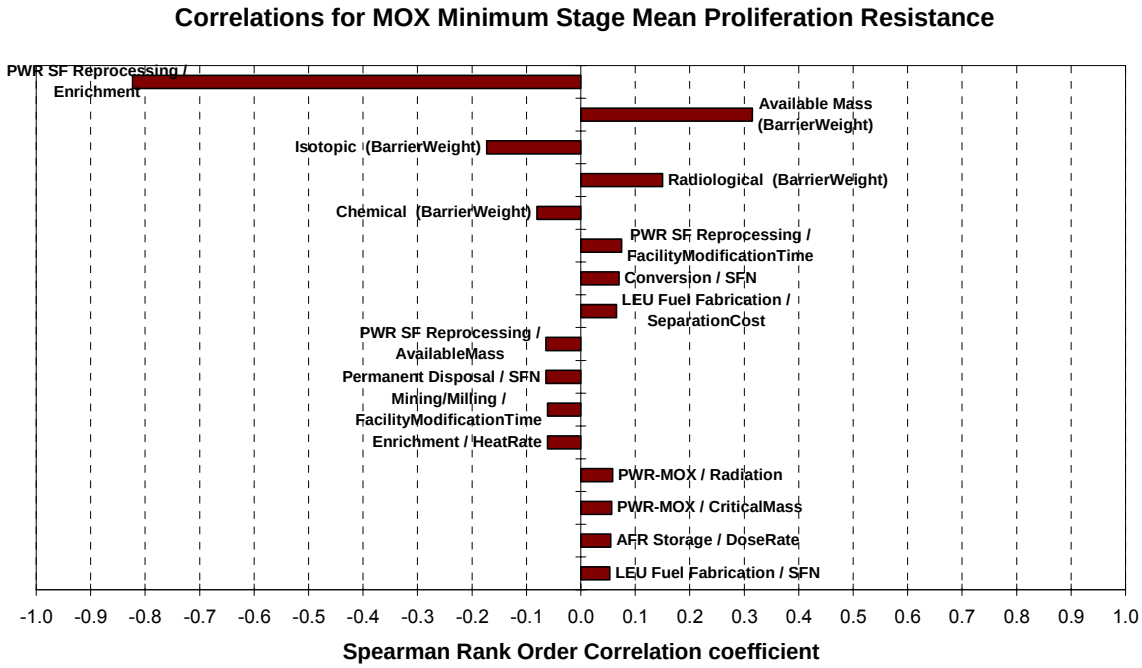

Figure 5-21 Correlations for MOX minimum stage mean proliferation resistance

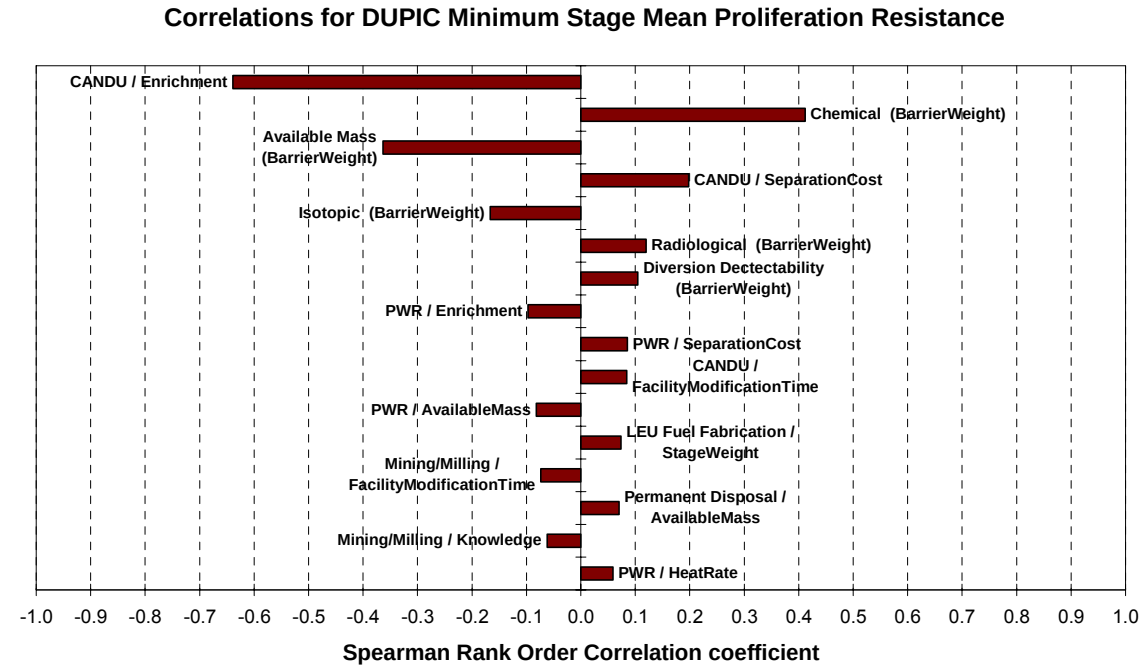

Figure 5-22 Correlations for DUPIC minimum stage mean proliferation resistance

5.6.3 Uncertainty of Fuel Cycle Cost

The distribution statistics information is from Ref 5-3 and Ref 5-4 (Table 5-53). Log normal distribution is assumed to avoid negative value during sampling when the standard deviation is large.

Table 5-53 Stochastic parameters for fuel cycle cost model

Parameter	Distribution Type	Distribution Statistics
Ore Purchase ($/KgHM)	Log Normal	Mean = 30, SD = 10
Conversion ($/KgHM)	Log Normal	Mean = 5, SD = 2
Enrichment ($/kgSWU)	Log Normal	Mean = 80, SD = 30
UOX Fabrication ($/KgHM)	Log Normal	Mean = 250, SD = 50
Waste Disposal ($/Cask)	Log Normal	Mean = 3902000, SD = 929000
Reprocessing ($/KgHM)	Log Normal	Mean = 800, SD = 100
MOX Fabrication ($/KgHM)	Log Normal	Mean = 1100, SD = 200
DUPIC Fabrication ($/KgHM)	Log Normal	Mean = 623, SD = 125
Maximum Loading (MTHM)	Log Normal	SD/Mean = 10% (assumed)
SD = Standard Deviation		

It can be seen from Table 5-54 that MOX has highest FCC and PWR-OT has lowest FCC. FCC of DUPIC is slightly higher than FCC of PWR-OT. The relative SD is around 10-15%. Important parameters indicated in Figure 5-25-Figure 5-27 are different for three cycles. The two most important parameters for FCC of PWR-OT are enrichment and ore purchase price, for FCC of MOX are enrichment and reprocessing price, and for FCC of DUPIC are enrichment and DUPIC fuel fabrication price. The enrichment price is so important in this study because high contribution of enrichment facility to total cost (32% in PWR-OT scenario, 15% in MOX scenario and 22% in DUPIC scenario) and its high uncertainty (37.5% relative SD). The uncertainty of max loading which is indicated by waste package (WP) density does not have significant correlation with FCC of all three cycles.

Table 5-54 FCC statistics (cents/kWhe)

	PWR-OT	MOX	DUPIC
Minimum	0.195	0.497	0.234
Maximum	0.750	1.146	0.776
Mean	0.461	0.820	0.499
Std Deviation	0.074	0.077	0.064
95% Percentile	0.580	0.947	0.603

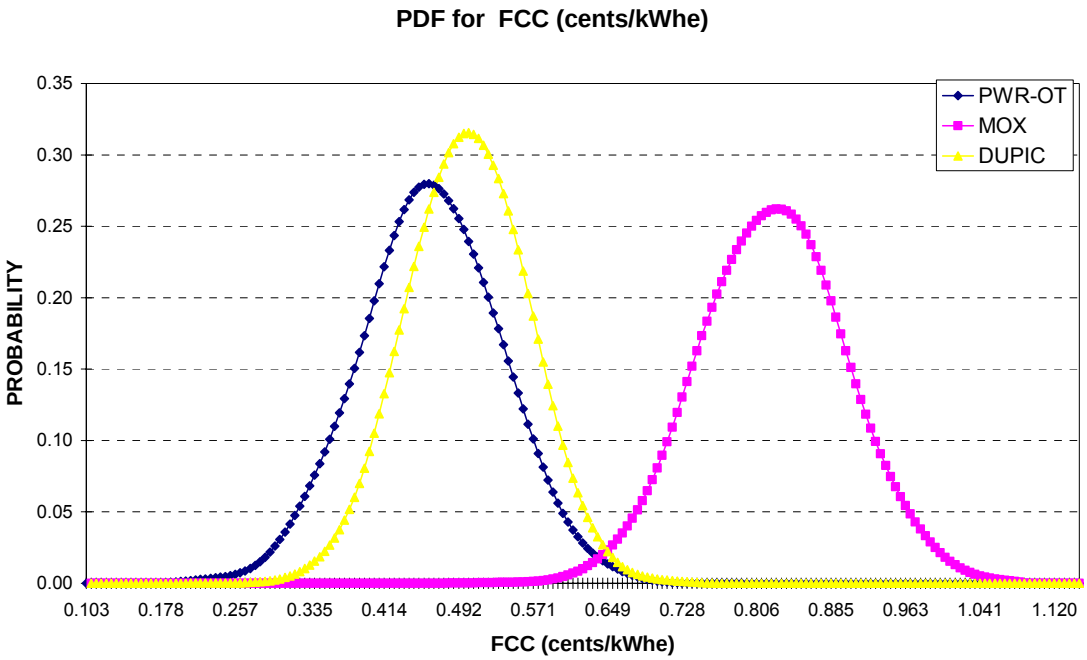

Figure 5-23 PDF for FCC

Table 5-55 Ranking of FCC for three scenarios

	PWROT	MOX	DUPIC
PD	0.05	0.83	0.07
PSD	0.17	0.83	0.17

Table 5-56 Ranking of FCC for PWROT and DUPIC

	PWROT	DUPIC
PD	0.88	0.89
PSD	0.32	0.65

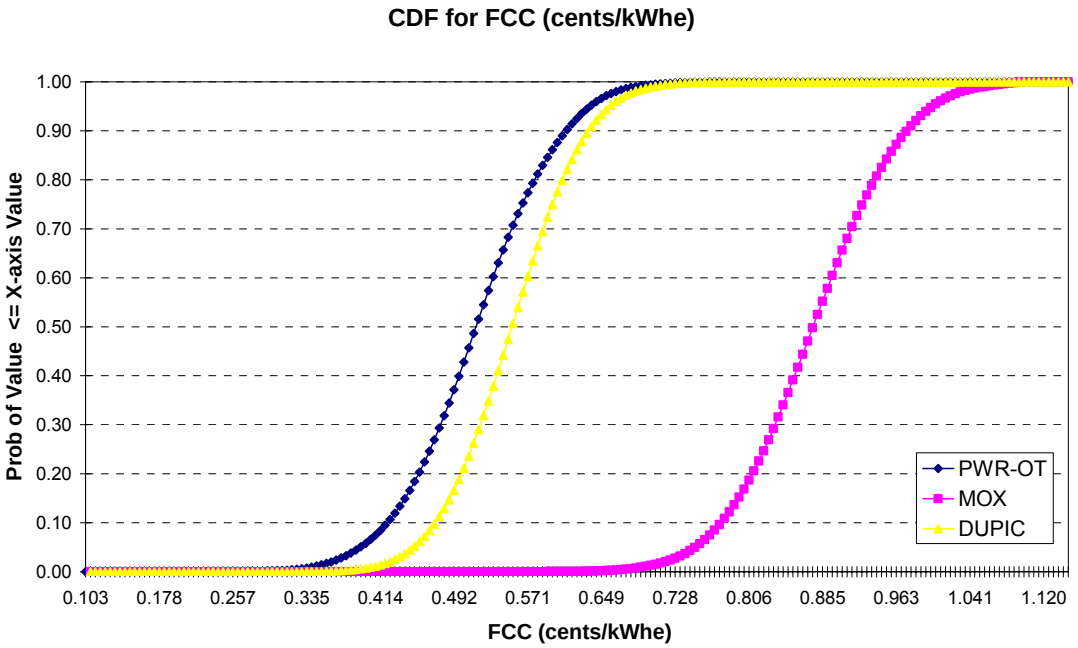

Figure 5-24 CDF for FCC

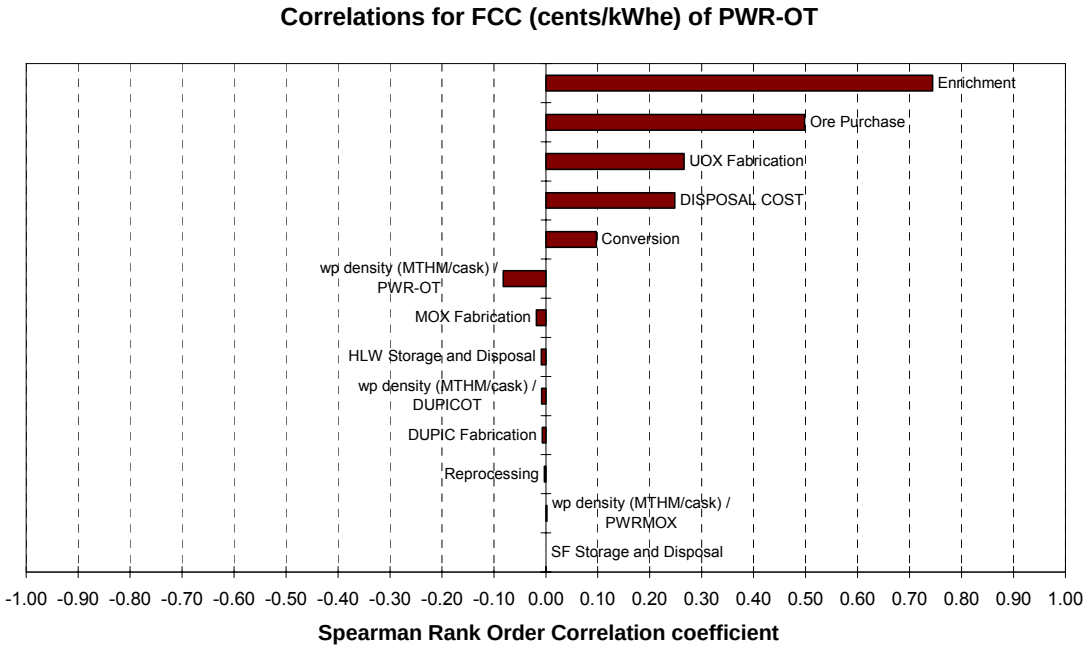

Figure 5-25 Correlations for PWR-OT FCC

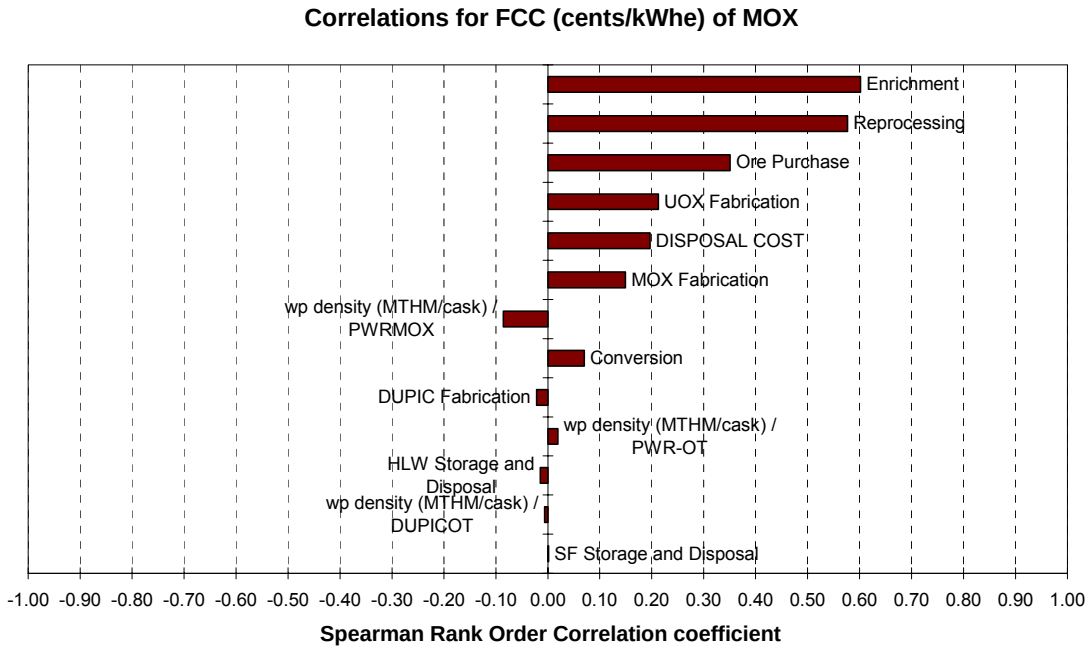

Figure 5-26 Correlations for MOX FCC

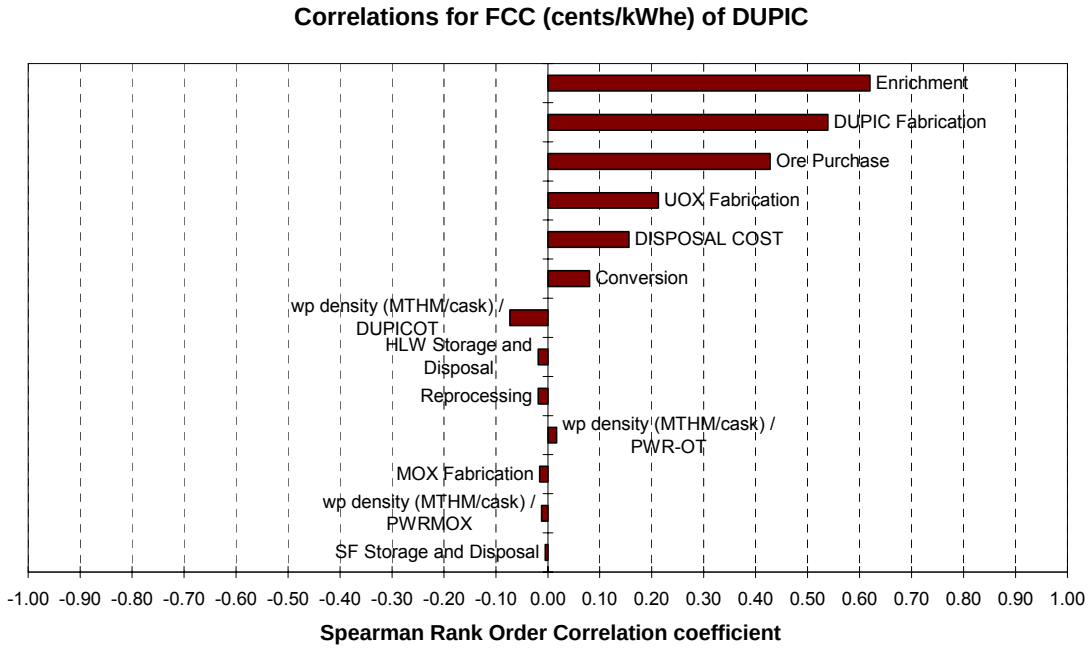

Figure 5-27 Correlations for DUPIC FCC

5.6.4 Uncertainty of Adjusted Fuel Cycle Cost

Assumed the uncertainties of parameters are listed in Table 5-46 and Table 5-53, the uncertainty of adjusted FCC is investigated and result is shown in Table 5-57.

It can be seen that since the nonproliferation charge is only 15% of FCC, the impact from uncertainty of system mean proliferation resistance is very limit and important parameters for adjusted FCC are same as those for FCC (Figure 5-30-Figure 5-32). The relative standard deviations are almost the same as FCC of the three scenarios (~16% for PWR-OT, ~10% for MOX and ~13% for DUPIC).

Table 5-57 Adjusted FCC statistics (cents/kWhe)

Adjusted FCC			
	PWR-OT	MOX	DUPIC
Minimum	0.319	0.666	0.405
Maximum	0.963	1.273	0.911
Mean	0.529	0.896	0.575
Std Deviation	0.084	0.087	0.073
95% Percentile	0.688	1.049	0.701

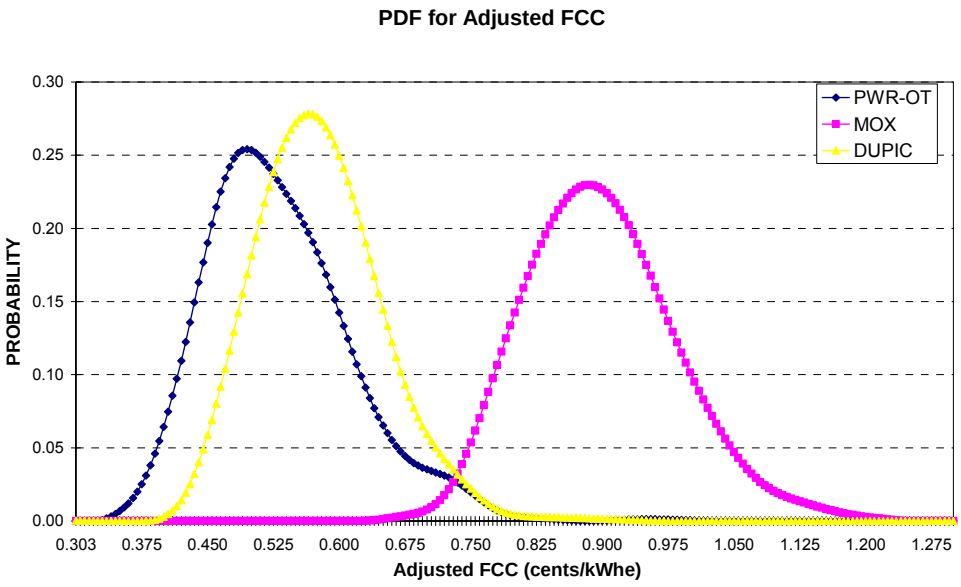

Figure 5-28 PDF for adjusted FCC

Table 5-58 Ranking of adjusted FCC for three scenarios

	PWROT	MOX	DUPIC
PD	0.10	0.83	0.11
PSD	0.17	0.83	0.17

Table 5-59 Ranking of adjusted FCC for PWROT and DUPIC

	PWROT	DUPIC
PD	0.83	0.11
PSD	0.83	0.17

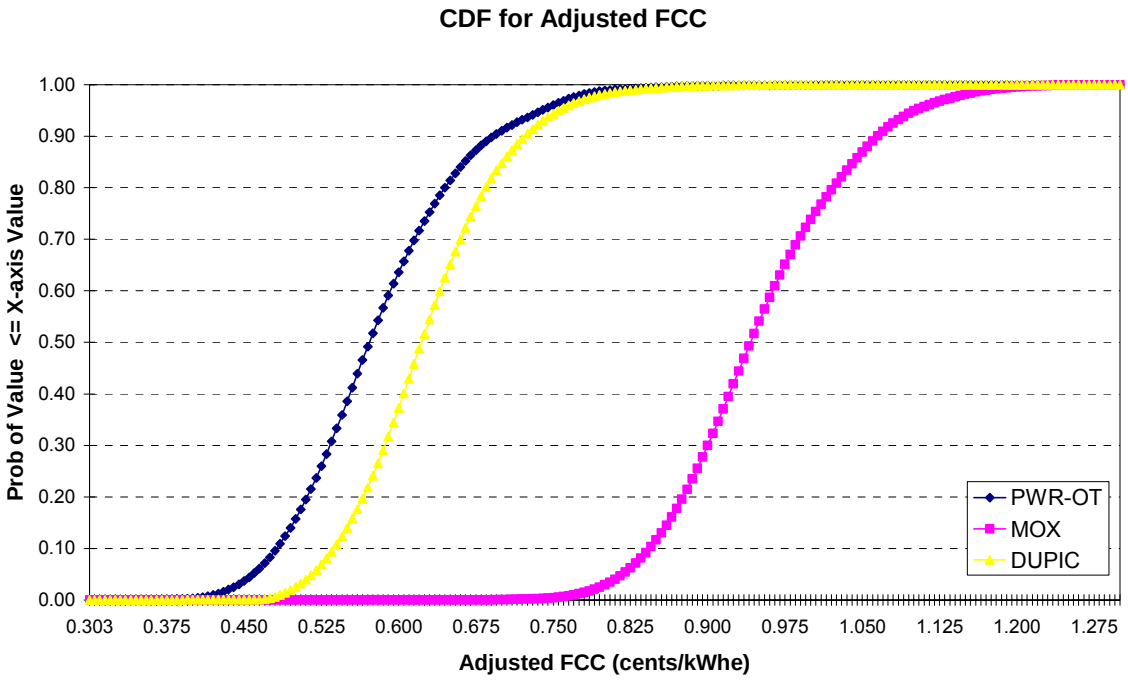

Figure 5-29 CDF for adjusted FCC

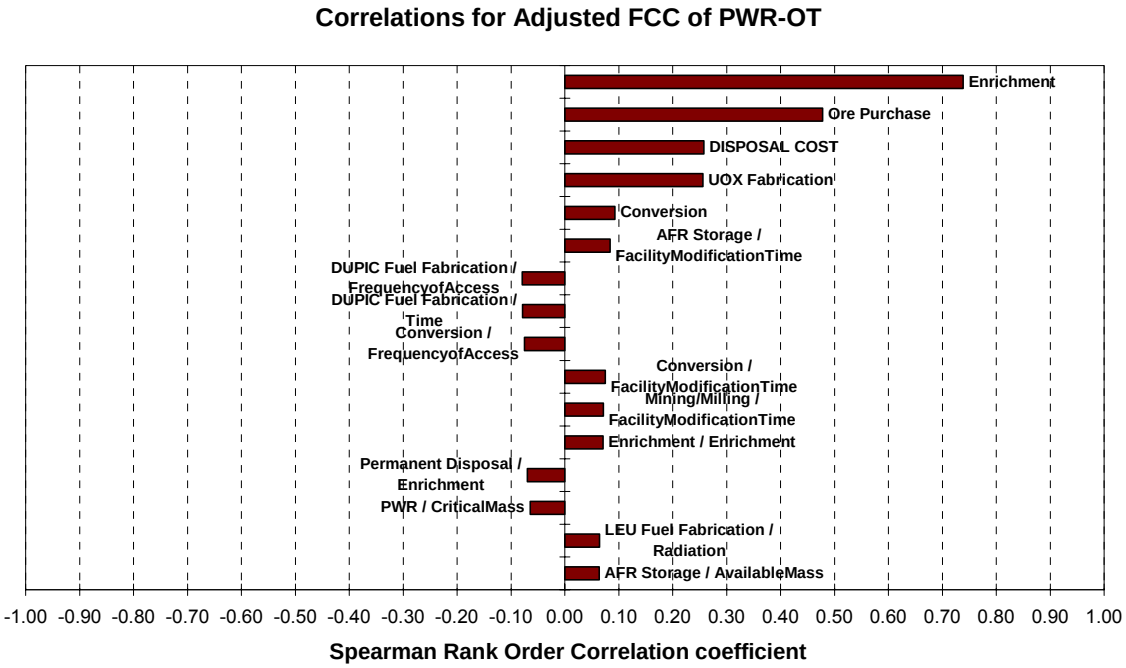

Figure 5-30 Correlations for PWR-OT adjusted FCC

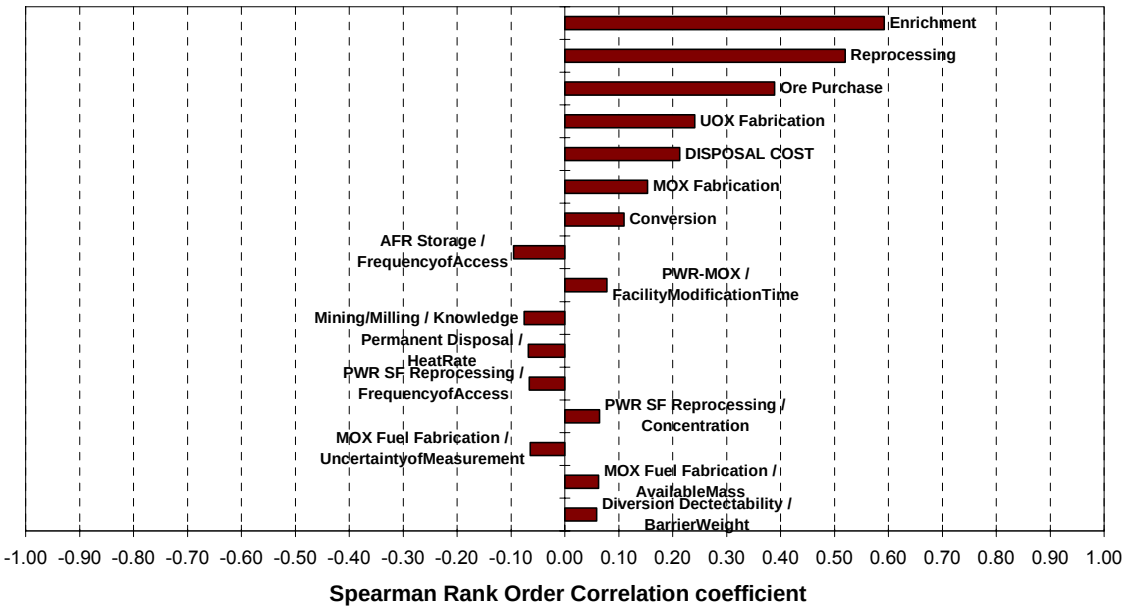

Figure 5-31 Correlations for MOX adjusted FCC

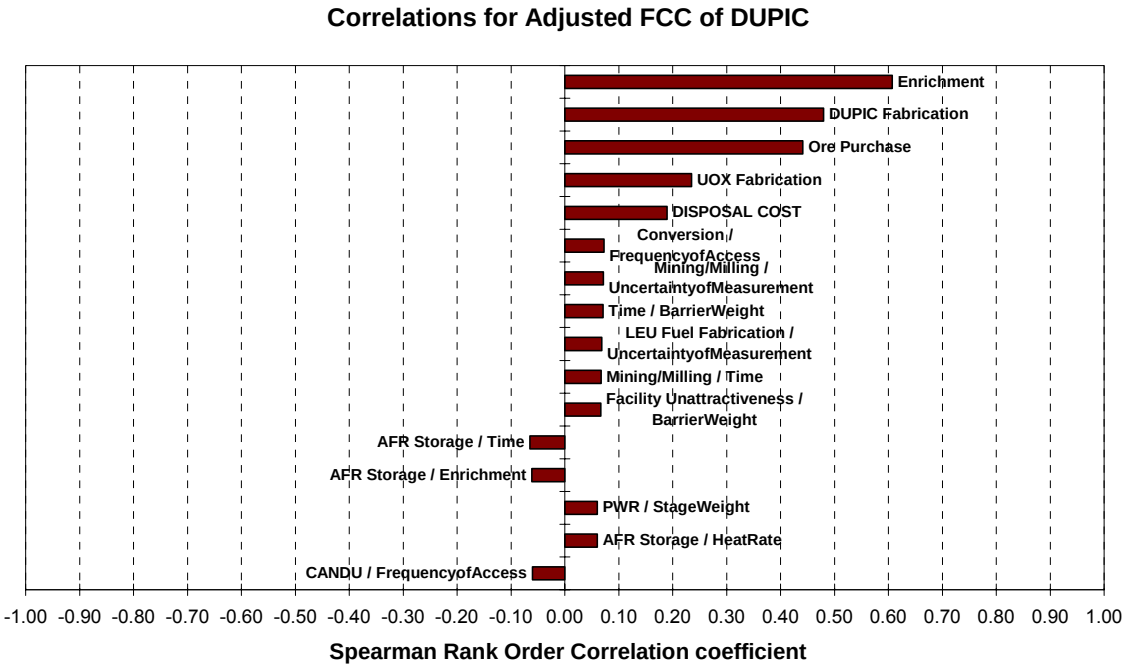

Figure 5-32 Correlations for DUPIC adjusted FCC

5.6.5 Uncertainty of Total Cost

Assumed the uncertainties of parameters are listed in Table 5-46 and Table 5-53, the uncertainty of total cost to generate the same amount of electricity under current policies and greenhouse policy are investigated and results are shown in Table 5-60 and Table 5-61. Compare Table 5-60 and Table 5-37, the ranking of three scenarios based on mean value in Table 5-60 is different as the ranking based on the total costs to generate the same amount electricity in Table 5-37, due to the assumed uncertainties from the parameters. Figure 5-33 shows the close total cost to generate the same amount of electricity of DUPIC and PWROT. Under greenhouse policy, the ranking of three scenarios is clearer by looking at Table 5-61 and Figure 5-34: DUPIC provides much lower total cost than other two scenarios. Even

PWROT has higher total cost than MOX to generate the same amount of electricity because the electricity gap that PWROT is short from other scenarios has to be compensated with higher cost traditional energy resources.

Figure 5-35 to Figure 5-37 show the important parameters to the total cost to generate the same amount of electricity for three scenarios. They are almost identical to the important parameters to adjusted fuel cycle cost and FCC.

Table 5-60 Total cost comparison under current policies (15% nonproliferation charge) $

	PWR-OT	MOX	DUPIC
Minimum	1.79E+12	1.91E+12	1.76E+12
Maximum	2.01E+12	2.11E+12	2.08E+12
Mean	1.85E+12	2.00E+12	1.87E+12
Std Deviation	2.63E+10	3.34E+10	4.14E+10
95% Percentile	1.90E+12	2.05E+12	1.94E+12

Table 5-61 Total cost comparison under greenhouse policies (15% nonproliferation charge) $

	PWR-OT	MOX	DUPIC
Minimum	2.87E+12	2.73E+12	1.76E+12
Maximum	3.09E+12	2.94E+12	2.08E+12
Mean	2.93E+12	2.82E+12	1.87E+12
Std Deviation	2.63E+10	3.34E+10	4.14E+10
95% Percentile	2.98E+12	2.88E+12	1.94E+12

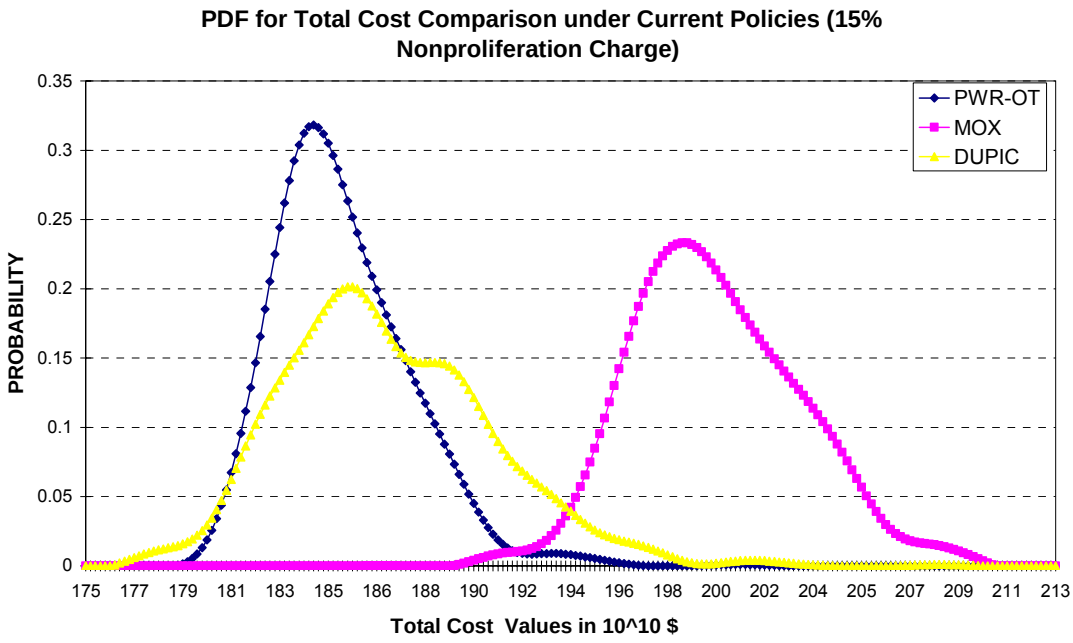

Figure 5-33 PDF for total cost comparison under current policies (15% nonproliferation charge)

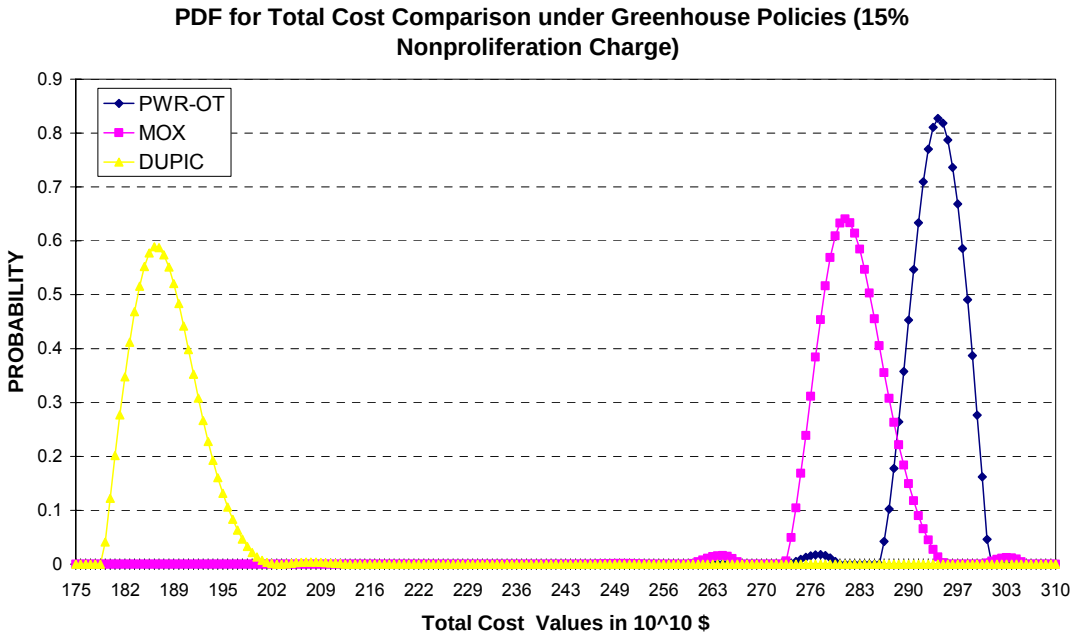

Figure 5-34 PDF for total cost comparison under greenhouse policies (15% nonproliferation charge)

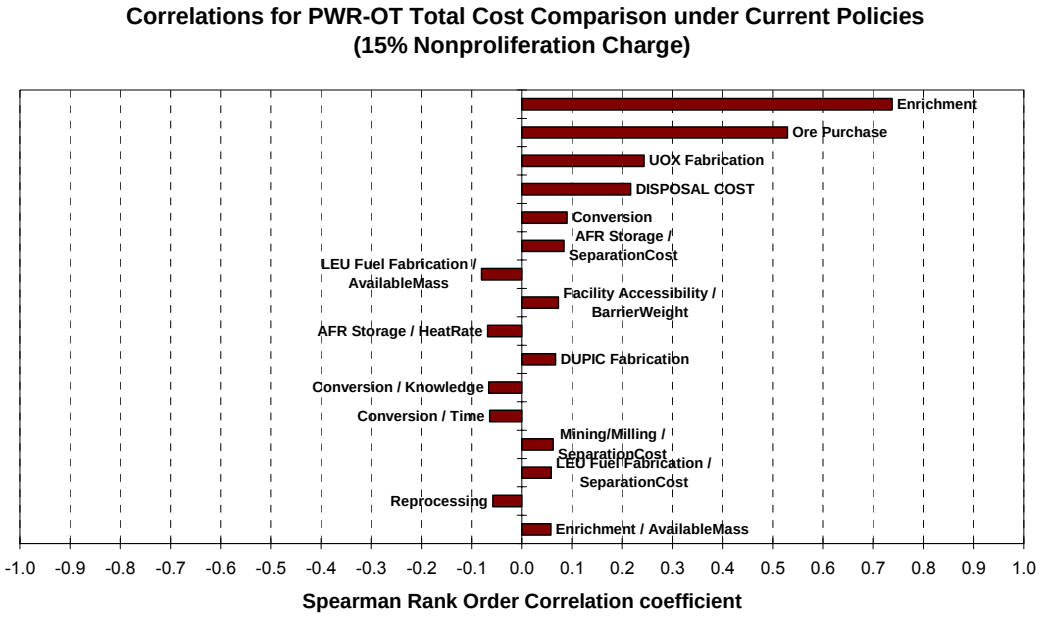

Figure 5-35 Correlations for PWROT total cost comparison under current policies (15% nonproliferation charge)

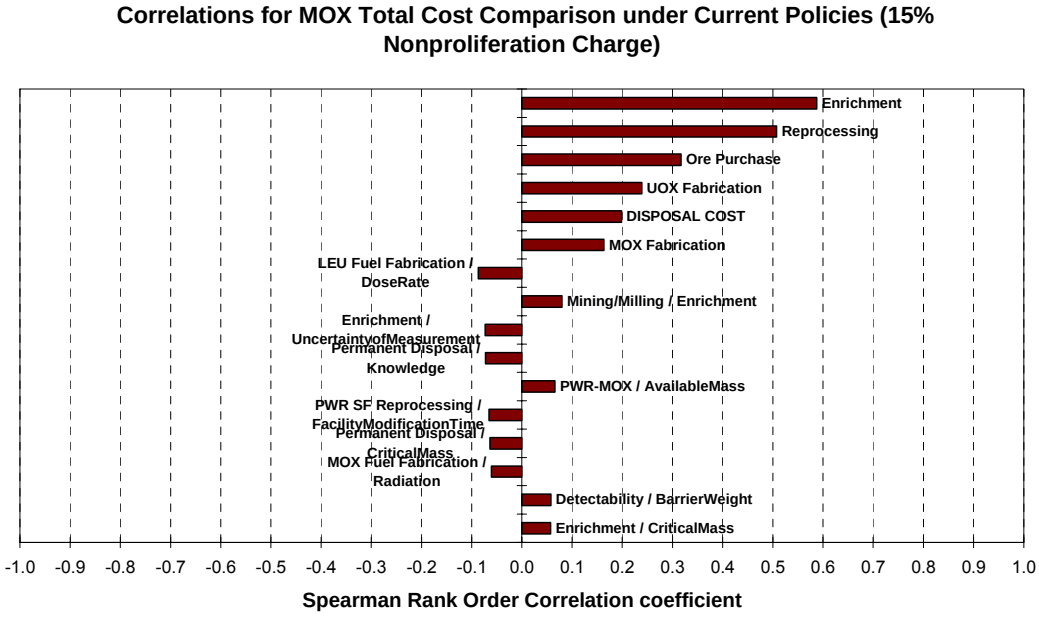

Figure 5-36 Correlations for MOX total cost comparison under current policies (15% nonproliferation charge)

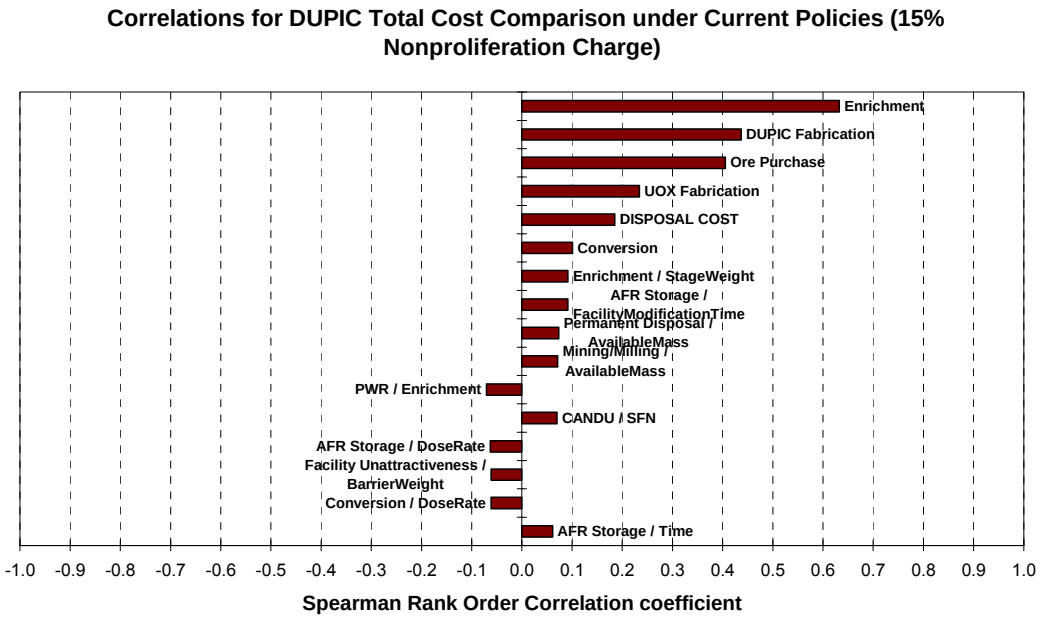

Figure 5-37 Correlations for DUPIC total cost comparison under current policies (15% nonproliferation charge)

5.7 References

Ref 5-1 Won Il KO, Ho Dong KIM, “Analysis of Nuclear Proliferation Resistance of DUPIC Fuel Cycle”, Journal of NUCLEAR SCIENCE and TECHNOLOGY, Vol. 38, No. 9, p. 757–765 September 2001

Ref 5-2 M. Bunn, S. Fetter, J. P. Holdren, B. V. D. Zwaan, “ The Economics of Reprocessing vs. Direct Disposal of Spent Nuclear Fuel”, Harvard University, 2003

Ref 5-3 “Accelerator-driven Systems (ADS) and Fast Reactors (FR) in Advanced Nuclear Fuel Cycles”, NEA, 2002

Ref 5-4 W.I. Ko, J.W.Choi, J.S.Lee, and H.S.Park, "Uncertainty analysis in dupic fuel-cycle cost using a probabilistic simulation Method", Nuclear Technology, Vol 127, pp123-140, July 1999

Ref 5-5 Bechtel SAIC Company, LLC, “Saturated Zone Flow and Transport Model Abstraction”, MDL-NBS-HS-000021 REV 02, October 2004

Ref 5-6 R. W. Barnard, M. L. Wilson, H.A. Dockery, J. H. Gauthier, P. G. Kaplan, R. R. Eaton, F. W. Bingham, T. H. Robey, “TSPA 1991: An Initial Total-System Performance Assessment for Yucca Mountain”, Sandia National Lab., SAND91-2795, Sept. 1992

Ref 5-7 U.S. Department of Energy, Office of Civilian Radioactive Waste Management, Yucca Mountain Site Characterization Office, “Viability Assessment of a Repository at Yucca Mountain”, DOE/RW-0508, Dec. 1998

Ref 5-8 United States Environmental Protection Agency, “Risk Assessment Guidance for Superfund: Volume 1- Human Health Evaluation Manual (Part A)”, EPA/540/1-89/002, Office of Emergency and Remedial Response, Washington, D.C., 1989

Ref 5-9 Mohanty, S., T. J. McCartin, and D. W. Esh, “Total-System Performance Assessment (TPA) Version 4.0 Code: Module Descriptions and User’s Guide”, Center for Nuclear Waste Regulatory Analyses, San Antonio, Texas, Jan. 2002.

Ref 5-10 “The Economic Future of Nuclear Power: A Study Conducted at The University of Chicago”, University of Chicago, August 2004

Ref 5-11 Palisade Corporation, “@Risk for Windows”, Version 3.5.2

6 Discussion

The major observations from the previous discussions are summarized in this chapter.

1. The toxicity index methods did not yield consistent results in evaluating repository performance for the test cases cited in chapter 2. Also, neither the mass inventory nor the toxicity index considers the contribution of the waste package and the repository in assessing the overall performance. If the waste packages could be constructed to maintain their integrity over the life of the repository, then the radiotoxicity of the waste would not be an issue. PA methods have to be used as the performance of the repository and the waste package are crucial components in the evaluation of the health impacts from the SNF/HLW.
2. In the three fuel cycle scenarios studied, the repository capacities are constrained by the required temperature limit at midway between drifts (96°C). Other temperature limits might be more limiting in different scenarios. The peak centerline temperature appears over fifteen hundred years after the drift ventilation system has been shut off and the drifts have been backfilled (Table 5-10). The temperature rise is principally due to the decay heat from the long half-life actinides. To increase the repository capacity in the MOX and DUPIC scenarios, a further reduction of the long half-life actinides should be considered.
3. Due to different decay heat characteristics of the spent fuels considered in these scenarios, the maximum loading for each is different. Of the three

fuel cycle scenarios studied, the highest loading was found for the DUPIC SNF, followed by the PWROT SNF and the MOX. As MOX SNF is not reprocessed, it contains more Pu and other actinides (Table 5-11) than the other two fuel cycles considered. MOX SNF, therefore, will produce more heat resulting in the lowest repository loading. In MOX scenario, the reactor is loaded with mixed fuel (15% MOX fuel and 85% PWR fresh fuel). Because of recycling of the Pu and U in the PWROT SNF, which is 85% of the total SNF discharged from the reactor, to develop MOX fuel, the volume of the generated HLW for final disposal to get one GWe-yr is the least (less than 30% of the other two fuel cycle scenarios). This benefit is offset by the larger actinide inventory in the MOX SNF and, consequentially, a hotter waste package. If MOX SNF could be reprocessed and actinides were recycled further, then the benefit of volume reduction and an increase in repository capacity could be achieved.

4. Even though the waste composition and the loading amounts are very different, it is observed that the performance of waste package/EBS is similiar for each of the three fuel cycles. The failure times of about 90,000 years and the projected peak dose rate in about 100,000 years in 100,000 years investigation period are nearly the same in each case. The dose rate is almost linear with the amount of SNF loaded for each case. Some error may be introduced for the DUPIC and the MOX results as a result of using the currently available source term model which was developed for PWR and BWR SNF waste packages. A more general source term model

may provide more accuracy in capturing the difference due to different waste forms.

5. Large uncertainties exist in estimating peak dose rate and the accumulated dose in these three scenarios (Table 5-40 and Table 5-43) from the uncertainty study. The geological structure and groundwater properties have the greatest influence on the projected dose rate and accumulated dose. The life style of future down gradient residents of the repository also strongly influences the projected dose in terms of consumed water volume. Even with the large uncertainty in the projected dose rate, none of the fuel cycle scenarios, with the repository fully loaded, exceeded the EPA standard for dose to the public out to 10,000 years (15 mrem/yr). The model developed in this study covers the projected dose rate from the repository to 100,000 years post closure. EPA has proposed amendments extending the coverage to one million years; a further development to the model presented herein would be required to meet this extension. The health risk based single number for repository performance was not used in the case study as part of the objective function, but it may be used as one constraint in the optimization of fuel cycles.

6. The stage mean PR figure (Figure 5-4) has shown the weaker stages in each scenario. More attention and effort is needed by the nuclear industry and research community to enhance the proliferation resistance of the weaker stages. Only intrinsic barriers were investigated in the case studies. Therefore, for an evaluation of the effectiveness of safeguards

represented by the extrinsic barriers, more studies are needed to include them in the current PR model.

7. The mean system PR and minimum stage PR highlight the relative difference between the three fuel cycle scenarios (Table 5-19). Qualitative interpretation helps the user to understand the meaning of the difference in the quantitative results. The PWROT cycle has stronger PR in terms of both the mean system and the minimum stage PR. The quantitative difference of mean system PRs of the MOX and DUPIC fuel cycles shows no difference in the qualitative interpretation (they can be classified into the same level). Based on the minimum stage PR, however, DUPIC is clearly better, at least with respect to poliferation resistance, than MOX.

8. As shown in the sensitivity study of proliferation resistance performance, the weighting scheme is very important in assigning proliferation resistance values. The weighting scheme for all barriers was developed based on available information from published reports and oral communications. Different probabilities and analytical methods may be applied to generate the weighting scheme. For example, pairwise comparison based model could be used for this purpose. The PRA method may be used to obtain the probability to overcome each barrier, and those results can be used as the basis for establishing the weighting scheme for the barriers. Input from experts can be used to refine or enhance the weighting scheme. As some of the quantities can be difficult to measure, the input from experts is valuable to ensure realistic results.

9. In the case study, a fuzzy number is defined as a Gaussian distribution for ease of calculations. For further uncertainty study, other shapes may be applied. The combination of fuzzy numbers requires a more complex calculation accomplished in this investigation with the use of Monte Carlo methods.

10. The impact on FCC from repository capacity expansion was demonstrated by varying the disposal cost in this study. The disposal cost was found to contribute only moderately to the overall FCC: 18% for the PWROT (Table 5-28), 8% for MOX (Table 5-29), and 9% for DUPIC (Table 5-30). Likewise, expanding the repository capacity does not significantly affect the FCC. This result can also be demonstrated by performing an economic study for a potential second repository. When the total mass of HLW exceeds the statutory limit for the Yucca Mountain Repository, the capacity will need to be expanded or a second repository will be required. The cost of the additional repositories would need to be included in the FCC.

11. When the repository capacity is represented as the total electricity that could be generated from the waste, the DUPIC fuel cycle becomes most favorable. By comparing the total cost to generate the same amount of electricity with one repository (Table 5-34, Table 5-35), DUPIC shows the least total cost when the cost of conventional power is higher than nuclear power if the electricity gap between fuel cycles will be compensated by conventional power. If a greenhouse policy is applied, the benefit of the

DUPIC system becomes even greater (62.2% less expensive than the PWROT cycle).

12. Two different methods of defining nonproliferation charges were presented and compared in the case study. Nonproliferation charges based on the FCC shows limited impact because the FCC accounts for about 20% of the total electricity cost. Using 15% of the total electricity cost (Captical cost + O&M cost + FCC) for nonproliferation charges results in the PWROT cycle being a better choice than DUPIC even through the DUPIC cycle generates more electricity. The value of 15% is comparable to the relative standard deviation of FCC in this study, which can be adjusted to reflect the level of concern for nonproliferation issues on the part of policy makers.

13. This study has demonstrated two methods for combining repository proliferation resistance and economic performance. Another option demonstrated would be with the use of health risk and proliferation resistance as constraints; the adjusted fuel cycle cost from the different repository performances could be used as one indicator to choose the fuel cycles with the EPA limits for projected dose rate from the nuclear waste disposal as the health risk constraint and the once-through LWR (PWROT) cycle as the standard for proliferation resistance. One additional choice is to use proliferation resistance as constraints, Once-through LWR cycle as the standard for proliferation resistance constraint. The projected health risk from the once-through LWR cycle can be used as a reference to adjust the charge for final waste disposal. Currently, 1 mill per kWh is charged to

consumers for the final waste disposal. For the fuel cycles other than PWROT, instead of charging the 1 mill per kWh for the disposal funding, a charge based on the ratio of the health risk projected from the alternative fuel cycle to the health risk projected from the once-through LWR spent fuel (PWROT) could be utilized.

7 Conclusion and Recommendation

7.1 Conclusion

A methodology has been developed to evaluate and compare nuclear fuel cycle and waste transmutation systems by considering and integrating a number of performance-attributes including repository performance and corresponding health risk, proliferation resistance performance and fuel cycle cost. A number of sub-models have also been developed or adapted: a simplified repository performance assessment model, a fuzzy logic PR barrier model to quantify the proliferation resistance of the various fuel cycles, and a fuel cycle cost model which integrates the repository and proliferation resistance performances.

A simplified repository performance model, based on the Yucca Mountain Repository, has been developed. By considering the temperature limits at different locations in the repository, the maximum loading was computed for given nuclear waste characteristics. The peak projected dose rate in 100,000 years to the future down gradient (20 km) residents was computed. The accumulated dose in 100,000 years is also presented as a single number index to show the health risk from the fully loaded repository. The single number index could be usefule to facilitate fuel cycle optimization calculations. The maximum capacity of the Yucca Mountain Repository was also computed based on the amount of electricity that could be generated from the nuclear waste.

To quantify the proliferation resistance of the various nuclear fuel cycles, a fuzzy logic based PR barrier model was developed by using the TOPS barrier concetps.

This latter model mimics the human logic process of experts who may use the TOPS barrier method to evaluate the proliferation resistance of a nuclear fuel cycle. Fifteen important quantities were chosen to determine the barrier strength against proliferation at each stage of a given fuel cycle. Barrier effectiveness functions were defined to relate the quantitative values to barrier strength levels. Fuzzy numbers were used to represent the strength of each barrier at 15 different levels. All barrier strength levels for each stage were weighted, then integrated to determine the proliferation resistance of the stage. The barrier weighting scheme was determined as the cost needed to overcome each of the 11 intrinsic barriers in this study. The fuzzy number was obtained by integrating the proliferation resistance information for all stages, thereby indicating the proliferation resistance of the nuclear fuel cycle. The quantified proliferation resistance can be qualitatively interpreted into category according to the definition of the fuzzy number. The plot of the proliferation resistance at each stage can be used as a valuable tool to observe (and compare) the relatively strong and weak barrier stages in terms of the overall proliferation resistance of nuclear fuel cycles.

Based on the assumed nonproliferation charge, an adjusted fuel cycle cost was computed which includes the impact from repository performance and proliferation resistance performance on the fuel cycle cost.

A case study was developed in which three fuel cycles: PWR-OT, MOX and DUPIC were investigated. The PWR-OT fuel cycle was shown to behave the best in this study in terms of its proliferation resistance and fuel cycle cost. But the DUPIC fuel cycle maximizes the capacity of the repository in terms of the amount of

total electricity that could be generated from the nuclear waste loaded. The total electricity that could be generated from the full loaded DUPIC spent fuel is 80% more than what could be generated from the PWR-OT spent fuel using the same enrichment factor, burnup, irradiation period and post irradiation storage time. Meanwhile, the DUPIC fuel cycle system's mean proliferation resistance only decreases by 11%; the fuel cycle cost increases by 8.3% (Table 5-25); and the adjusted fuel cycle cost which includes the nonproliferation charge (assumed to be 15% of FCC) increases by 8.9% (Table 5-31). In these analyses, the performance characteristics of the MOX fuel cycle showed the poorest mainly due to the separation of the plutonium during the MOX fuel fabrication and reprocessing stages and the high reprocessing cost associate with this cycle.

The MOX fuel cycle cost was determined to be the highest followed by the DUPIC cycle and finally the PWR-OT fuel cycle (Table 5-54). The fuel cycle cost of the DUPIC cycle, however, was only slightly higher than that for the PWR-OT fuel cycle. The relative Standard Deviations of FCCs was around 10-15%. There are a number of important variables indicated in Figure 5-25-27 which are different for the three cycles. For example, the two most important variables for the PWR-OT fuel cycle cost are enrichment factor and ore purchase price; for the MOX fuel cycle cost, enrichment and reprocessing cost; and for the DUPIC cycle, enrichment and fuel fabrication cost. The uncertainty in maximum waste fuel loading in the repository, which is a function of waste package density, does not have a significant correlation with the fuel cycle costs for any of the three fuel cycles investigated. Disposal cost is generally a less important parameter but is strongly correlated with

the overall fuel cycle costs. In this study, the calculation of fuel cycle cost was based on the assumption that there is a repository available for all of the spent fuel. If the cost of a potential second repository was included in the calculations, the impact of increasing the repository capacity would be enhanced and the disposal cost could be very important in computing the fuel cycle costs.

The nonproliferation charge used in these investigations was assumed at 15% of the overall fuel cycle costs. The impact from uncertainty of system mean proliferation resistance is very limited. Important variables for adjusted FCC are the same as those for FCC (Figure 5-30-Figure 5-32). The overall relative standard deviation (SD/Mean) was almost the same for each of the three fuel cycles (~16% for PWR-OT, ~10% for MOX and ~13% for DUPIC).

7.2 Recommendations

1. The repository performance model developed in this study considers that only one type of spent fuel is loaded into the repository. A general source term model is needed to cover the case where different types of nuclear waste would be loaded into the repository at the same time. The model should take into consideration the location of the waste from the different nuclear fuel cycles and the peak temperature shoud be mapped over the entire repository.
2. The repository performance model developed can perform for time zones out to 100,000 yrs. Because of the recent determinations of the time to peak dose, a revised model able to compute performance out to 1,000,000 years is needed.

3. The fuzzy logic based barrier method still needs development. Additional work is needed to investigate the impact of fuzzy definitions and barrier weights on the results.
4. Characterizing of the values of input important variables (currently they are calculated manually) in the fuzzy logic based barrier model needs further development. Ideally, the fuel cycle simulation model would automatically generate the values of important variables.
5. The repository performance and the proliferation resistance models need to be linked with a fuel cycle simulation model in order to allow for quick evaluations for optimizating the system design and loading plans.
6. The nonproliferation charge is more of a policy than an economics issue. How large the nonproliferation charge should be depends on how important is the consideration of proliferation resistance in fuel cycle decisions. To consider proliferation resistance more an economics issue, one could investigate the potential damage caused by proliferation. Alternatively, one could determine the safeguard cost to increase the proliferation resistance to a consistent standard.
7. Finally, using the adjusted fuel cycle cost is one way of integrating repository, proliferation resistance, and economics performance to evaluate the performance of the various fuel cycles. Another possible way is to use repository performance and/or proliferation resistance as constraints to screen the potential nuclear fuel cycles and then to use fuel cycle cost to determine the best one. For example, the EPA standard serves as the

minimum requirement for screening. For the screening of PR, consensus is required among the uses of the theshhold.